

# Catalytic asymmetric silicon-carbon bond-forming transformations based on Si–H functionalization

Li Li<sup>1</sup>, Wei-Sheng Huang<sup>1</sup>, Zheng Xu<sup>1</sup> & Li-Wen Xu<sup>1,2\*</sup>

<sup>1</sup>China Key Laboratory of Organosilicon Chemistry and Material Technology of Ministry of Education, Key Laboratory of Organosilicon Material Technology of Zhejiang Province, College of Material, Chemistry and Chemical Engineering, Hangzhou Normal University, Hangzhou 311121, China;

<sup>2</sup>State Key Laboratory for Oxo Synthesis and Selective Oxidation, Suzhou Research Institute, Lanzhou Institute of Chemical Physics, Chinese Academy of Sciences, Lanzhou 730000, China

Received October 5, 2022; accepted December 5, 2022; published online May 4, 2023

In view of the exciting advancement on silicon-carbon bond-forming transformations achieved in the past decade, this review intends to show a unified illustration of the recent findings on enantioselective Si–H bond functionalization aided by asymmetric catalysis. Accordingly, this review describes the enantioselective silicon-carbon bond-forming Si–H bond functionalization, focusing on the reactivity and stereoselectivity in catalytic asymmetric hydrosilylation, carbene Si–H insertion, C–H silylation, and Si–C bond-forming cross-coupling reactions that were achieved with high enantioselectivity in the presence of transition-metal catalyst systems. This review highlights recent and representative examples of the enantioselective Si–H bond functionalization, discusses the origins of silicon-involving stereoselectivities, and evaluates the substrate scopes and limitations in these catalytic asymmetric Si–H bond functionalization reactions due to the special reactivity of different hydrosilanes.

**Si–H functionalization, hydrosilylation, C–H silylation, carbene Si–H insertion, asymmetric catalysis**

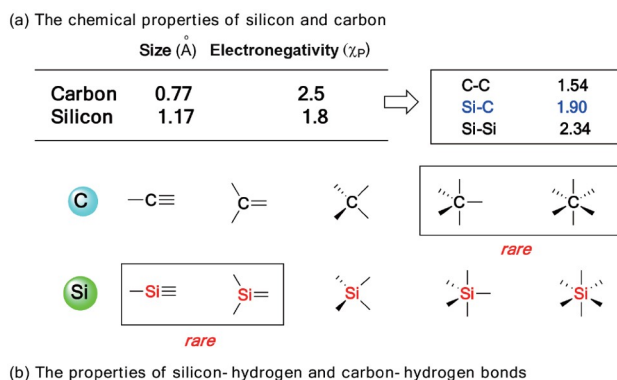
**Citation:** Li L, Huang WS, Xu Z, Xu LW. Catalytic asymmetric silicon-carbon bond-forming transformations based on Si–H functionalization. *Sci China Chem*, 2023, 66: 1654–1687, <https://doi.org/10.1007/s11426-022-1480-y>

## 1 Introduction

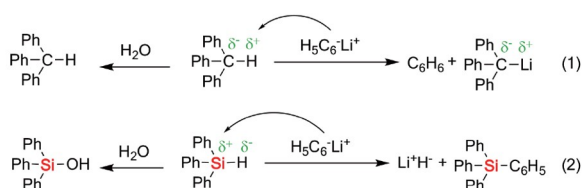
Organosilicon compounds, including the most common chlorosilanes and hydrosilanes, were created in chemical laboratories because they do not exist naturally. These compounds are versatile synthetic building blocks that are widely used in organic synthesis, polymer chemistry, and functional materials. Notably, they possess unique stability and are abundant in their propensity to prepare structurally diverse products through a variety of synthetic transformations [1]. In regard to the molecular level, the chemistry of silicon differs largely from carbon due to the atom size and electronegativity (Figure 1a) [2]. In addition, the availability

of the empty 3d orbitals makes it easy for silicon to form 5- or 6-coordinated complexes that is actually similar to that of some of the first-row transition metals. One of the featured properties of silicon also differs from carbon in forming far few stable multiple bonds but in the formation of stable molecules with more than four bonds due to the production of hypervalent silicon derivatives (Figure 1a). It is generally accepted that the lack of multiple bonds seriously hampers the development of a wide variety of synthetic strategies in organosilicon chemistry in comparison to carbon-centered synthetic chemistry. This is counterbalanced by the fact that there are some unexpected reaction pathways at tetrahedral silicon centers because of the relatively low activation energies in nucleophilic substitutions at silicon compared to carbon [3]. For example, although both Si–H and C–H bonds

\*Corresponding authors (email: [liwenxu@hznu.edu.cn](mailto:liwenxu@hznu.edu.cn); [20060054@hznu.edu.cn](mailto:20060054@hznu.edu.cn))



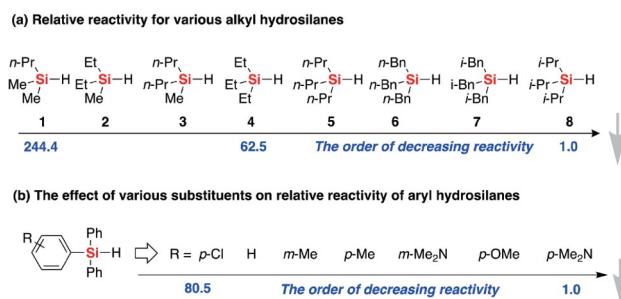
(b) The properties of silicon-hydrogen and carbon-hydrogen bonds



**Figure 1** The difference in the chemical properties of silicon and carbon (color online).

are thermodynamically stable (367–438 kJ/mol for the C–H bond and about 377 kJ/mol for the Si–H bond), the chemical properties of C–H and Si–H bonds are inverse of one another in the representative model reaction of phenyllithium (PhLi) on triphenylsilane ( $\text{Ph}_3\text{SiH}$ ) and triphenylmethane ( $\text{Ph}_3\text{CH}$ ). As shown in **Figure 1b**, the negatively polarized phenyl of PhLi acts as a nucleophile to abstract the positively polarized H of  $\text{Ph}_3\text{CH}$  (Eq. (1) in **Figure 1b**) but undergoes nucleophilic attack to the silicon center to form  $\text{Ph}_4\text{Si}$  (Eq. (2) in **Figure 1b**). Besides, the hydrosilanes can be easily hydrolyzed to yield silanols but a hydrocarbon is unchanged in the presence of a catalytic amount of base. Therefore, the Si–H bond functionalization of hydrosilanes is actually different from C–H functionalization.

Catalytic transformations of Si–H bonds with main-group reagents have become one of the most important synthetic methods due to the diverse applications of functionalized organosilicon products [4]. In a historic context, the application of hydrosilanes and their state-of-the-art transformations include the reduction of unsaturated carbonyl compounds or other unsaturated bonds, silylation of alcohols, and the preparation of polymeric materials [5]. For hydrosilanes used in organic synthesis, the reactivity of Si–H bonds largely depends on the substituents [6]. The begin of such investigation can look back to 70 years ago, Price and Eaboran [7] have ever determined the order of reactivity of various silanes in aqueous-ethanolic alkali liquid (**Figure 2**), in which the steric effects and electronic properties of substituted groups on hydrosilanes contribute largely to the reactivity of Si–H bond. In addition, the order of different types of hydrosilanes is probably represented as  $\text{SiH}_4 > \text{RSiH}_3 > \text{R}_2\text{SiH}_2 > \text{R}_3\text{SiH}$ , and the relative reactivities of the

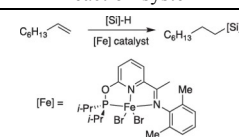
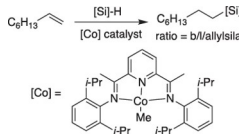
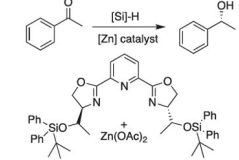
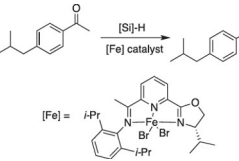
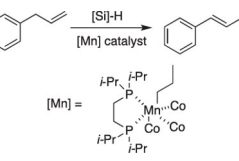
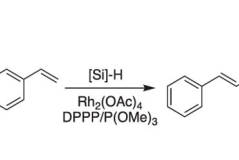
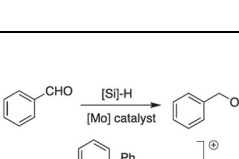
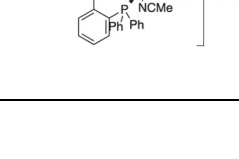


**Figure 2** Relative reactivity of various hydrosilanes (color online).

hydrosilanes  $\text{C}_6\text{H}_{11}\text{SiH}_3$ ,  $n\text{-Pr}_2\text{SiH}_2$ , and  $\text{Et}_3\text{SiH}$  are calculated as about 120:22:1. These hydrosilanes with different reactivities provide an inherently challenging problem in searching efficient catalysts for its wide-ranging utilities in the enantioselective synthesis of structurally diverse silanes. In the past decades, there are numerous examples reported for the chemoselective utility of certain hydrosilane in the catalytic synthesis of organic molecules [8]. For example, with  $t\text{-BuMe}_2\text{SiH}$  as a reducing agent for the reaction silane, the reductive coupling product was obtained with 80% yield and good enantioselectivity (92% *ee*). In addition, when the reaction mediated with bulky ( $i\text{-Pr}$ ) $_3\text{SiH}$ , it afforded only trace amounts of the desired product because of the inefficiencies of the bulky ( $i\text{-Pr}$ ) $_3\text{SiH}$  and its low reactivity in an effective  $\sigma$ -bond metathesis that occurred with the metallacycle intermediate [9]. For other hydrosilanes, the evaluation of hydrosilanes in the reductive hydroxymethylation of styrenes demonstrated that  $(\text{EtO})_3\text{SiH}$  (the desired product with 94% yield and 96% *ee*) and  $\text{Me}(\text{MeO})_2\text{SiH}$  (with 78% yield, 98% *ee*) showed excellent behavior for this transformation, in comparison to that with  $\text{MePh}_2\text{SiH}$  (not detected) or polymethylhydrosilane (PMHS, 64% yield and 82% *ee*) [10]. Besides, some representative examples shown in **Table 1** revealed the tip of the iceberg for the state-of-art advances in the use of hydrosilanes in organic synthesis, in which these reaction results were generally completed by specific hydrosilane related to a certain activity, selectivity, and fidelity activated by the transition-metal catalyst. In another word, the relatively narrow substrate scope of the silicon-based reaction with respect to the hydrosilanes shows the Si–H bond functionalization is a challenging task due to their substituent-induced differences in reactivity, especially for the enantioselective silicon-carbon bond-forming transformations of hydrosilanes. Each hydrosilane compound has its own special reactivity, which gives the magic and uncertainty of silicon-based transformations. At the same time, this feature of silicon-hydride bond gives it the advantage of fine-tuning the reactivity in catalytic asymmetric transformations of hydrosilanes with general organic functional groups, such as olefins, alkynes, and carbonyl compounds.

The differences between monohydrosilanes (SiH) and

**Table 1** The comparison of different reactivities for previously reported hydrosilanes in transition-metal-catalyzed catalysis

Reaction system	Hydrosilane ([Si]-H)	Yield (%)	Ref.
 $C_8H_{13} \xrightarrow{[Si]-H} C_8H_{13}[Si]$ [Fe] catalyst	PhSiH <sub>3</sub>	24	[11]
	Ph <sub>2</sub> SiH <sub>2</sub>	98	
	(EtO) <sub>3</sub> SiH	91	
	(EtO) <sub>2</sub> MeSiH	72	
 $C_8H_{13} \xrightarrow{[Si]-H} C_8H_{13}[Si]$ [Co] catalyst ratio = b/l/allylsilane	PhSiH <sub>3</sub>	91/9/0 <sup>a)</sup>	[12]
	Ph <sub>2</sub> SiH <sub>2</sub>	57/25/18 <sup>a)</sup>	
	(EtO) <sub>3</sub> SiH	12/36/52 <sup>a)</sup>	
	PhMe <sub>2</sub> SiH	0/0/>99 <sup>a)</sup>	
	Et <sub>3</sub> SiH	0/0/>99 <sup>a)</sup>	
 $C_6H_5CHO \xrightarrow{[Si]-H} C_6H_5CH_2OH$ [Zn] catalyst	(EtO) <sub>2</sub> MeSiH	>99 (74) <sup>b)</sup>	[13]
	(EtO) <sub>3</sub> SiH	>99 (16) <sup>b)</sup>	
	PMHS	0	
	PhSiH <sub>3</sub>	>99 (0) <sup>b)</sup>	
 $C_6H_4(t-Bu)CHO \xrightarrow{[Si]-H} C_6H_4(t-Bu)CH_2OH$ [Fe] catalyst	Ph <sub>3</sub> SiH	Trace	[14]
	Ph <sub>2</sub> MeSiH	Trace	
	(EtO) <sub>3</sub> SiH	92 (68) <sup>b)</sup>	
	(TMSO) <sub>2</sub> MeSiH	84 (75) <sup>b)</sup>	
	Et <sub>3</sub> SiH	Trace	
	PhSiH <sub>3</sub>	89 (71) <sup>b)</sup>	
 $C_6H_5C\equiv CMe \xrightarrow{[Si]-H} C_6H_5CH_2CH_2CH_2[Si]$ [Mn] catalyst	Et <sub>3</sub> SiH	87	[15]
	PhMe <sub>2</sub> SiH	93	
	(TMSO) <sub>2</sub> MeSiH	17	
	(MeO) <sub>3</sub> SiH	0	
	( <i>i</i> -Pr) <sub>3</sub> SiH	0	
	(EtO) <sub>3</sub> SiH	88	
 $C_6H_5C\equiv CMe \xrightarrow{[Si]-H} C_6H_5CH_2CH_2CH_2[Si]$ Rh <sub>2</sub> (OAc) <sub>4</sub> DPPFP/(OMe) <sub>3</sub>	(EtO) <sub>2</sub> MeSiH	85	[16]
	(EtO) <sub>3</sub> SiH	88	
	(TMSO) <sub>2</sub> MeSiH	93	
	Ph <sub>3</sub> SiH	88	
	Ph <sub>2</sub> MeSiH	88	
	( <i>i</i> -Pr) <sub>3</sub> SiH	Trace	
 $C_6H_5CHO \xrightarrow{[Si]-H} C_6H_5CH_2OH$ [Mo] catalyst	Et <sub>3</sub> SiH	90	[17]
	( <i>n</i> -Bu) <sub>3</sub> SiH	96	
	PhSiH <sub>3</sub>	33	
	Ph <sub>2</sub> SiH <sub>2</sub>	83	
	PhMeSiH <sub>2</sub>	67	
	PhMe <sub>2</sub> SiH	100	
	Ph <sub>2</sub> MeSiH	15	
	Ph <sub>3</sub> SiH	0	
	( <i>i</i> -Pr) <sub>3</sub> SiH	0	
(MeO) <sub>3</sub> SiH	100		
 $C_6H_5C\equiv CMe \xrightarrow{[Si]-H} C_6H_5CH_2CH_2CH_2[Si]$ CuCl NaO <i>t</i> -Bu Ph-BPE	( <i>n</i> -Bu) <sub>3</sub> SiH	0	[18]
	<i>t</i> -BuMe <sub>2</sub> SiH	0	
	EtMe <sub>2</sub> SiH	43	
	( <i>n</i> -Bu) <sub>2</sub> PhSiH	0	
	PhEt <sub>2</sub> SiH	17	
	PhMe <sub>2</sub> SiH	59	
Ph <sub>2</sub> Me <sub>2</sub> SiH	55		
Ph <sub>3</sub> SiH	52		

a) The ratio is branched/linear/allylsilane; b) the values in parentheses are enantioselectivity (*ee*, %) of the corresponding reaction with above [Si]-H.

multihydrosilanes ( $\text{SiH}_x, x > 1$ ) also demand different chemo- and enantio-selectivity preferences from the chiral catalyst systems for each Si–H transformation. Nowadays, catalytic asymmetric transformations of Si–H bond are among the hottest topics and most widely studied in organosilicon chemistry. The importance of these reactions based on enantioselective Si–H functionalization stems from the versatility and utility of chiral organosilicon molecules as potentially useful products in medicinal chemistry, advanced functional materials, and organic synthesis [19]. Especially in the past five years, dramatic progress in enantioselective Si–H transformations that resulted in Si–C bond-forming functionalization has been made on the basis of broad transition-metal catalysis as well as the development of chiral ligands. These new breakthroughs based on asymmetric hydrosilylation, C–H silylation, carbene insertion and other cross coupling-type Si–H functionalization promoted us to present advances in this topic. Thus, in view of the exciting advancement achieved in the past decade, this review intends to show a unified illustration of the recent findings on enantioselective Si–C bond-forming processes in the Si–H bond functionalization aided by asymmetric catalysis. Some synthetic strategies centered on catalytic hydrosilylation, C–H silylation, and carbene insertion will be presented as representative examples in this topic. In addition, it will be discussed the most attractive results of the transition-metal catalysis with particular emphasis on the stereoselective control for silicon-carbon bond-forming Si–H functionalization, leading to enantioselective synthesis of chiral organosilanes. Through the catalytic asymmetric reactions of these hydrosilanes, we can predict that the synthesis of chiral organosilanes will greatly promote the rapid development of silicon-containing functional molecules.

## 2 Asymmetric hydrosilylation of alkenes

Catalytic hydrosilylation, the addition of Si–H across unsaturated carbon–carbon or carbon–heteroatom (O, N, *etc.*) bonds, is one of the most important reactions in organosilicon chemistry for forming silicon–carbon bonds [20]. Although there are many types of hydrosilylation, hydrosilylation of alkenes and alkynes catalyzed by transition-metal complex [20a], such as platinum, rhodium, palladium, iron, cobalt and other earth-abundant metal catalysts, presents a straightforward tactic to access organosilicon products with high atom economy. Over the past decades, the scope of catalytic hydrosilylation has been expanded to structurally specific unsaturated carbon–carbon bonds, such as allenes and other substrates, to construct silicon-containing compounds difficultly achieved by other methods [21]. Recently, growing attention has been paid to catalytic asymmetric hydrosilylation as well as their application in the

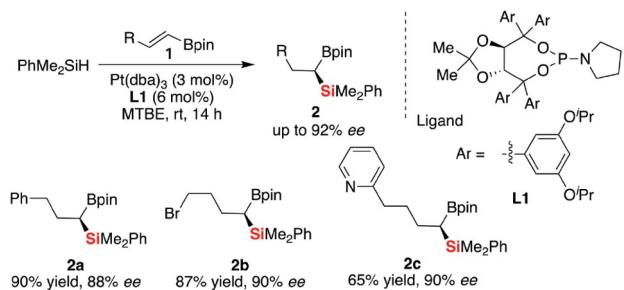
synthesis of functionalized silanes. Nevertheless, the development of an asymmetric version is challenging since effective chiral catalyst systems are still limited due to the difficulty in enantioselective Si–H bond activation and substrate-specific reactivity of hydrosilanes. In this regard, we will review some representative advances in the catalytic asymmetric hydrosilylation based on the different types of transition-metal catalysts, including platinum, rhodium, palladium, iron, cobalt, scandium, copper, and nickel.

### 2.1 Pt-catalyzed hydrosilylation of alkenyl boronates

Since the first hydrosilylation reaction was reported in 1947 [22], the platinum-catalyzed hydrosilylation reaction has gained increasing attention and is successfully employed in industrial applications because of their high activities and ease of handling [23]. In this context, many effective platinum complexes, such as the Karstedt catalyst, have been developed to catalyze the hydrosilylation of alkenes to organosilicon compounds and silicone materials [24]. However, the development of chiral versions of platinum-catalyzed hydrosilylation of alkenes is really rare. As the example of enantioselective Pt-catalyzed hydrosilylation of alkenes reported in 2018, Morken and co-workers [25] demonstrated the ability of TADDOL-derived phosphoramidite **L1** in the asymmetric platinum-catalyzed hydrosilylation of alkenyl boronates **1** with  $\text{PhMe}_2\text{SiH}$ , which gave the corresponding geminal silylboronate products **2** with high regio- and enantioselectivity (Scheme 1, eighteen examples, up to 92% *ee*). The mechanistic studies supported the reaction mechanism that olefin insertion into a platinum hydride led to a stabilized  $\alpha$ -boryl-organoplatinum intermediate, and this species governed the regiocontrol of the hydrosilylation.

### 2.2 Rh-catalyzed hydrosilylation of alkenes

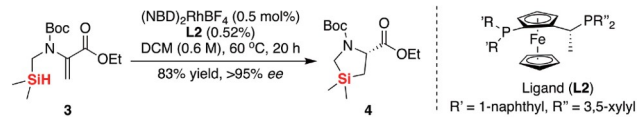
It is well-known that Wilkinson's catalyst  $[\text{RhCl}(\text{PPh}_3)_3]$  and its analogs can effectively catalyze the hydrosilylation of various ketones and alkenes [26]. In addition, asymmetric rhodium-catalyzed hydrosilylation of alkenes is an important strategy for the synthesis of chiral silanes and their derivatives, such as chiral alcohols [27]. Rhodium-catalyzed asymmetric hydrosilylation of alkenes using chiral ligands provides an efficient route to chiral silanes, which are of great significance in fine chemicals as well as biologically active molecules. Since Bosnich's pioneering work on the catalytic asymmetric intramolecular hydrosilylation of olefins [28], asymmetric rhodium-catalyzed intramolecular hydrosilylation of olefins has become an important strategy to access silicon-containing chiral heterocycles and its derivatives in the past decades. In this regard, Jeon and co-workers [29] contributed additional rhodium catalyst systems as an alternative protocol in intramolecular hydrosilylation. Sub-



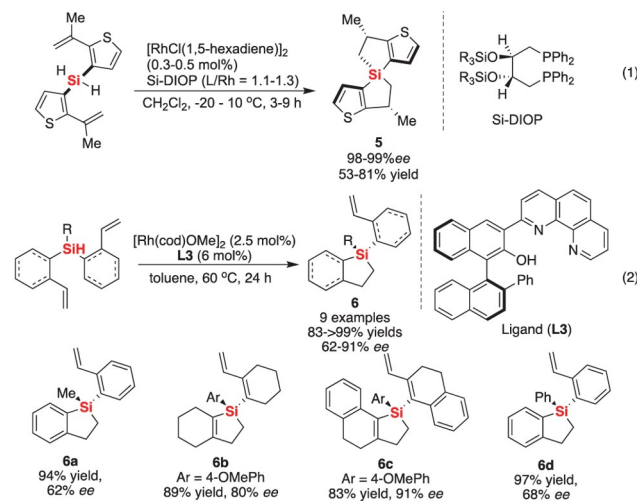
**Scheme 1** Asymmetric Pt-catalyzed hydrosilylation of alkenyl boronates (color online).

sequently later, the year 2016 brought a report by Chung and co-workers [30] for a catalytic asymmetric intramolecular hydrosilylation (Scheme 2). This reaction was able to convert a group of Si–H into the corresponding Si–C bond for the synthesis of silicon-containing chiral amino acid derivatives. In the enantioselective Rh-catalyzed intramolecular hydrosilylation reaction of **3**, several Joisphos ligands were found to afford the most reactive Rh catalyst with good selectivity. Interestingly, higher catalyst loadings (5 mol%–10 mol%) at two different concentrations (0.08 or 0.2 M) led to a lower yield of the desired product. Interestingly, using 3 mol% Rh catalyst with chiral Joisphos ligand **L2**, the reaction was nearly complete in less than 5 min at room temperature to afford good yield (91%) and enantioselectivity (98.7% *ee*) along with 6% unreacted starting material.

Despite the potential of intramolecular hydrosilylation, highly enantioselective synthesis of this chiral spiroisilabiindanes and cycloisomerization-derived silyl products is little reported [31]. In 1996, Tamao and co-workers [32] reported the first example of the asymmetric Rh-catalyzed intramolecular hydrosilylation for the enantioselective synthesis of chiral thiophene-containing spiroisilane (Scheme 3, Eq. (1)). This work opened a new entry to the enantioselective synthesis of silicon-stereogenic organosilicon compounds by hydrosilylation. However, the development of conformationally more constrained silicon-centered spiroisilane is still limited to the enantioselective control of intramolecular hydrosilylation. As described in 2015, inspired by Tamao's strategy, Naganawa and Nishiyama *et al.* [33] reported an enantioselective rhodium-catalyzed desymmetrizing intramolecular hydrosilylation of SiH-tethered symmetrically disubstituted alkenes (Scheme 3, Eq. (2)). The axially chiral BINOL-derived phenanthroline ligand **L3** (simplified as BinThro) was found to be an effective chiral catalyst that worked efficiently for this catalytic asymmetric hydrosilylation (Scheme 3). The silicon-stereogenic center on cyclic five-membered organosilanes **6** was constructed with promising enantioselectivity in the present protocol (up to 91% *ee*). Although the reaction mechanism is not clear at present, the experimental result provided direct evidence that the role of the hydroxy group of (*S*)-BinThro was crucial to



**Scheme 2** Enantioselective Rh-catalyzed intramolecular hydrosilylation (color online).

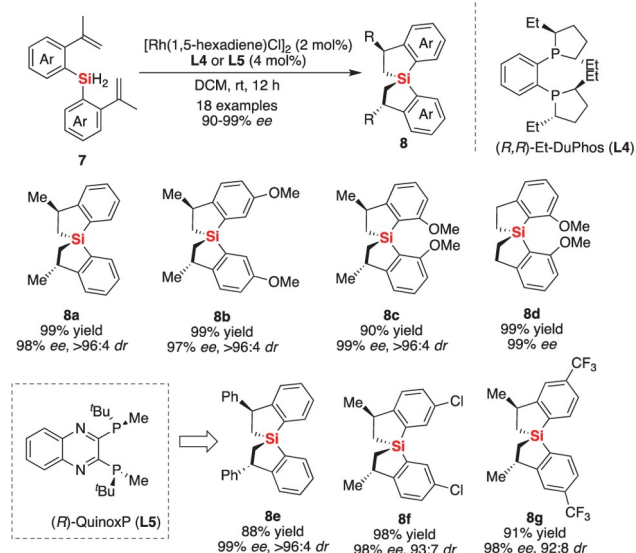


**Scheme 3** Asymmetric Rh-catalyzed intramolecular hydrosilylation of alkenes to access silicon-stereogenic centers (color online).

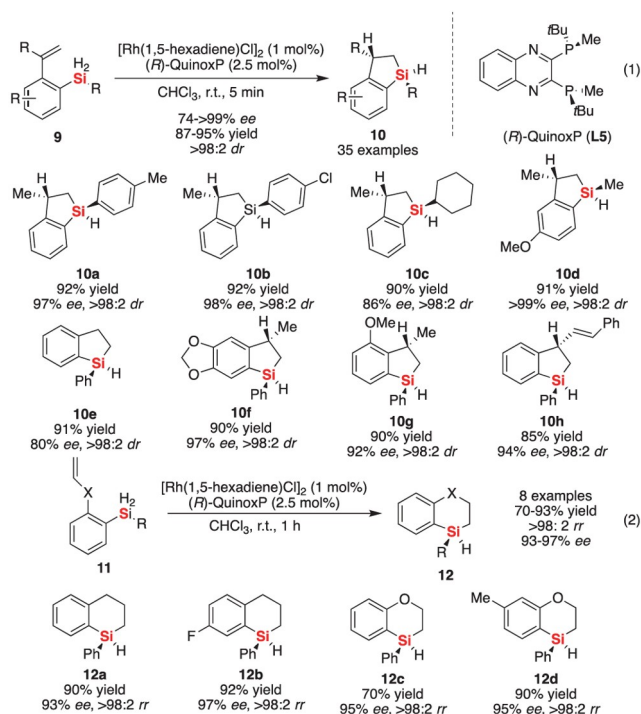
the enantioselective Si–H activation by the *N,N,O*-tridentate Rh complex.

Later in 2020, Wang and Li [34] reported the enantioselective synthesis of chiral spiroisilabiindane scaffolds by Rh/P-ligand complex-catalyzed double and intramolecular hydrosilylation of hydrosilane-linked alkenes (Scheme 4). This reaction could be applied to the synthesis of a wide range of structurally diverse silicon-stereogenic spiroisilabiindanes **8** with excellent yields and enantioselectivities (84%–99% yield and 90%–99% *ee*) as well as good diastereoselectivities (91:9–>96:4 *dr*). In addition, enantiopure derivatives (spiroisilabiindane diol, SPSiOL) could be used as a new building block for the preparation of various chiral P-ligands for asymmetric Rh-catalyzed hydrogenation to give methyl acetyl-L-phenylalaninate with 99.8% *ee* and a Pd-catalyzed intramolecular carboamination to give *tert*-butyl(*R*)-2-(4-methoxybenzyl)pyrrolidine-1-carboxylate with 88% *ee*.

Very recently, Wang and co-workers [35] have further demonstrated an intramolecular and desymmetric hydrosilylation of dihydrosilanes **9** to access silicon-stereogenic monohydrosilanes **10** with the aid of Rh/QuinoxP complex (Scheme 5). This strategy is suitable for the enantioselective synthesis of a wide range of five- and six-membered cyclic monohydrosilanes with excellent diastereo-, regio-, and enantioselectivities. Notably, this reaction was completed within 5 min without the loss of *ee* value and yield. Further mechanistic studies and density functional theory (DFT)



**Scheme 4** Asymmetric Rh-catalyzed intramolecular hydrosilylation of alkenes to access chiral spirocyclic silanes (color online).



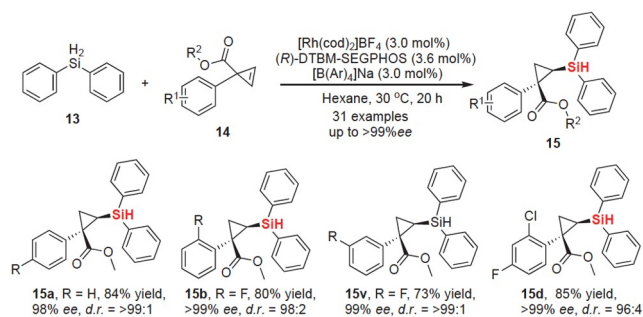
**Scheme 5** Asymmetric Rh-catalyzed intramolecular hydrosilylation of alkenes to access silicon-stereogenic centers (color online).

calculations supported that this asymmetric Rh-catalyzed intramolecular hydrosilylation reaction might proceed *via* a Chalk-Harrod mechanism and the oxidative addition of the Si-H bond might be the enantio-determining step.

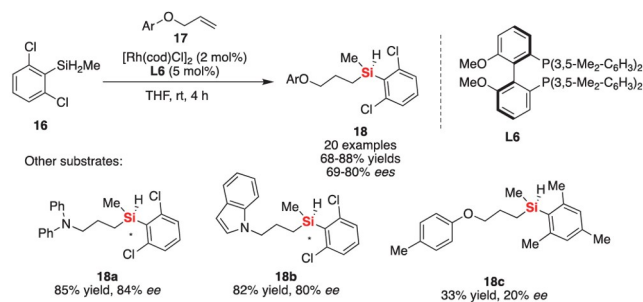
Although catalytic hydrosilylation of general olefins have been developed to make structurally diverse linear or branched alkylsilanes with good yields and stereoselectivities, the limitation of deficiency of enantioselective hydrosilylation

of cyclopropenes motivates Xu group [36] to explore catalytic asymmetric hydrosilylation of cyclopropenes **14** for the construction of chiral silyl carbocycle compounds. In 2019, they presented the Rh-catalyzed asymmetric hydrosilylation reaction of 1,1-disubstituted cyclopropenes **14** in the presence of chiral DTBM-SEGPHOS (**Scheme 6**), allowing for desymmetrization-based enantioselective access to achieve chiral organosilicon compounds **15** in high yields with excellent stereoselectivities (up to >99:1 *dr* and >99% *ee*). In addition, the rhodium-catalyzed process featured a broad scope of enantioselective construction of three-membered carbocycles bearing a carbon quaternary stereocenter, and these silyl products could be transferred into a variety of substituted cyclopropanes and silanols.

The success in Tamao's intramolecular hydrosilylation by asymmetric rhodium catalysis inspired further exploration of the possibility of enantioselective rhodium-catalyzed intermolecular hydrosilylation for the synthesis of silicon-stereogenic monohydrosilanes. In 2020, He and Zhang [37] developed an enantioselective Rh-catalyzed intermolecular hydrosilylation of alkene with prochiral dihydrosilanes **16** to access a new hydrosilanes bearing a Si-stereogenic center with good yields and enantioselectivities (**Scheme 7**, up to 84% *ee*). Compared with known methods for the synthesis of silicon-stereogenic silacycles, this substrate-sensitive finding further revealed the difficulty in stereoselective construction of linear silicon-stereogenic silanes **18** [38]. For example, changing the Cl into Me on the aryl ring of dihydrosilane resulted in a low yield and *ee* value for the desired



**Scheme 6** Asymmetric Rh-catalyzed hydrosilylation of cyclopropenes (color online).



**Scheme 7** Asymmetric Rh-catalyzed intermolecular hydrosilylation of alkenes to access silicon-stereogenic monohydrosilanes (color online).

product. In addition, the steric environment around the silicon atom is also essential for both the reactivity of Si–H bond activation and subsequent stereocontrol.

The above examples on enantioselective Rh-catalyzed hydrosilylation of alkenes show that the rhodium-based catalyst systems have good catalytic performance in the intramolecular hydrosilylation reactions, which could successfully realize the catalytic asymmetric construction of carbon- and silicon-stereogenic centers with high level of enantioselectivities. However, for the intermolecular hydrosilylation reaction of alkenes, the rhodium catalyst system still has a limited ability to realize the desymmetrization reaction of dihydrosilane to construct a silicon-stereogenic center. Meanwhile, the hydrosilylation reaction of internal olefins needs to be further strengthened because there was only one example reported by Xu and co-workers [36], and it is expected that there will be more examples to be developed in the future to demonstrate the unique ability of rhodium catalysts in enantioselective Si–H bond functionalization reactions.

### 2.3 Pd-catalyzed intermolecular hydrosilylation of alkenes

Palladium has a unique historical role in catalytic asymmetric hydrosilylation reactions. Since the first example of enantioselective palladium-catalyzed hydrosilylation of styrene with highly reactive  $\text{HSiCl}_3$  reported by Kumada in 1972 [39], enantioselective palladium-catalyzed hydrosilylations of carbon–carbon double bonds with  $\text{HSiCl}_3$  (trichlorosilane) have been intensively investigated with the aid of chiral monodentate ligands from the early 1990s to early 2000s [40]. Although the asymmetric palladium-catalyzed hydrosilylation of alkyl-substituted terminal alkenes, styrene derivatives, and the other alkenes with trichlorosilane has been established for 20 years with excellent regioselectivities and enantioselectivities, the development of chiral ligands for enantioselective hydrosilylation of terminal alkenes with tertiary hydrosilanes (but not trichlorosilane) remains an underexplored and ongoing task, as presented in Figure 3 which shows the various well-established P-ligands for asymmetric Pd-catalyzed hydrosilylation of styrene with trichlorosilane [41].

Notably, during the evolution of chiral ligand for the palladium-catalyzed hydrosilylation, it was found that the potential secondary donation could be an important factor to be considered for this reaction as it might have a significant impact on palladium catalyst activity and stereoselectivity [42]. Of course, for such P-ligands based on the biaryl skeleton, the importance of secondary interactions in the enantioselectivity enhancement is less clear. Although the palladium-catalyzed hydrosilylation of aromatic alkenes with trichlorosilane has been well-established in the past

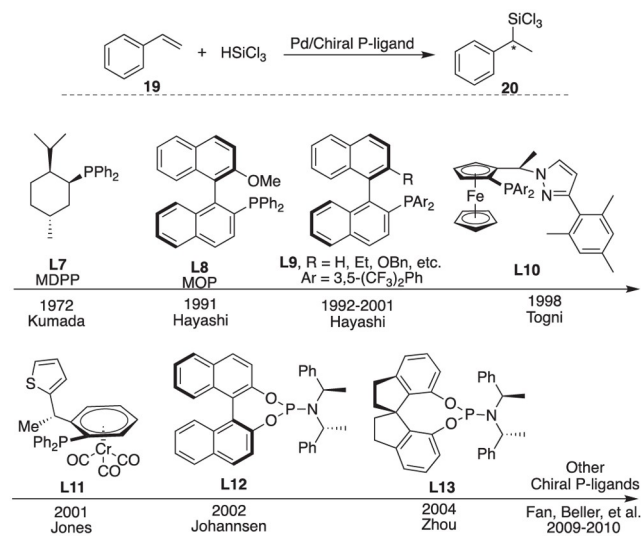
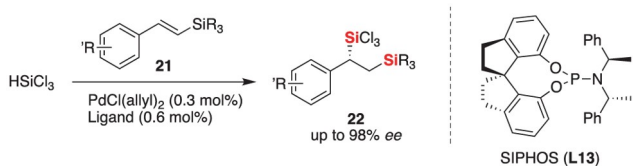


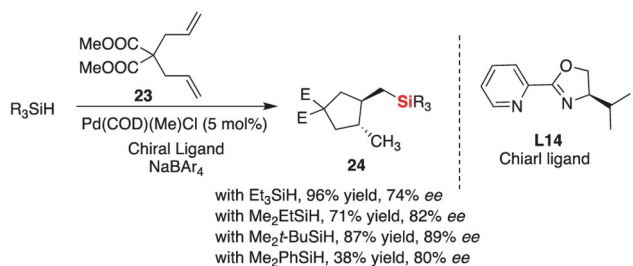
**Figure 3** Some representative P-ligands for the evolution of Pd-catalyzed asymmetric hydrosilylation of styrene with  $\text{HSiCl}_3$ .

decades, the powerful potentials of previously developed P-ligands continued to be proved in recent work. For instance, Li and co-workers recently reported an enantioselective hydrosilylation of  $\beta$ -silyl styrenes **21** with trichlorosilane by a chiral palladium catalyst system with the aid of Zhou's SI-PHOS, which produced chiral 1,2-bis(silyl) compound **22** with excellent yield and good to excellent enantioselectivities (Scheme 8) [43].

Except for the trichlorosilane-involved silicon–carbon bond-forming hydrosilylation, the use of general chloride-free alkyl or aromatic hydrosilanes did not get successful accumulation in the past decades because of its low reactivity and selectivity in palladium-catalyzed hydrosilylation. Before 2020, there are few examples reported for the enantioselective palladium-catalyzed Si–H functionalization by the use of organosilanes other than trichlorosilane. A notable example was shown in 1998 reported by Widehoefer and co-workers [44]. They found that an optically active palladium/bisoxazoline complex was effective for the cyclization/hydrosilylation of dimethyl diallylmalonate or its analogs with triethylsilane, which provides a facile route to form the silylated carbocycle **24** in a good yield and with up to 91% *ee* (Scheme 9). Although dimethylphenylsilane was not particularly efficient, a number of hydrosilanes, such as  $\text{HSiMe}_2\text{Et}$  and  $\text{HSiMe}_2t\text{-Bu}$ , were employed to give the corresponding silylated products with good *ee* values. Notably, based on the investigation of substrate scope (15 examples), it was found that the enantioselectivity of this reaction roughly paralleled the steric bulk of the homoallylic substituents and ranged from 33% *ee* for hydrosilylation/cyclization of diallyltrifluoroacetamide to 91% *ee* for the reaction of 4,4-bis(trimethylacetoxymethyl)-1,6-heptadiene. Notably, the reaction was also applicable to various 1,*n*-dienes to form a cyclopentane ring as well as a new carbon–



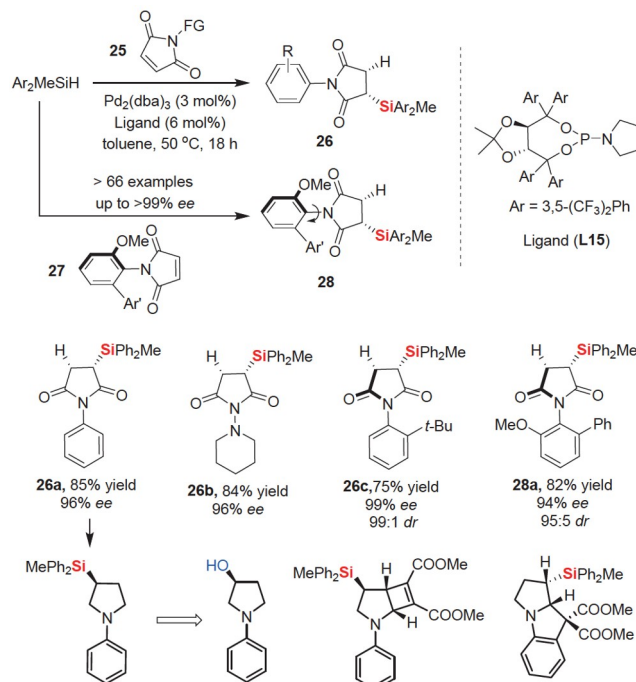
**Scheme 8** Asymmetric Pd-catalyzed hydrosilylation of  $\beta$ -silyl styrene with trichlorosilane (color online).



**Scheme 9** Enantioselective Rh-catalyzed cyclization/hydrosilylation of dimethyl diallylmalonate and its analogs (color online).

silicon bond at a remote site [45], whereas no enantioselective version was achieved in this case.

Encouraged by previous success for the palladium-catalyzed hydrosilylation of alkenes with trichlorosilane ( $\text{HSiCl}_3$ ), Xu and co-workers [46] want to design a novel one-pot and multicomponent asymmetric allylic alkylation and cascade hydrosilylation in the presence of different hydrosilanes. However, the reaction of benzene-1,2-diol with but-2-ene-1,4-diol-derived allylic acetate as well as different hydrosilanes, such as  $\text{Ph}_2\text{SiH}_2$ ,  $\text{MePhSiH}_2$ , and  $\text{MePh}_2\text{SiH}$ , resulted into the reductive product through double allylic alkylation and cascade reduction of olefin moiety. Therefore, although transition-metal-catalyzed hydrosilylation has been successfully developed for the enantioselective synthesis of chiral silanes, the catalytic asymmetric hydrosilylation of internal alkenes or its analogues are uncommon and not easy due to the lack of effective catalyst systems, and the synthetic capabilities for the enantioselective hydrosilylation of activated alkenes are also presently limited. For example, the palladium-catalyzed hydrosilylation of electron-withdrawing group-activated alkenes, especially for  $\alpha,\beta$ -unsaturated carbonyl compounds, generally generate mixtures because of the competitive reduction and silylation reactions, including  $\alpha$ - and  $\beta$ -adducts, and silyl ketene acetals, silyl ethers/amines, and polymeric byproducts [47]. Subsequently in 2020, Xu and co-workers [48] report the first example for a highly enantioselective palladium-catalyzed Si–C bond-forming hydrosilylation of carbonyl-activated alkenes **25** with the aid of a chiral TADDOL-derived phosphoramidite ligand **L15** (Scheme 10), in which the stereospecific Si–C coupling/hydrosilylation of maleimides **25** afforded a series of chiral silyl succinimides **26** with excellent yields and diastereoselectivity as well high enantioselectivity (up to

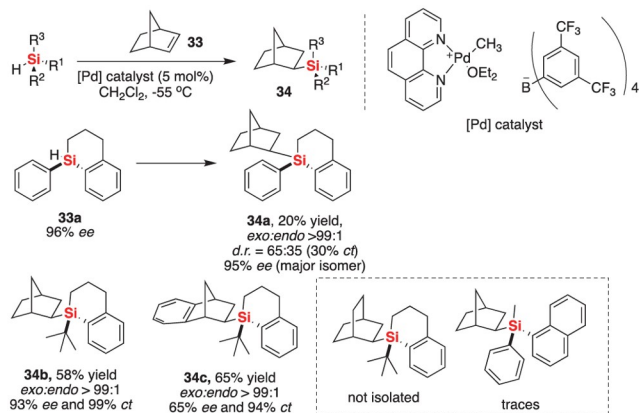


**Scheme 10** Enantioselective palladium-catalyzed hydrosilylation of maleimides (color online).

99%, >99:1 *dr*, and >99:1 *ee*). Except for general aryl maleimides with electron-withdrawing or electron-donating groups on the aromatic ring that reacted efficiently with hydrosilane to give desired products with excellent stereoselectivity, other substrates bearing an additional N- or S-heterocycle also performed smoothly to give the corresponding products **26** under the optimized reaction conditions. In addition, this reaction could be applied in the enantioselective construction of C–N axial chirality due to the remote chiral control in Pd-catalyzed hydrosilylation of *ortho*-substituted *N*-aryl maleimides **27**. The one-step formation of both point chirality and axial chirality provided a facile process to pick up synthetically useful intermediates in the enantioselective synthesis of complex molecules benefited from the palladium-catalyzed hydrosilylation of maleimides.

For palladium-catalyzed hydrosilylation, the direct use of silicon-stereogenic hydrosilanes in the silicon–carbon bond-forming process is quite rare. Early in 2005, Oestreich and Rendler [49] investigated the stereochemical information at the chiral-at-silicon in the process of silicon-to-carbon chirality transfer based on the palladium-catalyzed hydrosilylation (Scheme 11). Notably, the Pd-catalyzed hydrosilylation of norbornene **33** with acyclic silane proved to be extremely sluggish and cyclic silanes could be suitable substrates in this reaction, whereas the hydrosilylation itself was extremely sensitive to slight steric alternations of silanes and alkenes. In addition, based on the study of nonlinear effect, asymmetric amplification was observed in this reagent-controlled





**Scheme 11** Pd-catalyzed hydrosilylation of silicon-stereogenic silane with alkene (color online).

process because the enantiomeric excess of silyl product **34b** (93% *ee*) was substantially higher than the *ee* value of starting silicon-stereogenic silanes. These experimental results would be beneficial to the application of silicon-stereogenic hydrosilanes in enantioselective synthesis.

Although asymmetric palladium-catalyzed intermolecular hydrosilylation of alkenes has achieved numerous successful examples, most of them are limited to hydrosilanes containing electron-withdrawing groups, such as  $\text{HSiCl}_3$ . Given the strong catalytic ability of palladium in asymmetric catalysis, it is believed that in the near future, palladium-catalyzed hydrosilylation reactions of olefins will be able to solve the long unresolved problems for hydrosilylation of activated olefins with simple and general hydrosilanes.

## 2.4 Fe-catalyzed hydrosilylation of terminal alkenes

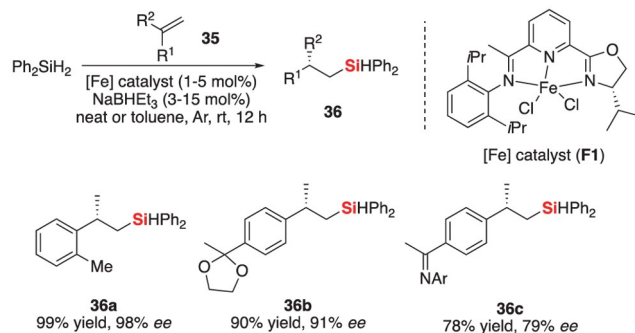
The use of iron as a catalyst in hydrosilylation has become an attractive method during the past year [50]. As an alternative to the aforementioned Pt, Rh, and Pd catalysis, asymmetric Fe-catalyzed hydrosilylation provides a new operation to the enantioselective synthesis of chiral silanes. In sharp contrast to palladium catalysis, iron-catalyzed hydrosilylation of 1,1-disubstituted olefins proceed smoothly in the presence of diphenylsilane ( $\text{Ph}_2\text{SiH}_2$ ) or phenylsilane ( $\text{PhSiH}_3$ ).

Catalytic asymmetric hydrosilylation of 1,1-disubstituted alkenes is a challenging task due to the low enantioselectivities achieved by several groups [51]. In 2015, Lu and co-workers [52] developed a highly enantioselective hydrosilylation of 1,1-disubstituted alkenes **35** in the presence of chiral oxazoline iminopyridine iron complex **F1** (Scheme 12). With the optimized reaction conditions in hand (only 1 mol% of chiral iron precatalyst and 3 mol% of additive ( $\text{NaHBET}_3$ ) are needed for this transformation), the catalytic asymmetric hydrosilylation of 1,1-disubstituted styrenes **35** with *ortho*, *meta*, and *para*-substitutions on phenyl ring gave the corresponding monohydrosilanes **36** in good yields and

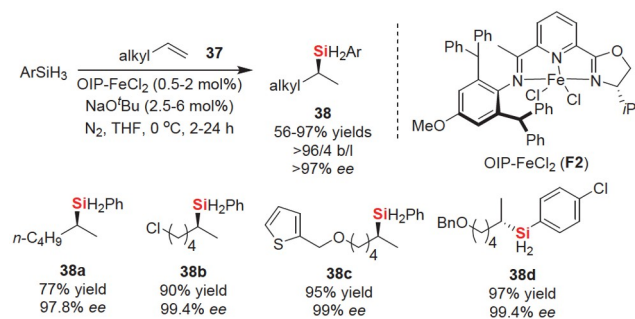
excellent enantioselectivities (up to 99%). In this case,  $\text{NaHBET}_3$  was used as an additive for *in-situ* reduction of the iron precatalyst to form active iron species. In comparison to previous findings in the field of catalytic asymmetric hydrosilylation, this Si–H bond functionalization transformation provided an improved and practical method alternative to the synthesis of chiral organosilanes due to the operational simplicity, low catalyst loading, as well as using a sustainable and cheap transition metal as a catalyst precursor.

In 2018, Lu and co-workers [53] further reported a highly enantioselective iron-catalyzed Markovnikov-type hydrosilylation of terminal aliphatic alkenes **37** with arylsilanes ( $\text{ArSiH}_3$ ). This process featured good functional group tolerance from readily available hydrosilanes and aliphatic alkenes, operationally simple protocol by using of earth-abundant transition metal catalyst, and the chiral organosilane products **38** achieved with better than 99% *ee* in most cases (Scheme 13). The control experiment suggested that the iron silyl species were initially obtained from reducing  $\text{OIP}\cdot\text{FeCl}_2$  (**F2**) by hydrosilane ( $\text{PhSiH}_3$ ) with the aid of  $\text{NaO}^t\text{Bu}$  and then coordinated with an alkene to generate a key iron species. The alkene was inserted into the Fe–Si bond and subsequently formed iron alkyl species, which reacted with  $\text{PhSiH}_3$  to afford the hydrosilylation product and regenerate iron-silicon species for the next catalytic cycles.

Recently, with phenylsilane as a silicon source, Lu and co-workers [54] established an enantioselective iron-catalyzed

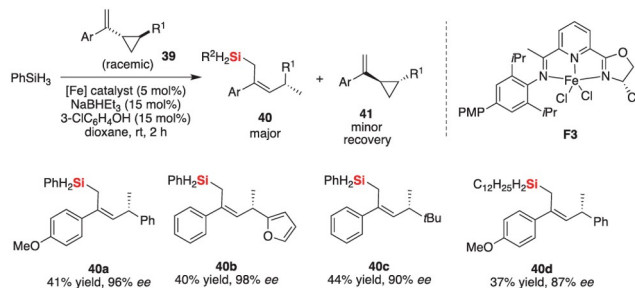


**Scheme 12** Iron-catalyzed hydrosilylation of 1,1-disubstituted alkenes with  $\text{Ph}_2\text{SiH}_2$  (color online).



**Scheme 13** Iron-catalyzed hydrosilylation of alkenes with  $\text{ArSiH}_3$  (color online).

hydrosilylation of vinylcyclopropanes (VCPs) with anti-Markovnikov-selectivity *via* stereospecific C–C bond cleavage (Scheme 14). The transformation of trihydrosilanes (RSiH<sub>3</sub>) with a wide range of VCPs **39** generated the desired allylic dihydrosilanes **40** in excellent *ee* and recovered minor amount of chiral VCPs in moderate to excellent *ee* through a kinetic resolution pathway. In this reaction, the addition of 3-chlorophenol was found to be an effective additive to promote the formation of proposed iron silyl species from the chiral iron catalyst and RSiH<sub>3</sub> to accelerate the hydrosilylation reaction.



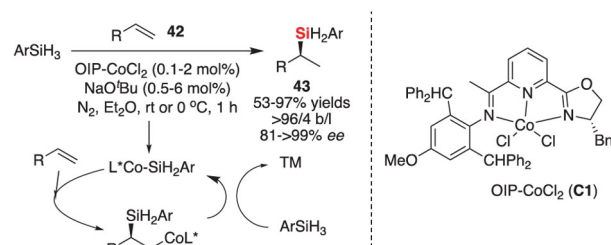
**Scheme 14** Iron-catalyzed hydrosilylation of vinylcyclopropanes with ArSiH<sub>3</sub> (color online).

## 2.5 Co-catalyzed hydrosilylation of alkenes

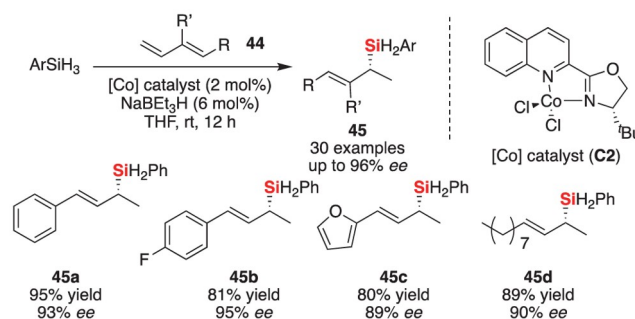
Similarly to iron, the inexpensive cobalt is an abundant element and comprises 0.0029 wt% of the Earth's crust, which is much higher than the heavier platinum group metals, such as rhodium and iridium [55]. Since Chalk and Harrod's finding [56] of cobalt-catalyzed hydrosilylation of terminal alkenes in 1965, hydrosilylation of alkenes catalyzed by cobalt has become a promising and particularly expected approach to synthesize organosilanes [57]. Especially, significant progress in the enantioselective version of silicon-hydrogen activation for hydrosilylation has also been achieved in the past years.

In 2017, Lu and co-workers [58] developed an enantioselective cobalt complex (C1)-catalyzed Markovnikov-type hydrosilylation of olefins with ArSiH<sub>3</sub> to give the chiral benzyl silanes **43** in good yields (53%–97%) and excellent *ee* values (up to >99% *ee*). Beside the aryl alkenes, the aliphatic alkenes were also found to be suitable substrates under optimized reaction conditions to afford the chiral dihydrosilanes **43** in 81%–87% *ee* (Scheme 15). Notably, this protocol could be easily carried out in a gram-scale without loss of enantioselectivity using 0.1 mol% of catalyst loading (86% yield and 98% *ee*). In this case, the turnover frequency (TOF) and turnover number (TON) are quite high (up to 1,800 and 860, respectively).

In 2019, Huang and co-workers described an asymmetric quinoline-oxazoline cobalt complex (C2)-catalyzed 1,2-Markovnikov hydrosilylation of conjugated dienes **44** with aromatic primary silanes (Scheme 16) [59]. This protocol provided efficient access to chiral allyl dihydrosilanes **45** with excellent enantioselectivity (up to 96% *ee*) and high regioselectivity. In addition, this cobalt catalyst system featured with good substrate scope, in which a wide array of conjugated dienes with aryl and/or alkyl substituents could be used in this reaction. Furthermore, the dihydrosilane products are useful starting materials for the synthesis of polyorganosiloxanes containing side chains of enantioenriched allylic functionalities by cobalt-catalyzed step-growth polymerization with terephthalaldehyde. The mechanistic studies, including the experimental result of a



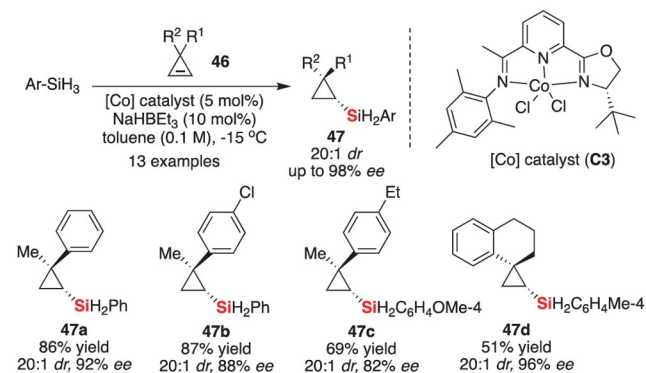
**Scheme 15** Cobalt-catalyzed hydrosilylation of olefins with ArSiH<sub>3</sub> (color online).



**Scheme 16** Cobalt-catalyzed hydrosilylation of conjugated dienes with ArSiH<sub>3</sub> (color online).

deuterium-labeling experiment with PhSiD<sub>3</sub>, revealed that the hydrosilylation most likely occurred through a modified Chalk-Harrod mechanism, involving the key step of 1,2-insertion of the terminal double bond of the alkene into the Co–Si bond.

In the past years, the development of atom-economy approach to access silylated saturated three-membered rings became an attractive topic that could constitute a new and additional tool for the direct and enantioselective functionalization of three-membered carbocyclic skeleton [60]. In 2020, Marek and co-workers [61] reported a highly diastereo- and enantioselective cobalt-catalyzed hydrosilylation reaction of achiral 3,3-disubstituted cyclopropanes **46** with arylsilanes (Ar-SiH<sub>3</sub>). In this protocol (Scheme 17), various monoaryl silanes could be activated by cobalt catalyst to react with substituted 3,3-disubstituted cyclopropanes smoothly, which gave the desired silylcyclopropanes **47** with



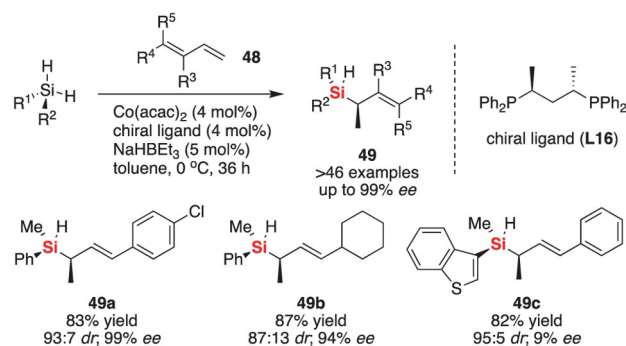
**Scheme 17** Cobalt-catalyzed hydrosilylation of cyclopropenes with Ar-SiH<sub>3</sub> (color online).

good to excellent stereoselectivities (20:1 *dr* and 64%–98% *ee* for 13 examples). The deuterium labeling experiments showed that the *in-situ* formed cyclopropylcobalt intermediate was protonated by the hydrosilane to give the desired *syn*-addition product and regenerate the active catalytic cobalt species.

Very recently, Meng and Chong *et al.* [62] reported a cobalt-catalyzed protocol for regio- and stereo-selective hydrosilylation of 1,3-dienes **48** to furnish a wide range of silicon-stereogenic silanes **49** in high efficiency and selectivity (up to 99% *ee*, Scheme 18). In addition, the simultaneous construction of both carbon- and silicon-stereogenic centers in an acyclic molecule is really interesting. The Si–H functionalization also featured a broad scope of prochiral silanes without the special requirement for the installation of steric substituents, enabling access to a high diversity of silicon-stereogenic molecules. The cobalt catalyst system was proved to be practical, and the synthetic utility of corresponding products was demonstrated by some transformations, such as the reduction of the alkene and stereospecific functionalization of the “silicon-centered” Si–H bond, in which a series of useful enantioenriched building blocks could be achieved that are otherwise difficult to access. In this work, the authors carried out a series of control experiments, deuterium-labeling and kinetic experiments, these experiment results revealed that the establishment of the silicon-stereogenic center by addition of the Si–Co complex is the rate-determining step, and the  $\sigma$ -bond metathesis at the silicon-stereogenic center occurred rapidly with complete retention of stereochemistry.

## 2.6 Sc-catalyzed hydrosilylation of terminal alkenes

Although the first example of highly efficient scandium-catalyzed hydrosilylation of olefins only appeared in 2017, the enantioselective version of scandium-catalyzed hydrosilylation was proved to be an effective strategy to access silicon-stereogenic silanes [63]. In 2018, Hou and co-



**Scheme 18** Cobalt-catalyzed hydrosilylation of 1,3-dienes with prochiral silanes (color online).

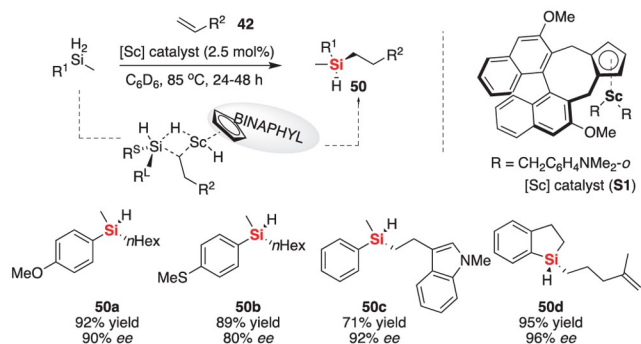
workers [64] have achieved a highly enantioselective hydrosilylation of alkenes with dihydrosilanes by using their newly developed chiral scandium catalyst **S1** (Scheme 19). The half-sandwich Sc catalyst **S1** made this intermolecular hydrosilylation process to constitute an efficient and general route for the enantioselective construction of silicon-stereogenic hydrosilanes. A broad range of prochiral dihydrosilanes can be applied in this intramolecular hydrosilylation of alkenes, efficiently affording a unique class of silicon-stereogenic hydrosilanes **50** in enantioenriched form that are really difficult to be synthesized by other catalysts. The high enantioselectivity is proved to be induced through  $\sigma$ -bond metathesis between an Sc–alkyl bond and a Si–H bond in a prochiral dihydrosilane, in contrast to classic late-transition-metal-involving hydrosilylation reaction mechanisms.

## 2.7 Cu-catalyzed hydrosilylation of alkenes

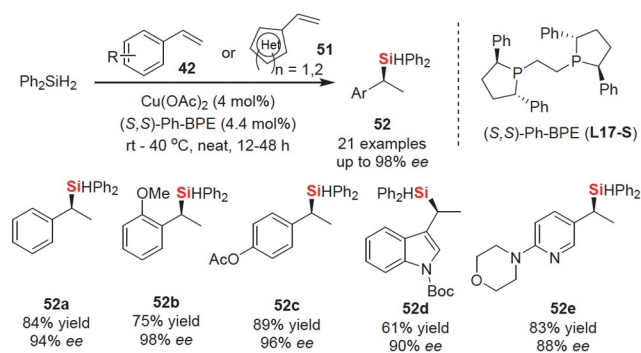
The past decade witnessed numerous and significant progress toward the use of copper catalyst in the hydrosilylation of carbonyl compounds [65]. However, in the copper-catalyzed hydrosilylation of alkenes, the reduction process generally occurred and the silicon–carbon bond-forming hydrosilylation was rare.

In 2017, Buchwald group [66] reported the first example of asymmetric copper-catalyzed Markovnikov-type selective hydrosilylation of vinylarenes and vinyl heterocycles with Ph<sub>2</sub>SiH<sub>2</sub> (Scheme 20). This CuH catalysis exhibited a broad substrate scope and enabled both the enantioselective synthesis of isolable monohydrosilanes **52** and the conversion of crude products to chiral alcohols when PhSiH<sub>3</sub> was used as a hydrosilane. DFT calculations supported that the reaction mechanism proceeded by hydrocupration and then followed by  $\sigma$ -bond metathesis with the hydrosilane (Figure 4).

Very recently, You and co-workers [67] reported an enantioselective Cu(OAc)<sub>2</sub>-catalyzed hydrosilylation of 1,2-dihydroquinolines **53** with hydrosilanes (Ph<sub>2</sub>SiH<sub>2</sub> or PhSiH<sub>3</sub>)



**Scheme 19** Scandium-catalyzed hydrosilylation of alkenes to access silicon-stereogenic centers (color online).



**Scheme 20** Copper-catalyzed hydrosilylation of alkenes (color online).

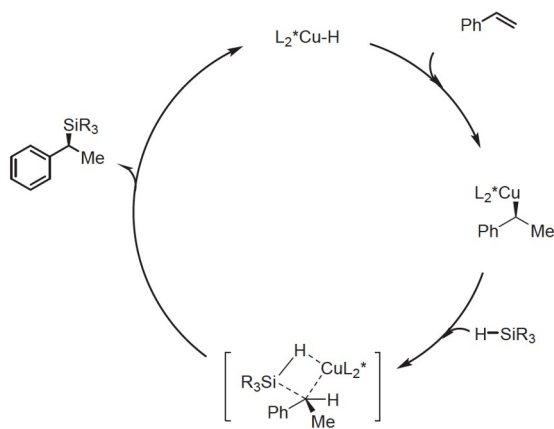
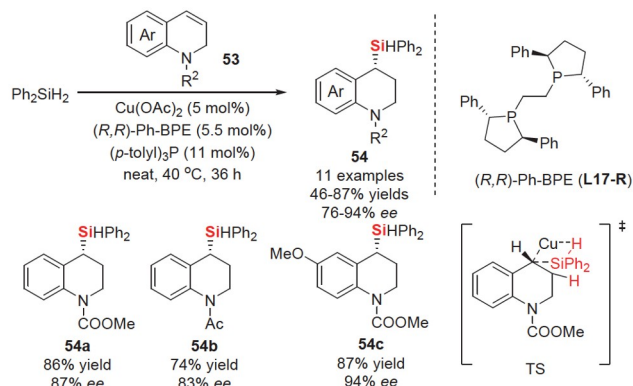


**Figure 4** The proposed mechanism for copper-catalyzed hydrosilylation of alkenes.

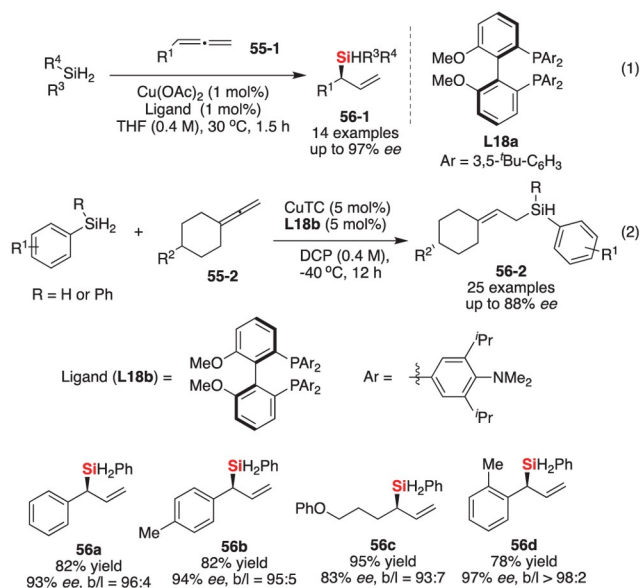
with the aid of both chiral (*R,R*)-Ph-BPE (**L17-R**) and (*p*-tolyl)<sub>3</sub>P. The presence of racemic P-ligand could accelerate the reaction to give a higher yield from 56% to 86% without the loss of enantioselectivity (**Scheme 21**). Similarly to Buchwald's copper catalysis, the mechanistic studies showed that the ligated copper hydride (LCuH) might be generated *in situ* from the Cu(OAc)<sub>2</sub>, the P-ligand (L) and diphenylsilane. The activated species was then inserted into 1,2-dihydroquinoline with the formation of a copper intermediate



**Scheme 21** Copper-catalyzed hydrosilylation of 1,2-dihydroquinolines (color online).

bearing a stereogenic center with a C–Cu bond. Subsequent stereoretentive *s*-metathesis between active copper species and another diphenylsilane resulted in the desired product and the regeneration of LCuH for the next catalytic cycles.

Very recently, Xu and co-workers [68a] determined a copper-catalyzed regiodivergent hydrosilylation of simple allenes **55** with aryl silanes (ArSiH<sub>3</sub>) and an unprecedented asymmetric version, which gave a wide range of linear allylsilanes by CuTC (copper(I) thiophene-2-carboxylate) in dichloromethane (DCM) and branched allylsilanes by Cu(OAc)<sub>2</sub> in tetrahydrofuran (THF) (Eq. (1) in **Scheme 22**). In addition, the corresponding branched allylsilanes **56** could be obtained with high regio- and enantioselectivity (*b/l* = 90:10 to >98:2 and *ee* = 82%–97%) with the aid of chiral bisphosphine ligand **L18a** [(*R*)-3,5-*t*-Bu-MeOBIPHEP]. It should be noted that substituted aryl allenes exhibited high reactivity to form the corresponding allylsilanes with high regio- and enantioselectivities (91%–95% *ee*), while aliphatic allenes resulted in the desired products in good yields but with slightly decreased enantioselectivities (82%–86% *ee*). Furthermore, except for PhSiH<sub>3</sub>, other hydrosilanes including *n*-C<sub>8</sub>H<sub>17</sub>SiH<sub>3</sub>, diethylsilane (Et<sub>2</sub>SiH<sub>2</sub>), and diphenylsilane (Ph<sub>2</sub>SiH<sub>2</sub>) were found to be an inactive substrate to form the desired allylsilanes. The specific activation of phenylsilane by copper catalyst further revealed the distinguished reactivity of the Si–H bond on different hydrosilanes leading to an exciting and challenging choice of matching catalysts and hydrosilanes in synthetic organosilicon chemistry. In 2022, Xu and co-workers [68b] have further reported an interesting protocol to synthesize axially chiral (cyclohexylidene)ethyl silanes (Eq. (2) in **Scheme 22**) by Cu-catalyzed asymmetric hydrosilylation of 4-substituted vinylidenecyclohexanes with arylsilanes (ArSiH<sub>3</sub> or Ph<sub>2</sub>SiH<sub>2</sub>). Different vinylidenecyclohexanes with aryl substituted and alkyl-substituted groups at *para*-position of cyclohexane ring were tolerated to afford the corresponding silanes in moderate to good yields (56%–90%) and enantioselectivities (34%–88% *ee*). In this protocol, the reactive Cu–H species was proposed as a key



**Scheme 22** Copper-catalyzed hydrosilylation of allenes (color online).

intermediate to coordinate with allenes and then to form an active allylcopper species. And the steric interaction between the R group on the allene and the P–Ar moiety of the ligand on the structure of Cu-allene species is considered to be key factor in the control of the regio- and enantioselectivity of hydrosilylation.

The recent year has witnessed the prosperity of copper catalyzed hydrosilylation. In this context, Zhang and co-workers [69] recently expanded the copper-catalyzed hydrosilylation to the enantioselective synthesis of chiral geminated disilyl and borylsilyl compounds from silyl and boryl alkenes. In the presence of CuTC or Cu(OH)<sub>2</sub> as catalyst (Scheme 23) and Ph-BPE as chiral ligand, the desired geminated Si/B or Si/Si products **57** with various valuable functional groups, such as ester, cyano, amide and heterocyclic groups, could be afforded with good enantioselectivities (87%–99% ee). Importantly, the synthetic application of the corresponding product from copper-catalyzed hydrosilylation has been well illustrated by downstream transformations in this work.

## 2.8 Ni-catalyzed hydrosilylation of gem-difluoroalkenes

Although nickel salts and their complexes have long been considered as the catalyst in alkene hydrosilylation, these reaction systems suffered from narrow substrate scope, low yield or harsh reaction conditions [70]. Thus the development of effective ligands for nickel-catalyzed hydrosilylation has become one of the active areas of research [71].

Interestingly, the first example of asymmetric version of nickel-catalyzed alkene hydrosilylation was not found until

2022. In this case, Bai and Chang *et al.* [72] developed an enantioselective nickel(0)-catalyzed hydrosilylation of *gem*-difluoroalkenes with dihydrosilanes to afford chiral  $\alpha$ -difluoromethylsilanes **58** with moderate to good yields (42%–99%) in good to excellent enantioselectivity (71%–96% ee). The nickel-catalyzed hydrosilylation featured with a broad substrate scope and good regio- and stereoselectivity, demonstrating the considerable potential for silyl modifications of bioactive molecules introduced with a *gem*-difluoroalkene moiety. Among these, some special substrates, such as the 6-chloropyridin-3-yl substituted *gem*-difluoroalkene, were not suitable for this reaction because they are found to be unreactive but with starting materials recovered. The reaction of 1,1-difluoro-4-phenyl-1-butene gave complex products with only 11% yield of the diphenyl(4-phenylbutyl)silane, presumably due to the competitive and unavoidable  $\beta$ -F elimination process. Mechanistic studies, including controlled experiments, linear effects and deuterium-labeling studies, have been performed to support that the Si–C bond-forming process but not Si–H bond activation might be the rate-determining step (Scheme 24). Notably, the additives combined with anisidine and B(C<sub>6</sub>F<sub>5</sub>)<sub>3</sub> might form a frustrated Lewis pair to accelerate the Si–H bond activation and subsequent oxidative addition of Ni<sup>0</sup> to the Si–H bond. In addition, the selective insertion of Ni–H species into the *gem*-difluoroalkene to give the chiral  $\alpha$ -difluoromethylated intermediates, owing to the  $\sigma$ -withdrawing-induced effect by difluorine group.

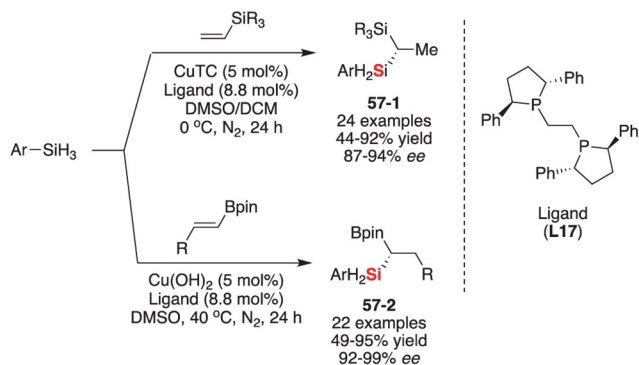
## 3 Asymmetric hydrosilylation of alkynes

Similar to the alkene hydrosilylation, catalytic hydrosilylation of alkynes is one of the most efficient processes for preparing vinylsilane derivatives with 100% atomic economy [73]. In the past decades, continuous studies on the control of selectivity, including regio- and stereoselectivity, which is one of the critical problems of Hydrosilylation [74], promoted the development of enantioselective Si–H bond functionalization.

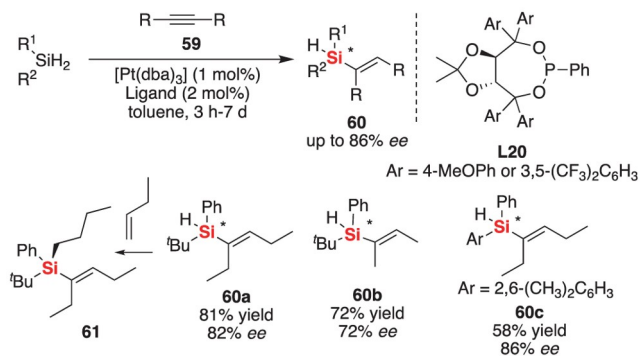
### 3.1 Pt-catalyzed hydrosilylation of internal alkynes

Due to their high catalytic performance, platinum complexes (such as Karstedt catalyst) are still the most important metal catalysts for the hydrosilylation in industrial processes [75]. However, the development of enantioselective platinum-catalyzed hydrosilylation of alkynes is a challenging topic in the past years, some efforts to explore the new ligands for the enantioselective version of platinum catalysis in Xu groups [76] revealed the deficient control in enantioselectivity during the enantioselective Si–H bond activation.

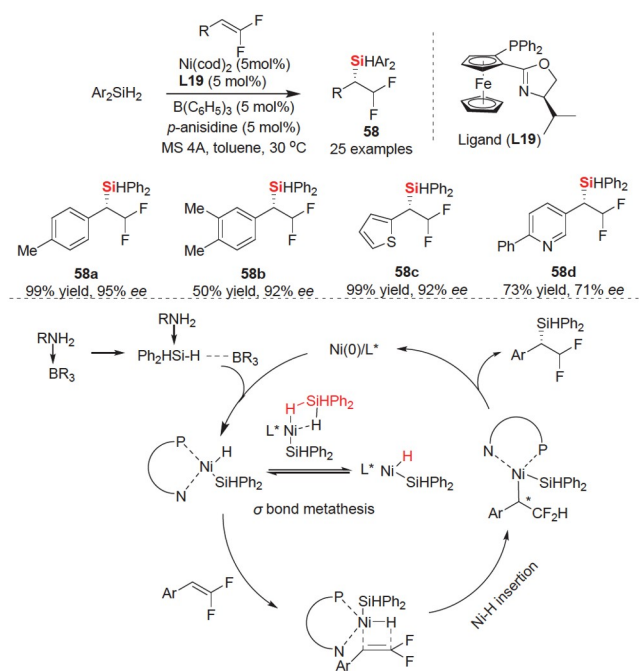
The first example of platinum-catalyzed asymmetric



**Scheme 23** Copper-catalyzed hydrosilylation of silyl or boryl alkene (color online).



**Scheme 25** Platinum-catalyzed asymmetric hydrosilylation of symmetric alkynes (color online).



**Scheme 24** Nickel-catalyzed hydrosilylation of *gem*-difluoroalkenes to access difluoromethylsilanes (color online).

hydrosilylation of alkynes **59** was reported in 2012 by Tomooka and co-workers [77], in which they found a catalytic asymmetric transformation of dihydrosilanes based on Pt(0)-catalyzed desymmetric hydrosilylation of alkynes with the aid of TADDOL-derived phosphonite ligands (Scheme 25). Although the enantioselectivity of present reaction was not excellent enough (up to 86% *ee*), this method afforded a facile process for catalytic synthesis of silicon-stereogenic alkenylhydrosilanes **60** that are synthetically valuable silicon-containing building blocks.

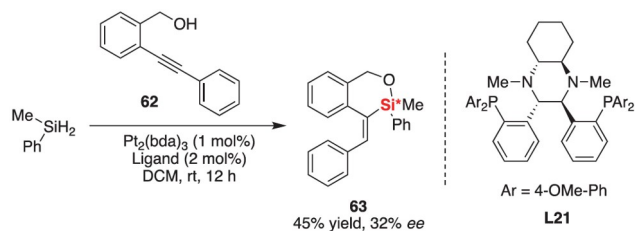
Although it is difficult to control the platinum-catalyzed desymmetrization of MePhSiH<sub>2</sub> in hydrosilylation, Xu and co-workers [78,79] screened their multifunctional P-ligands and found that their Fei-Phos and its analogues **L21** exhibited promising ability in enantioselective induction, leading to the formation of silicon-stereogenic oxasilane **63**

with up to 32% *ee* (Scheme 26). These preliminary explorations into asymmetric platinum catalysis have opened up an alternative pathway to enantioselective silicon-hydrogen bond functionalization, which has previously had limited success.

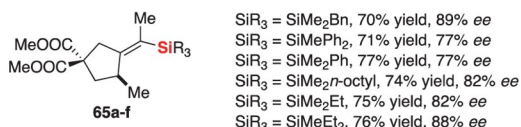
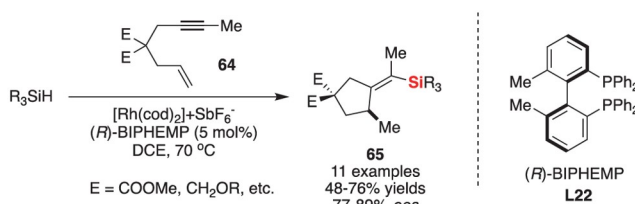
### 3.2 Rh-catalyzed hydrosilylation of internal alkynes

Similar to the alkene hydrosilylation, a series of rhodium catalyst systems were proved to be effective with good chemoselectivity in hydrosilylation of alkynes [80]. However, it is difficult to construct stereocenter in the hydrosilylation of general alkynes. Accordingly, the hydrosilylation-initiated cyclization of enynes might provide a direct platform to realize enantioselective silicon-hydrogen functionalization. For example, Widenhofer group [81] has presented another example of enantioselective cationic rhodium (*R*)-BIPHEMP complex -promoted enyne cyclization/hydrosilylation with various hydrosilanes. The silylated alkylidene cyclopentanes **65** were achieved with 70%–76% yields and 77%–89% *ee* (Scheme 27), which revealed that oxidative addition of the H–Si bond of the hydrosilane to Rh(I) species worked well in the presence of tertiary hydrosilanes. However, there is no additional data for the reaction results with other hydrosilanes, including dihydrosilanes.

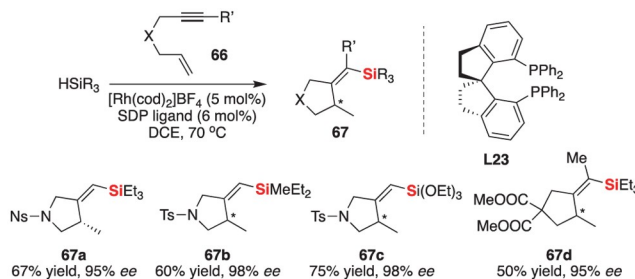
Subsequently, Zhou and co-workers [82] have developed an efficient rhodium complex based on their spiro diphosphine SDP **L23** for the catalytic asymmetric silylcyclization of 1,6-enynes **66** (Scheme 28). In this work, a series of hydrosilanes were used in this silylcyclization reaction of 1,6-enyne under the optimized reaction conditions. It was found that both trialkylsilanes (HSiR<sub>3</sub>) and trialkoxysilanes (HSi(OR)<sub>3</sub>) could serve as suitable hydrosilanes (>93% *ee*), although other hydrosilanes with phenyl groups give slightly lower enantioselectivities (89% *ee*). In addition, only a trace amount of silylcyclization product was obtained when hydrosilanes containing bulky alkyl groups (such as *i*-Pr<sub>3</sub>SiH) are used. The use of excess amount of hydrosilane is necessary to limit the dimerization of 1,6-enynes and other side reactions.



**Scheme 26** Platinum-catalyzed intramolecular hydrosilylation to access silicon-stereogenic center (color online).

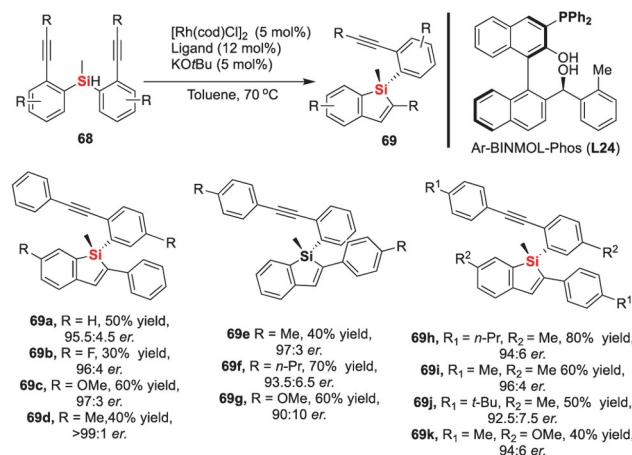


**Scheme 27** Rhodium-catalyzed asymmetric cyclization/hydrosilylation of enyne (color online).



**Scheme 28** Enantioselective Rh-catalyzed hydrosilylation-initiated cyclization of 1,6-enynes (color online).

Although the catalytic asymmetric hydrosilylation of alkenes based on desymmetrization has been achieved successfully to construct silicon-stereogenic center, the desymmetric hydrosilylation of Si-tethered bisalkynes was not reported until 2020. In this context, enantioselective control of intermolecular hydrosilylation of alkynes with prochiral hydrosilanes to provide silicon-stereogenic silanes is really a challenging task. In 2020, Xu group [83] accomplished a highly enantioselective Rh-catalyzed intramolecular hydrosilylation of silicon-tethered bisalkynes **68**, which provided a direct and practical approach to the construction of silicon-stereogenic benzosiloles **69** that are AIE and CPL-active molecules. It should be noted that only their newly developed multifunctional ligand, chiral Ar-BINMOL-Phos **L24** with hydrogen-bond donors, could be efficiently used as a P-ligand in the desymmetrization of silicon-tethered bisalkynes (Scheme 29). With the Rh/Ar-

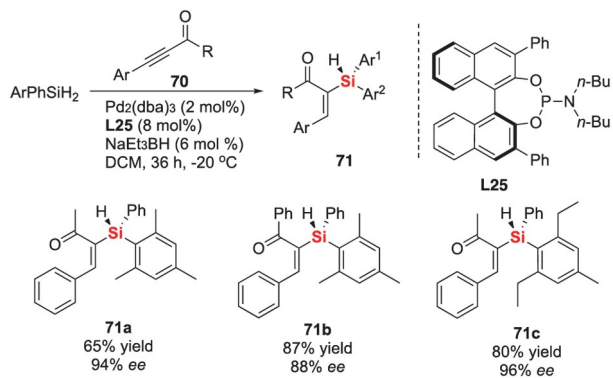


**Scheme 29** Enantioselective Rh-catalyzed hydrosilylation of bisalkynes (color online).

BINMOL-Phos catalyst system under the optimal reaction conditions, the reaction is operationally robust and 100% atom-economy with good functional group tolerability as well as high enantioselectivity (up to >99:1 er). More specially, the use of the  $\text{KOtBu}$  as the basic additive is crucial to maintaining excellent enantioselectivity in this reaction because the catalytic amount  $\text{KOtBu}$  might be responsible for the formation of an active Rh complex.

### 3.3 Pd-catalyzed hydrosilylation of ynones

Most of palladium-catalyzed hydrosilylation to date largely focused on generation of carbon-stereogenic centers [84], and the straightforward and enantioselective construction of silicon-stereogenic centers by palladium-catalyzed hydrosilylation presented a challenge due to a shortage of effective chiral ligand with high level of enantioselective induction. In 2021, Xu and co-workers [85] reported an unprecedented example of palladium-catalyzed hydrosilylation of ynones **70** that could be applied in the highly efficient construction of enantioenriched silicon-stereogenic compounds (Scheme 30). In this reaction, the newly developed P-ligand **L25** made the stereospecific Si-H activation to afford a series of silicon-stereogenic silylenones **71** with up to 94% yield, and good enantioselectivity (96% ee) as well as high regioselectivity (>20:1 *rr*). It is the first example for the enantioselective synthesis of silicon-stereogenic silylenones through hydrosilylation of ynones. In this work, the DFT calculations were also conducted to elucidate the mechanism of selective palladium-catalyzed hydrosilylation reaction of dihydrosilanes as well as the origin of high degree of stereoselectivity. The mechanistic studies showed that both the regioselectivity and enantioselectivity were determined in the step of oxidative hydrometallation (Figure 5). In the key step, the oxidative addition of  $\text{ArPhSiH}_2$  and hydride transfer to the triple bond of ynone took place concertedly via a four-



**Scheme 30** Pd-catalyzed hydrosilylation of ynones for the enantioselective construction of silicon-stereogenic center (color online).

membered square planar Pd(II) complex, in which the chiral ligand played a crucial role in the stereocontrol addition due to the powerful potential of aromatic interaction in this reaction that is highlighted by the multiple C–H- $\pi$  interaction and aromatic cavity-oriented desymmetric functionalization of Si–H bond in the enantioselectivity-determining step. The Pd complex with chiral binaphthyl-phosphoramidite has the ability to differentiate between unsymmetrical substituent groups on hydrosilanes due to the chiral microenvironment constructed by the interaction between the palladium catalyst and the substrates through aromatic interactions. This guarantees the asymmetric activation of Si–H bond on hydrosilanes during the hydrosilylation of ynones.

### 3.4 Co-catalyzed hydrosilylation of alkynes

Cobalt-catalyzed alkyne hydrosilylation is a powerful pro-

cess to construct vinylsilanes and chiral silanes [86]. As one of the earth-abundant transition metal catalysts, the development of asymmetric cobalt-catalyzed hydrosilylation of alkynes is a very important task with potential applications in organosilicon chemistry. In this regard, asymmetric cobalt-catalyzed hydrosilylation reaction of alkynes has no promising breakthrough until 2017. While developing asymmetric cobalt-catalyzed alkene hydrosilylation, Lu and co-workers [87] developed a novel regio- and enantioselective cobalt-catalyzed one-pot hydrosilylation/hydrogenation of alkynes to give structurally diverse chiral silanes and silicon-containing chiral compounds (Scheme 31). In this reaction, various aryl alkynes bearing electron-donating or -withdrawing substituents on the phenyl ring were tolerated, in which the corresponding products **72** were achieved with good to excellent *ee* values (up to >99% *ee*). The mechanistic studies demonstrated that the regioselectivity might be controlled by the alkyne hydrosilylation step and the enantioselective induction occurred in the step of asymmetric hydrogenation of the corresponding vinyl silanes (Figure 6) [88].

Huang and co-workers [89] have developed an efficient and stereoselective method for the catalytic asymmetric construction of silicon-stereogenic vinylhydrosilanes **73** with high *ee* (up to 91% *ee*) that is based on a new cobalt/PyBox complex (**C5**)-catalyzed hydrosilylations of prochiral dihydrosilanes with alkyne (Scheme 32). In addition, the reactions proceeded as Markovnikov mode with high regioselectivities for terminal arylalkynes. Notably, this is an elegant example for alkyne hydrosilylation reaction with dihydrosilanes that occurs with high chemo-, regio- and

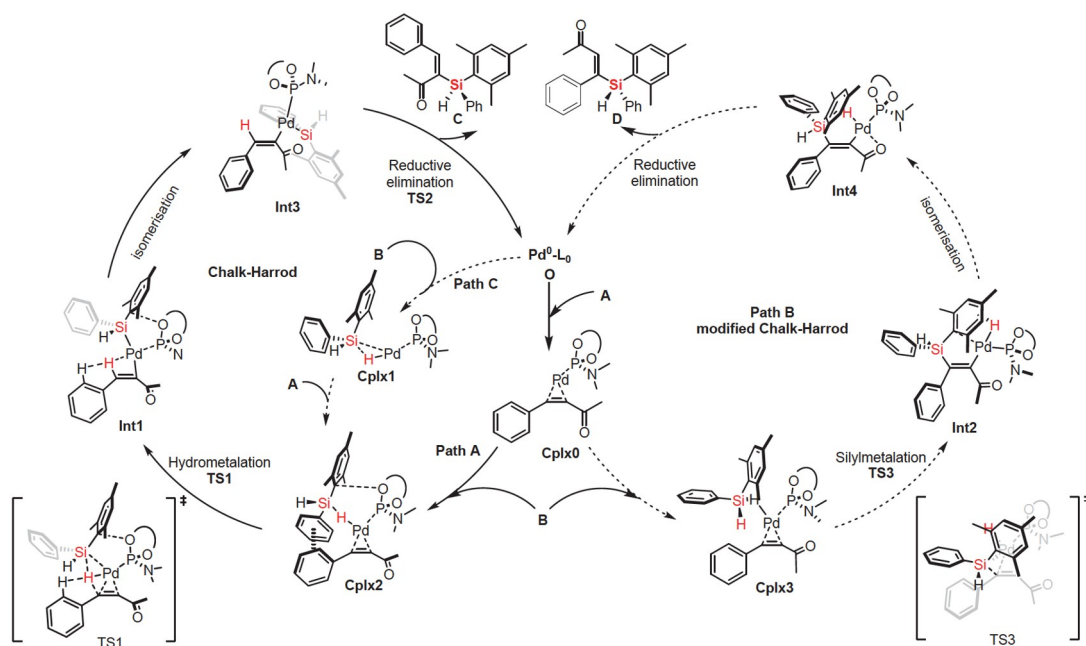
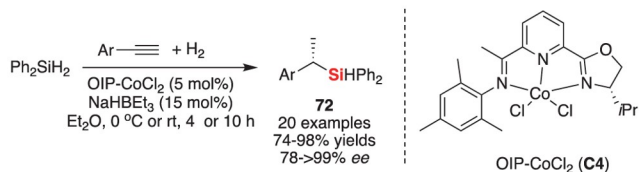
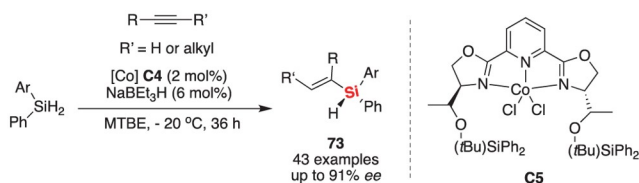


**Figure 5** Reaction mechanism for Pd-catalyzed hydrosilylation of ynones (color online).





**Scheme 31** Enantioselective Co-catalyzed hydrosilylation/hydrogenation of alkynes (color online).



**Scheme 32** Desymmetrization of prochiral silanes by Co-catalyzed hydrosilylation (color online).

enantioselectivity.

Lu and co-workers [90] recently developed a highly enantioselective cobalt complex (C6)-catalyzed sequential double hydrosilylation of aliphatic alkynes to synthesize enantioenriched *gem*-bis(silyl)alkanes **74** from two different hydrosilanes (Scheme 33). This protocol featured with high chemo-, regio-, and enantioselectivity to construct valuable chiral *gem*-bis(silyl)alkanes **74** through three-component

tandem hydrosilylation of simple aliphatic alkynes, trihydrosilanes (PhSiH<sub>3</sub>) and dihydrosilanes (Ar<sub>2</sub>SiH<sub>2</sub>). In addition, the mechanistic studies, including control experiments, kinetic studies, isotopic labeling experiments, and DFT calculations revealed that the CoBr<sub>2</sub>·Xantphos catalyzed hydrosilylation of alkynes with Ph<sub>2</sub>SiH<sub>2</sub> is quite fast to give vinylsilane intermediates that could further react with PhSiH<sub>3</sub>. The rate-determining step (RDS) is the vinylsilane-based coordination and insertion process. Notably, the synthetic versatility of *gem*-bis(silyl)alkanes bearing two different Si-H moieties was demonstrated by hydrolysis and new Si-C bond-forming process, which could be not only used in the clarification of the different reactivity of dihydrosilanes and monohydrosilanes, but also useful for the synthesis of chiral organosilanols **75** and **76**, α-hydroxysilanes, and chiral *gem*-bis(silyl)alkanes **78** containing adjacent C-stereocenter and Si-stereocenter.

Very recently, Song and co-workers [91] found that the product of hydrosilylation of alkyne with dihydrosilane was a reactive intermediate for the hydroboration, in which this protocol could be used in the enantioselective construction of chiral 1,1-silylboryl alkanes **79** in the presence of (*R,S*)-Joisphos **L26** (Scheme 34). Notably, reaction enantioselectivity for the alkynes with aliphatic chains was relatively insensitive to structural variation, and such a type of alkynes could be smoothly converted to enantioenriched 1,1-si-

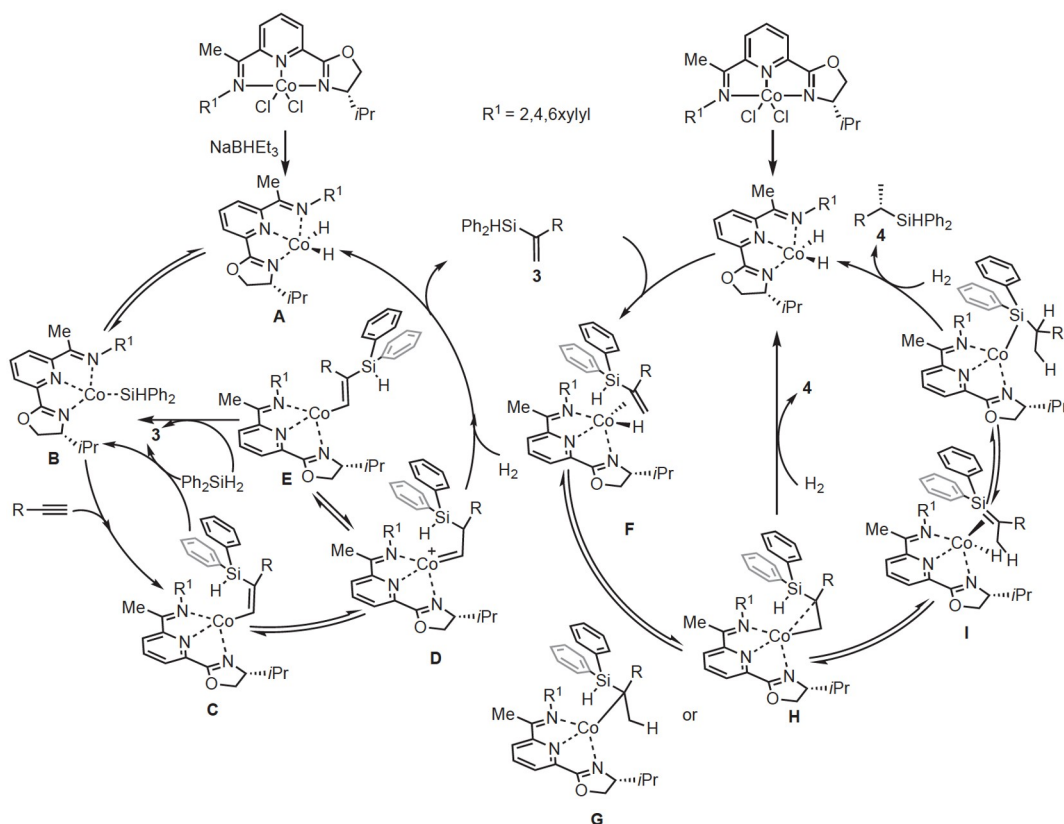
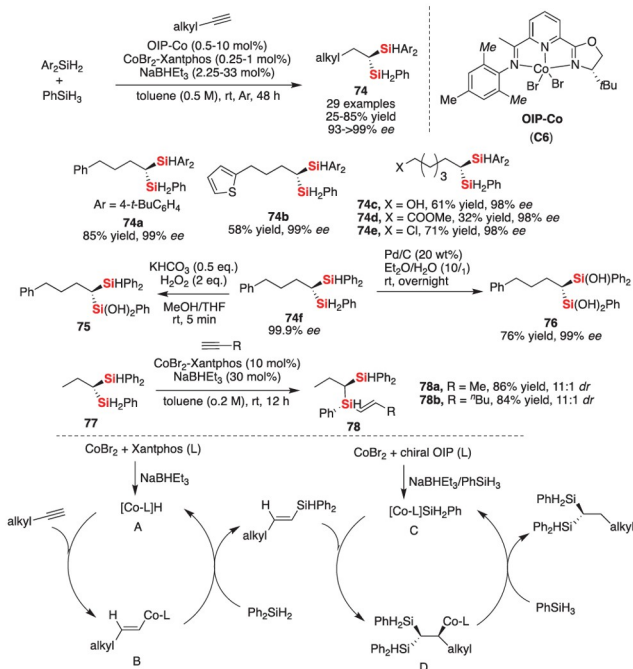
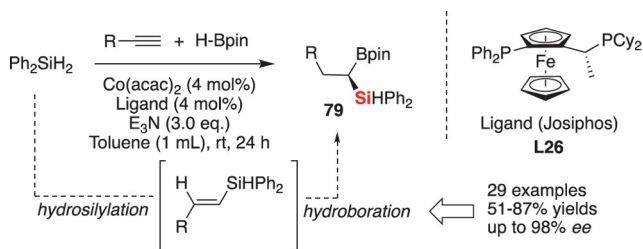


**Figure 6** Reaction mechanism for the cobalt-catalyzed hydrosilylation.



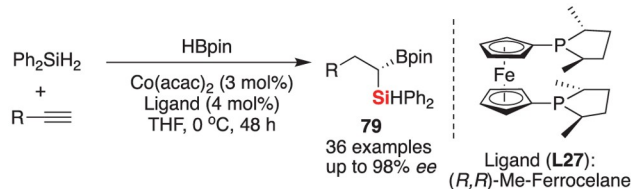
**Scheme 33** Cobalt-catalyzed sequential double hydrosilylation of alkynes with two different hydrosilanes (color online).



**Scheme 34** Enantioselective cobalt-catalyzed cascade hydrosilylation and hydroboration of alkynes (color online).

ylboryl alkanes with good yields and excellent enantioselectivity. However, the substituent on the aromatic ring of aryl alkynes exhibited obvious effect on the enantioselectivity. For example, the aryl alkynes with *para*- or *meta*-substituted OMe on the aromatic ring led to excellent *ee* value (96%–99% *ee*), but only 32% *ee* of the corresponding product was achieved when *i*-Pr or *t*-Bu was on the *para*-position of aryl alkynes.

Almost at the same time, Ge and co-workers [92] reported a highly enantioselective cobalt-catalyzed one-pot hydrosilylation/hydroboration of terminal alkynes through a chiral cobalt catalyst generated from Co(acac)<sub>2</sub> and (*R,R*)-Me-Ferrocene **L27** (Scheme 35). In this reaction, a variety of terminal alkynes could undergo one-pot hydrosilylation and enantioselective hydroboration, affording the corresponding *gem*-(borylsilyl)alkane products **79** with good yields and excellent enantioselectivity (up to 98% *ee*). This protocol further represented the most straightforward approach developed independently by Song's and Ge's groups who

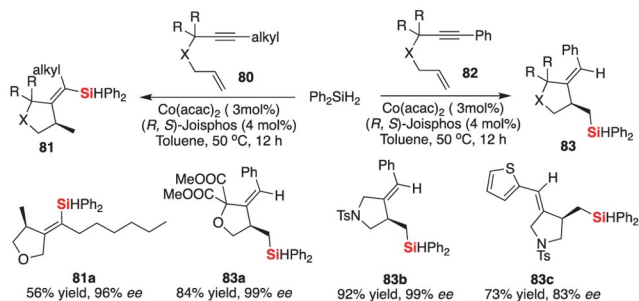


**Scheme 35** Enantioselective cobalt-catalyzed cascade hydrosilylation and hydroboration of alkynes (color online).

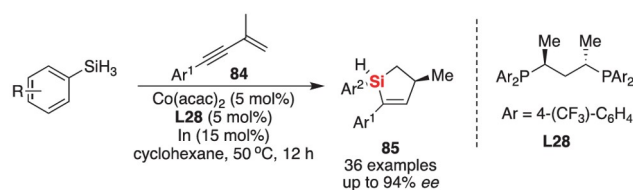
provided a well-defined cobalt catalyst to access versatile chiral *gem*-(borylsilyl)alkanes from readily available alkynes and commercially available diphenylsilane.

Ge and co-workers [93] have recently developed an enantioselective CoH-initiated cyclization protocol for the synthesis of silyl-functionalized chiral heterocycle compounds, in which a variety of carbon-, oxygen-, and nitrogen-tethered 1,6-enynes **80** reacted smoothly with secondary or tertiary hydrosilanes by cobalt-catalyzed hydrosilylation/cyclization (Scheme 36). The chiral cobalt complex generated *in situ* from Co(acac)<sub>2</sub> and (*R,S*)-Josiphos was found to be highly effective for the synthesis of corresponding alkylsilane products in good yields and excellent enantioselectivity. Interestingly, the Co-catalyzed hydrosilylation/cyclization of alkyl-substituted 1,6-enynes **80** resulted into chiral vinylsilane products **81** with high enantioselectivity, in which the product was different from Co-catalyzed hydrosilylation/cyclization of aryl-substituted 1,6-enynes **82**. Mechanistic studies suggest that the chelation of 1,6-enyne to the Co complex and the subsequent hydrocobaltation controlled the regioselectivity of this catalytic asymmetric hydrosilylation/cyclization reaction to give different products. Notably and very recently, Lu and co-workers [94] reported a similar strategy for sequential hydrosilylation/hydrohydrazidation of terminal alkynes with hydrosilanes and diazo compounds to afford 1,2-N, Si compounds by cobalt/Xantphos/tridentate anionic N-ligand catalyst system. Specifically, it was found that Ph<sub>2</sub>SiH<sub>2</sub> was proved to be an effective hydride donor in the palladium-catalyzed bicyclization of enynes, whereas PhSiH<sub>3</sub> and Et<sub>2</sub>SiH<sub>2</sub> were less effective in this reaction because of their different reactivities [95].

Cascade hydrosilylation reactions, in which two Si–H bonds on hydrosilanes are sequentially added to a single alkyne, olefin, enynes, or other unsaturated molecules with high chemo- and stereo-selectivity, remain rare [96]. Very recently, Meng and co-workers [97] developed a new protocol for catalytic chemo- and enantio-selective hydrosilylation of 1,3- and 1,4-enynes promoted by chiral phosphine (**L28**)–Co complexes (Scheme 37). Under the optimized reaction conditions, diverse and unique reaction pathways could be accurately tuned by a chiral bisphosphine ligand **L28** bearing electron-deficient CF<sub>3</sub> group on *para*-position of the phenyl ring. In this reaction, a wide range of



**Scheme 36** Enantioselective Co-catalyzed hydrosilylation of 1,6-enynes (color online).



**Scheme 37** Enantioselective Co-catalyzed hydrosilylation of enynes (color online).

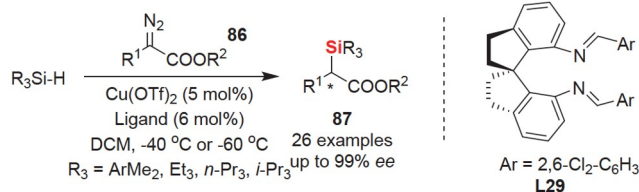
Si-stereogenic alkenylsilanes **85** and its further functionalization of the stereogenic Si–H bond were achieved in high efficiency and stereoselectivity.

## 4 Asymmetric carbene Si–H bond insertion

The catalytic carbene Si–H insertion reaction of diazo compounds is a very powerful organic transformation due to the environmentally benign and highly synthetic potential of the generated Si-based building blocks [98]. In the past few decades, various synthetic methods using diverse metal catalysts have been developed sharing the common aim to explore new reaction processes and enhance the enantioselectivity of these Si–H bond insertion reactions [99]. This review focuses on the recent advancements made in the past decade in catalytic asymmetric carbene Si–H bond insertion reactions.

### 4.1 Cu-catalyzed carbene insertion of Si–H bond of monohydrosilanes

Among various copper catalyst systems, Zhou's method [100,101] could be ranked as an important progress in this reaction, in which they have developed chiral spirodiimine ligands for the determination of a highly enantioselective copper-catalyzed carbenoid insertion into Si–H bonds (Scheme 38). By using this copper/Schiff base (L29) catalyst system, a wide range of  $\alpha$ -aryl silylestere were produced in excellent yields (85%–97%) and enantioselectivities (90%–99% *ee*). Notably, the  $\alpha$ -aryl group in the diazoester substrate was vital for obtaining good reaction results. For example,



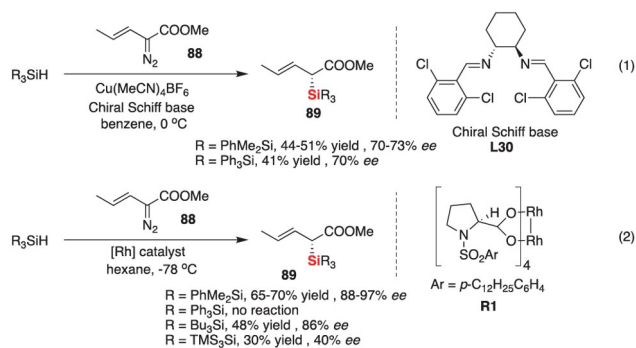
**Scheme 38** Copper-catalyzed carbene insertion of Si–H bond (color online).

the reactions of methyl  $\alpha$ -diazopropionate with  $\text{PhMe}_2\text{SiH}$  or (*o*-Tol)- $\text{Me}_2\text{SiH}$  resulted into very low yields and *ee* values (<60% yield and <35% *ee*). Similarly, the Si–H insertion of  $\alpha$ -allyldiazoacetate with  $\text{PhMe}_2\text{SiH}$  afforded a complicated mixture of products. In addition, similarly to the classic method reported by Panek and Stavropoulos *et al.* [102], 2,6-dichlorophenyl moiety on the Schiff base ligand played an obvious enhancement of enantioselectivity in comparison to that with other aryl backbones.

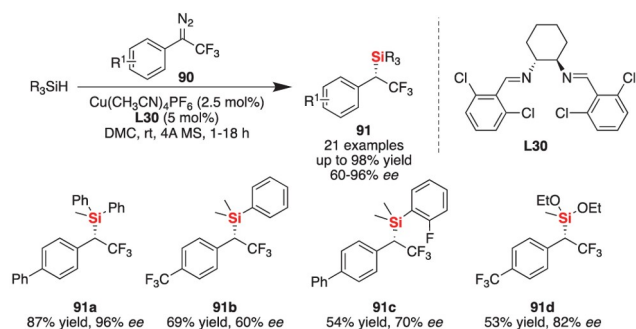
Later, Panek and co-workers [103] have extended the use of Jacobsen's chiral copper(I) diimine complexes derived from ligand L30 to carbene insertions of hydrosilanes with diazovinylacetates, resulting in the formation of enantiomeric excess crotylsilanes **89** bearing carbon-centered chirality with 70%–73% *ee*. In addition, the authors also carried out additional experiments to allow a comparison of chiral Cu(I) (Eq. (1) in Scheme 39) vs. Rh(II) catalysis (Eq. (2) in Scheme 39). For example, when  $\text{Rh}_2(\text{S-DOSP})_4$  (**R1**) was used as a chiral catalyst, comparable selectivity was achieved with *n*- $\text{Bu}_3\text{SiH}$  compared with  $\text{Me}_2\text{PhSiH}$ , while the use of  $\text{Ph}_3\text{SiH}$  and  $\text{TMS}_3\text{SiH}$  resulted into low yield and poor enantioselectivity. Therefore, the different chemical structures or physical properties of hydrosilanes is an important parameter in this reaction.

Inspired by previous reports on the copper catalysis, Ollivier and co-workers [104] developed a catalytic asymmetric Si–H insertion reaction of 1-aryl-2,2,2-trifluoro-1-diazoethanes **90** (Scheme 40). Similarly to previous work [105], it was found that the bis((2,6-dichlorobenzylidene)diimino)cyclohexane exhibited good activity and enantiocontrol in the Si–H insertion reaction to give up to 98% yields and up to 96% *ee*.

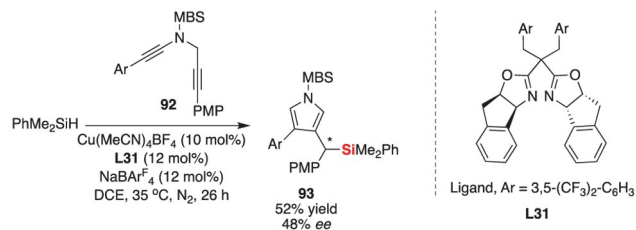
Different from previously used diazo compounds for the Si–H bond insertion reaction, Ye and co-workers [106] reported an efficient Cu-catalyzed synthesis of 4-silyl-substituted pyrroles **93** from *N*-propargyl ynamides **92** via Si–H bond insertion reaction of hydrosilanes (Scheme 41). In particular, the asymmetric copper-catalyzed Si–H bond insertion reaction of *N*-propargyl ynamides **92** was also investigated by screening of various chiral ligands, including bis(oxazoline) ligands and biphosphine ligands, which disclosed that the chiral copper/Box (L31) complex-catalyzed Si–H bond insertion reaction of *N*-propargyl ynamide with



**Scheme 39** The difference in copper and rhodium-catalyzed carbene insertion reaction of Si-H bond (color online).



**Scheme 40** Copper-catalyzed carbene insertion reaction of Si-H bond (color online).

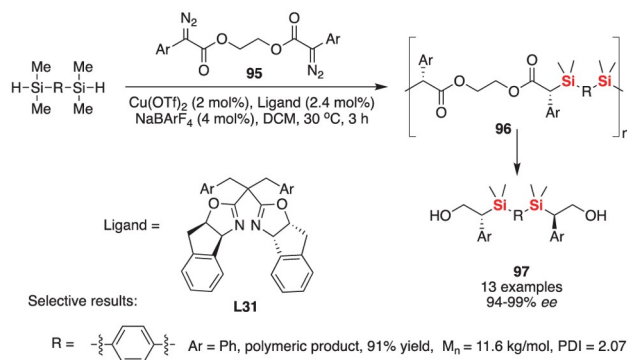


**Scheme 41** Copper-catalyzed synthesis of 4-silyl-substituted pyrroles from  $N$ -propargyl ynamides via Si-H bond insertion reaction of hydrosilanes (color online).

$PhMe_2SiH$  resulted into the desired silylpyrrole product **93** in 52% yield and promising enantioselectivity (48% ee).

Very recently, Zhou and Wu *et al.* [107] demonstrated the application of asymmetric Cu-catalyzed Si-H insertion of diazocarbonyl compounds **95** with hydrosilanes in polymeric condensation to synthesize a series of optically active silicon-linked polyesters **96** (up to 99% yield, 14.6 kg/mol). The resulting chiral polymers with good thermal stability could be transferred into chiral diols **97** by the reduction of DIBAL-H as a reductant, which indirectly revealed its highly enantioselective control in the Si-C bond-forming polycondensation (Scheme 42).

Judging from the previous progress of copper-catalyzed carbene insertion reaction of Si-H bond in recent years, copper catalysts have wide applicability and can be applied



**Scheme 42** Catalytic synthesis of silicon-containing macromolecule via Cu-catalyzed Si-H insertion of diazocarbonyl compounds with hydrosilanes (color online).

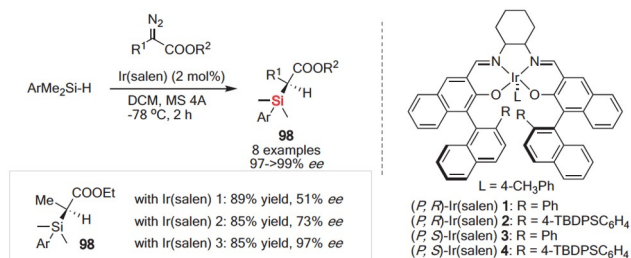
to carbene insertion reactions of various types of diazo compounds and  $N$ -propargyl ynamides, and can also be used in the synthesis of chiral polycarbosilanes. In particular, the copper-based catalyst system is quite suitable for the carbene insertion reaction of monohydrosilanes. At present, there is no report on the carbene insertion reaction-based desymmetriation of dihydrosilanes that can be used for the enantioselective construction of silicon-stereogenic silanes.

## 4.2 Ir-catalyzed carbene insertion of Si-H bond of dihydrosilanes

Iridium is one of the rarest elements in the earth's crust, with an average mass ratio of only 0.001 parts per million (about one-tenth that of platinum). In addition, this element is chemically stable, but still has the promising ability to form coordination compounds, which makes iridium can be used as an effective catalyst in the synthesis of fine chemicals and natural products. For example, iridium complexes can be used to catalyze asymmetric hydrogenation reactions, which is capable of hydrogenating otherwise difficult-to-hydrogenate substrates, such as non-functionalized olefins, to one of their enantiomers. Therefore, the asymmetric catalytic synthesis reaction promoted by iridium has the characteristics that other metals do not have.

In 2010, Katsuki *et al.* [108] have ever examined the Si-H insertion reaction of dimethylphenylsilane and ethyl  $\alpha$ -diazopropionate in the presence of Ir(salen) complex bearing axial and central chirality. The desired Si-H insertion process could occur at -78 °C to give promising enantioselectivities. The chirality matching is an important factor, as the enantioselectivity was moderately by using (*P,R*)-Ir(salen) **1** but significant improvement to 97% ee was achieved by using (*P,S*)-Ir(salen) complex.

As shown in Scheme 43, the Ir(salen) complex-catalyzed Si-H insertion reactions proceeded with good yields and excellent enantioselectivities; however, the central chirality was induced only on the carbon atom during the Si-C bond-



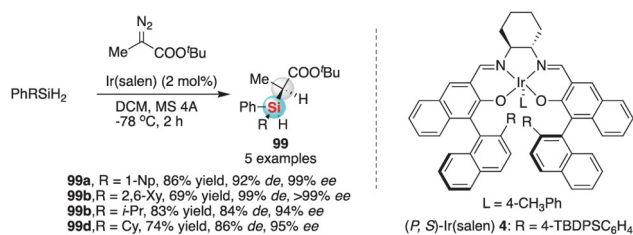
**Scheme 43** Iridium-catalyzed Si-H insertion reaction (color online).

forming process. If the hydrosilane compound is prochiral, additional silicon-stereogenic chirality should also be formed to provide a pair of diastereomers. To explore this possibility, Katsuki *et al.* [108] further examined the Si-H insertion reaction between prochiral (1-naphthyl)phenylsilane with *tert*-butyl  $\alpha$ -diazopropionate (Scheme 44). It is the first example of highly enantioselective Si-H insertion reaction that can give the silicon-stereogenic products **99** with good diastereo- and enantioselectivities. In addition, the study on kinetic isotope effect (KIE) supported the notion that the step of Si-H bond activation is key to the carbenoid Si-H insertion. Subsequently in 2012, Che and co-workers [109] also reported another important example for the Ir-catalyzed Si-H bond insertion reactions featuring high enantio- and diastereo-selectivity as well as high product turnovers with chiral iridium porphyrin as catalyst.

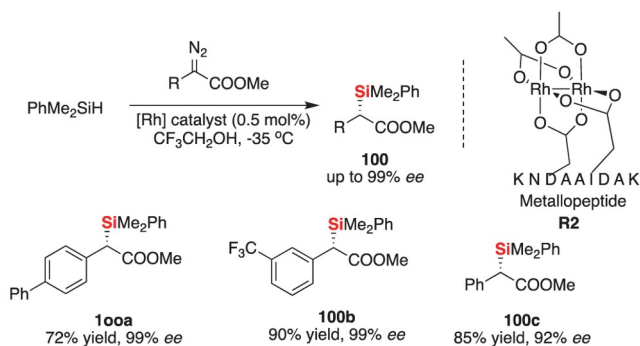
### 4.3 Rh-catalyzed carbene insertion of Si-H bond

Rhodium plays an important role in the asymmetric catalyzed carbene insertion reaction of silicon-hydrogen bond, and it is one of the most successful metal catalyst systems to realize the enantioselective control in this reaction. For example, inspired by their previous findings on the side-chain carboxylates of a peptide as bidentate ligand for dirhodium catalysis [110], Ball and co-workers [111] examined the metallopetide complex from Rh<sub>2</sub>(OAc)<sub>2</sub> and a chelating bis-carboxylate peptide ligand for the asymmetric insertion of diazoacetates into Si-H bond of PhMe<sub>2</sub>SiH (Scheme 45). In this work, the authors determined that the generation of a small peptide library (>22 examples) allowed structural optimization of peptide sequence and produced an efficient dirhodium catalyst **R2** for enantioselective carbenoid insertion into Si-H bonds (99% *ee* and 90% yield).

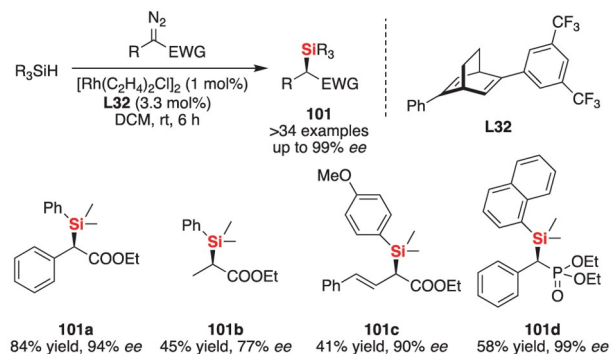
In 2016, Xu and co-workers [112] reported a highly efficient rhodium(I)-catalyzed asymmetric Si-H insertion reaction with the aid of a C<sub>1</sub>-symmetric chiral diene ligand **L32** (Scheme 46). The reaction enabled the asymmetric synthesis of valuable chiral  $\alpha$ -silyl esters and phosphonates **101** from a broad range of substrates, with excellent enantioselectivities under exceptionally mild conditions. Various tertiary hydrosilanes, such as substituted aryl silanes, triethylsilane, and



**Scheme 44** Iridium-catalyzed Si-H insertion reaction to give silicon-stereogenic silanes (color online).



**Scheme 45** Rhodium-catalyzed Si-H insertion reaction (color online).



**Scheme 46** Rhodium-catalyzed Si-H insertion reaction (color online).

tripropylsilane were found to be suitable silicon reagents successfully applied in this *trans*-formation, affording the desired  $\alpha$ -silylesters and its analogues **101** with good to excellent enantioselectivities (up to 99% *ee*). The deuterium-labeling kinetic isotopic studies and DFT calculations showed that the reaction proceeds *via* a concerted, stereospecific Rh(I)-carbene mediated transition state, in which the addition of Si-H bond onto the aromatic interaction-stabilized electrophilic Rh(I) carbenoid intermediate took place preferentially from the unlocked *Re*-face at the site adjacent to electron-withdrawing group and Cl anion to give the *R*-product.

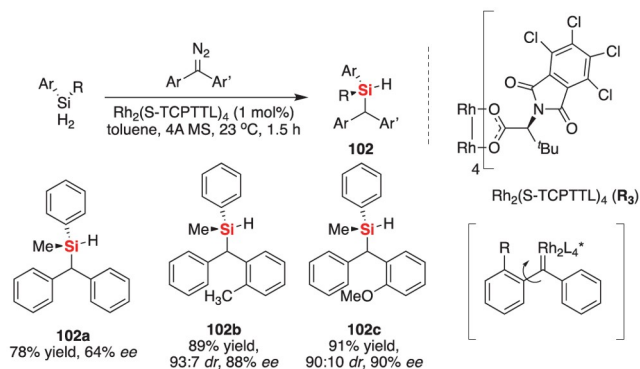
Although the chiral catalyst is able to achieve enantioselective control by discriminating the reactive center of the substrate between two prochiral faces with largely dif-

ferent steric interactions, it is quite difficult to identify prochiral faces of the reactive center when it is attached to two structurally or sterically similar substituents. In 2020, Shaw and Franz *et al.* [113] reported an interesting example of intermolecular and enantioselective diarylcarbene insertion into Si–H bonds of dihydrosilanes for the direct synthesis of silicon-stereogenic hydrosilanes **102** (Scheme 47). It was found that dirhodium(II) carboxylates **R3** could smoothly promote the Si–H insertion to the facile construction of an enantioenriched silicon center with moderate to good *ee* values (42%–90% *ee*) in most cases. The mechanistic studies supported that the Si–H insertion was probably determined as the rate-determining step.

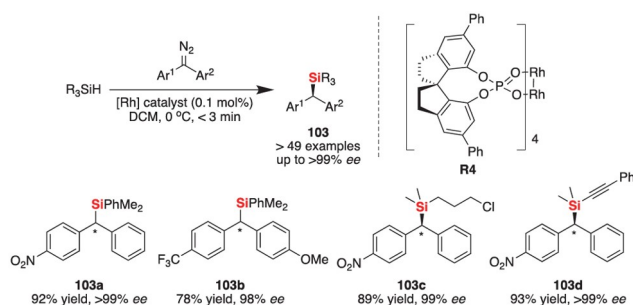
Almost at the same time, Zhou and Zhu *et al.* [114] also independently discovered a carbene Si–H insertion reaction in which the enantioselective control depended primarily on the electronic characteristics of the carbene compound, and it was found that the  $\log(er)$  values were linearly related to Hammett parameters. It showed excellent conversion and enantioselectivity for the diarylcarbene insertion reaction of hydrosilanes by a newly developed chiral tetraphosphate dirhodium catalysts **R4** (Scheme 48). Computational and mechanistic studies showed that the chiral environment of the Rh catalyst could fix the conformations of the transition state for the Si–H bond insertion reaction. And accordingly, the energy difference of the transition states, which is directly related to the enantioselective control of the Si–H insertion reaction, is primarily due to the electronic difference between two aryls of carbene substrate.

Very recently, Zhou and Zhu *et al.* [115] further found the chiral spiro dirhodium phosphate catalyst  $[\text{Rh}_2(\text{SPA})_2]$  was highly effective for catalytic asymmetric insertion of carbene intermediates into Si–H bonds (Scheme 49 and Figure 7). Notably, this Rh catalyst **R5** exhibited a good functional group tolerance, in which this process provided a variety of new chiral organosilanes **105** or **106** with high enantioselectivity from readily available hydrosilanes and alkynyl *N*-trisylhydrazones **104** or  $\alpha$ -aryldiazoacetates **86**. Interestingly, the structure of hydrosilanes also played important effect in this reaction. For example, the use of *i*-Pr<sub>3</sub>SiH, Ph<sub>2</sub>SiH<sub>2</sub>, and (EtO)<sub>3</sub>SiH resulted into complex mixtures and no desired product in Si–H insertion of methyl  $\alpha$ -diazophenylacetate.

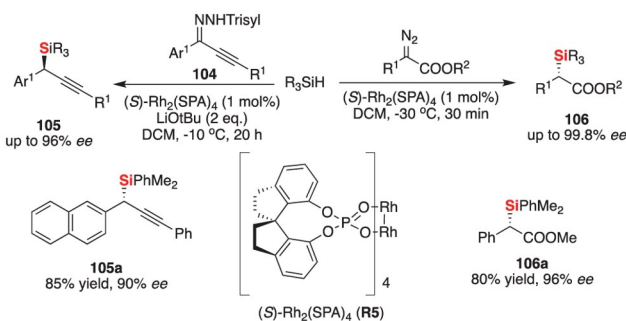
Catalytic asymmetric carbene insertion into Si–H bonds is an important reaction. For preparing chiral organosilicon. However, most of the carbene precursors used in this reaction have always been diazo compounds or its analogues [116]. In 2019, Zhu and co-workers [117] reported a highly efficient rhodium-catalyzed Si–H bond insertion reactions with functionalized alkynes **107** as carbene precursors. With chiral Rh(II) tetracarboxylates as catalysts (Scheme 50), the insertion reactions of carbonyl-ene-yne and various hydrosilanes smoothly resulted into chiral organosilanes **108** in high yields (up to 98%) with a good excellent enantio-



**Scheme 47** Rhodium-catalyzed Si–H insertion reaction for the construction of silicon-stereogenic centers (color online).



**Scheme 48** Dirhodium-catalyzed Si–H insertion reactions (color online).



**Scheme 49** Catalytic asymmetric insertion of carbene intermediates into Si–H bonds by rhodium catalysis (color online).

selectivity (76%–98% *ee*). It is the first example of highly enantioselective Rh(II)-catalyzed Si–H bond insertion reaction with functionalized alkynes as carbene precursors, which presented a new approach to the preparation of chiral organosilicon with widely structural diversity from readily available hydrosilanes and alkynes. Kinetic studies and other mechanistic studies suggested that insertion of the *in situ*-generated Rh(II) carbenes into the Si–H bonds of the tertiary hydrosilanes was probably the rate-determining step.

#### 4.4 Ru-catalyzed carbene insertion of Si–H bond of monohydrosilanes

Among the transition-metal-catalyzed Si–H insertion reac-

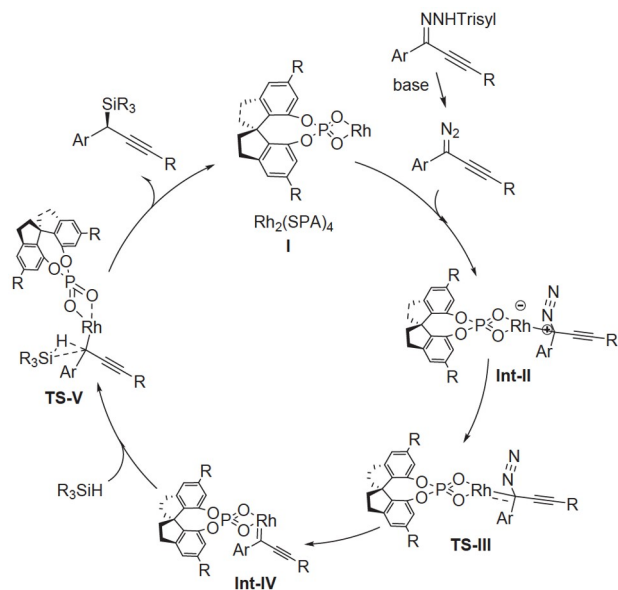
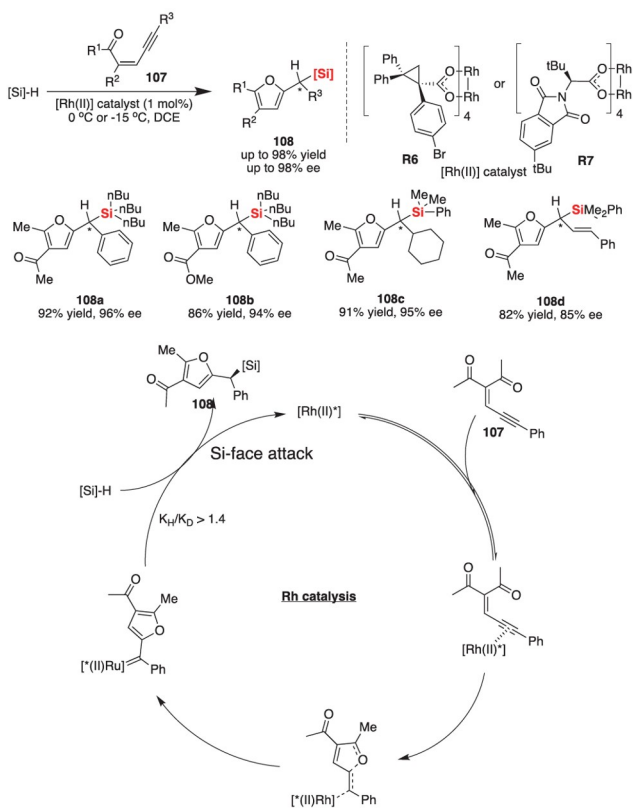


**Figure 7** The reaction mechanism for the rhodium-catalyzed insertion of alkynyl carbenes into Si-H bonds.



**Scheme 50** Rhodium-catalyzed Si-H insertion reaction with functionalized alkynes as carbene precursors (color online).

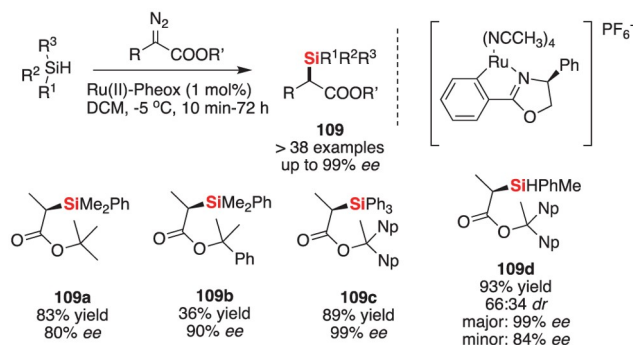
tions, there are a few examples related to the studies on ruthenium-catalyzed Si-H insertion reaction. In the first example reported in 2017, that Iwasa and Chanthamath *et al.* [118] established a highly efficient Ru-catalyzed Si-H insertion reaction with different hydrosilanes to  $\alpha$ -methyl-

substituted  $\alpha$ -diazoesters (Scheme 51), which provide an enantioselective protocol to construct carbon or silicon-stereogenic silanes **109** in high yields (up to 99%) and with moderate excellent enantioselectivities (up to 99% *ee*). It should be noted that the enantioselectivity depended largely on the steric hindrance of hydrosilane and  $\alpha$ -diazoester. Although the Si-H insertion reactions of dihydrosilanes ( $\text{PhRSiH}_2$ ) using Ru(II)-pheox suffered from low to moderate diastereoselectivity (58:42 to 79:21 *dr*), the experimental results indicated that chiral Ru(II) catalyst can be possibly applied for the development of highly enantioselective Si-H insertion reactions to construct enantioenriched silicon-stereogenic centers **109d** using a prochiral hydrosilanes.

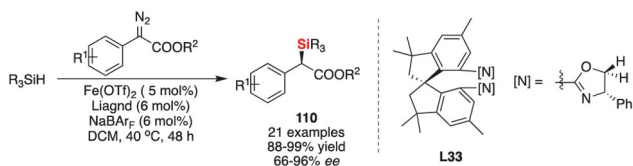
Subsequently in 2020, Che and co-workers [119] also investigated the catalytic activity of chiral *cis*- $\beta$ -[Ru<sup>II</sup>(salen)(CO)<sub>2</sub>] complexes in the enantioselective carbene Si-H insertion of  $\alpha$ -diazoester under light irradiation, and fortunately, this Ru catalyst exhibited good performance to give the desired product with up to 96% yields and up to 84% *ee*.

#### 4.5 Fe-catalyzed carbene insertion of Si-H bond of monohydrosilanes

Although an iron(II)-catalyzed Si-H insertion reaction of  $\alpha$ -diazo carbonyl compounds was developed in 2017 [120], the first enantioselective version was reported by Lin and co-workers [121], in which they reported a highly enantioselective iron-catalyzed Si-H insertion reaction with their hexamethyl-1,1'-spirobiindane-based bisoxazoline ligands (HMSI-BOX, **L33**). This protocol provided rapid and facile access to structurally diverse chiral  $\alpha$ -silyl esters **110** in high yields and good *ee* values (Scheme 52). Similarly to previous work,  $\alpha$ -diazoarylacetaes were suitable for this reaction with various tertiary hydrosilanes (such as  $\text{Et}_3\text{SiH}$  and  $\text{PhMe}_2\text{SiH}$ ); however, the use of  $\alpha$ -diazoalkyl compounds in the asymmetric Si-H insertion reaction resulted into no reaction with the same chiral iron catalyst system. The deuterium-labeling KIE experiments and DFT calculations suggested that the reaction proceeded *via* a concerted quintet transition state, in which the phenyl group on  $\alpha$ -



**Scheme 51** Ruthenium-catalyzed Si-H insertion reaction (color online).



**Scheme 52** Iron-catalyzed Si–H insertion reaction (color online).

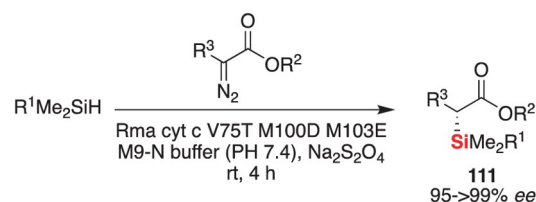
diazoarylacetaate has obvious steric repulsions with the ester group in the key quintet transition state that is responsible for the exceptional enantioselectivity.

#### 4.6 Enzyme-catalyzed carbene insertion of Si–H bond of monohydrosilanes

Although enzyme catalysis has been well-known in enantioselective synthesis, enzymes-catalyzed carbon–silicon bond formation is quite rare in nature. The first example was reported by Arnold group in 2016 [122]. They discovered that heme proteins could catalyze the formation of chiral organosilicon compounds **111** under physiological conditions *via* carbene Si–H insertion reaction of hydrosilane with diazo esters (Scheme 53). Using directed evolution, Arnold and co-workers [122] enhanced the catalytic function of cytochrome *c* from *Rhodothermus marinus* to achieve better reaction results with more than 15-fold higher turnover than synthetic catalysts. Notably, the biocatalytic reaction proceeded both *in vitro* and *in vivo*, accommodating a broad range of aryl and alkyl diazo esters as well as monohydrosilanes with high chemo- and enantioselectivity.

through C–H bond activation of ferrocene with a Si–H or Ge–H bond on aromatic ring (Scheme 54). In this work, they found Carreira’s dienes drastically improved the enantioselectivity (60% *ee*) in comparison to that of chiral BINAP (31% *ee*) [128]. Then the determination of chiral diene ligand **L34** as the best ligand in this reaction makes the selective synthesis of silicon-containing planar-chiral molecules possible (up to 86% *ee*).

Kuninobu and Takai *et al.* [129] developed a double dehydrogenative cyclization of bis(biphenyl)silane by the rhodium catalyst ( $[\text{RhCl}(\text{PPh}_3)_3]$  or a mixture of  $[\text{Rh}(\text{cod})\text{Cl}]_2$  and *rac*-BINAP) for the synthesis of a spiro-silabifluorene derivatives. And this reaction could be applied to the enantioselective synthesis of chiral spiro-silabifluorene derivatives (70%–81% *ee*) in the presence of chiral phosphine ligands ((*R*)-BINAP, Scheme 55). Subsequently, the authors further optimized the reaction conditions to improve the enantioselectivity for this Rh-catalyzed double dehydrogenative cyclization with the same BINAP as the ligand but under lower temperature and long reaction time, which resulted into the chiral spiro-9-silabifluorenes **115** with higher stereoselectivity (up to 95% *ee*) [130]. The mechan-



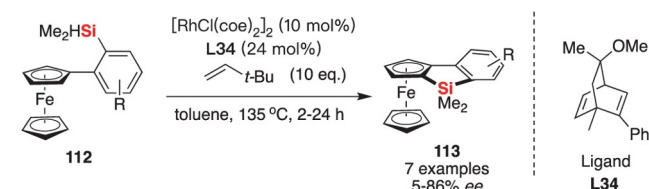
**Scheme 53** Enzyme-catalyzed Si–H insertion reaction (color online).

## 5 Asymmetric C–H silylation

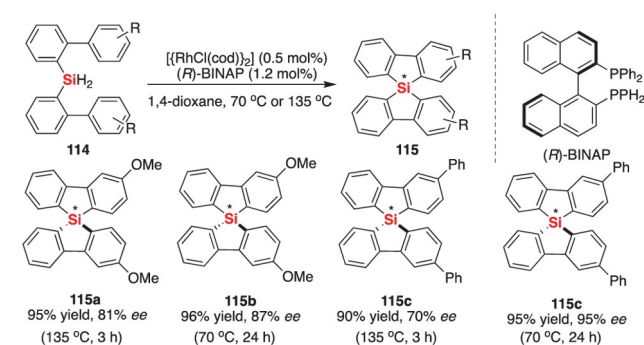
In the past decade, the C–H bond functionalization, including C–H silylation [123], has become a useful and efficient strategy for the synthesis of organosilicon compounds [124]. Herein, we will summarize recent and exciting findings for the enantioselective Si–H bond functionalization through C–H silylation catalyzed by rhodium or iridium complexes.

### 5.1 Rh-catalyzed intramolecular C–H silylation

Among the transition metal catalysts, rhodium catalysis was proved to be a superior strategy for the C–H silylation. In this regard, Hartwig *et al.* [125] contributed greatly to the rhodium-catalyzed C–H silylation reaction. Interestingly, although there are numerous exciting examples reported in the past years [126], the enantioselective version of C–H silylation was revealed until 2015. In this year, Shibata and co-workers [127] reported their effort in the asymmetric synthesis of ferrocene-fused benzo-siloles **113** and benzo-germole by intramolecular cross dehydrogenative coupling



**Scheme 54** Rhodium-catalyzed intramolecular C(sp<sup>2</sup>)–H silylation (color online).



**Scheme 55** Rhodium-catalyzed intramolecular C(sp<sup>2</sup>)–H silylation (color online).



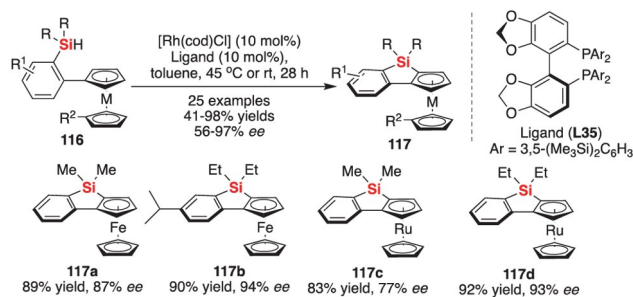
istic studies revealed that the rhodium catalyst promoted dehydrogenative silylation for the formation of spiro-9-silabifluorenes **115** through both Si–H and C<sub>sp<sup>2</sup></sub>–H activation, and interconversion of two Rh/monohydrosilane intermediates occurred through cleavage of C<sub>sp<sup>2</sup></sub>–Si bonds.

Subsequently in 2015, He and co-workers [131] reported a rhodium-catalyzed enantioselective intramolecular silylation of cyclopentadiene rings in metallocenes (Fe or Ru) through systemic investigation of chiral diphosphine ligands (Scheme 56). It was found that the (*S*)-TMS-Segphos **L35** could control the enantioselective rhodium-catalyzed C–H bond silylation reaction of Fe or Ru-based metallocenes under mild reaction conditions. In this intramolecular silylation, various planar-chiral ferrocene and ruthenocene siloles **117** were achieved with moderate to high enantioselectivity as well as good yields.

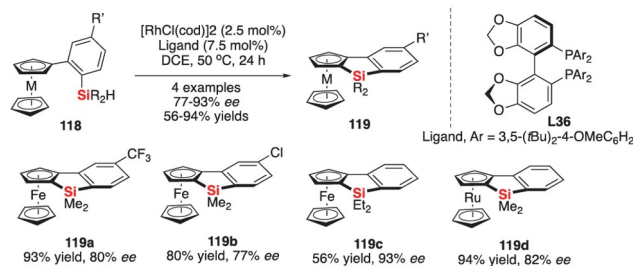
Almost at the same time in 2015, Murai and Takai *et al.* [132] developed an enantioselective rhodium-catalyzed intramolecular C–H silylation for the synthesis of several benzosilole-fused ferrocenes and ruthenocene **119** (Scheme 57). This protocol offered a practical and environmentally friendly strategy to the enantioselective construction of functionalized planar chiral metallocenes with good yields and enantioselectivities (up to 93% *ee*).

Different from the intramolecular C(sp<sup>2</sup>)–H silylation, the intramolecular dehydrogenative silylation of C(sp<sup>3</sup>)–H bonds is a more challenging reaction process. In 2015, Murai and Takai *et al.* [133] described the acceleration effect of phosphine ligands for the intramolecular dehydrogenative silylation of C(sp<sup>3</sup>)–H bonds (Scheme 58). Besides the diphosphine ligands, the role of hydrogen acceptors is also highly important. On the basis of screening experiments, P-ligand **L37** was found to be the most effective ligand to facilitate the intramolecular dehydrogenative silylation of C–H bonds, in which it could suppress the competitive hydro-silylation of a hydrogen acceptor, 3,3-dimethyl-1-butene. In addition, by employing bulky and electron-rich chiral diphosphine ligands, desymmetrizations of 2-(isopropyl)silylbenzene **120** or dihydrosilane **122** *via* the intramolecular silylative cyclization were achieved to give the enantiomeric rich products **121** or **123** with carbon or silicon-centered chirality respectively. Although the *ee* was quite low, this is a rare example of the catalytic asymmetric dehydrogenative functionalization of C(sp<sup>3</sup>)–H bonds with Si–H bond activation.

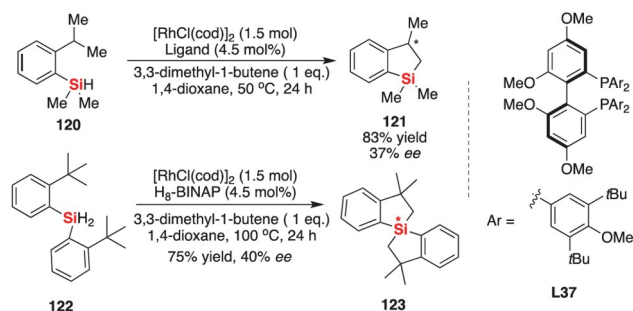
The combinational use of iridium-catalyzed Si–O bond-forming silylation and rhodium-catalyzed C–H silylation of diaryl ketones **124** provides a powerful strategy for the synthesis of silacycles **125**. Hartwig and co-workers [134] have shown that the direct silylation of aryl C–H bonds could create a new class of silacycles **125** (Scheme 59). In addition, such reaction process could be expanded to enantioselective silylation of C(sp<sup>2</sup>)–H bonds directed by a (hydrido)silyl



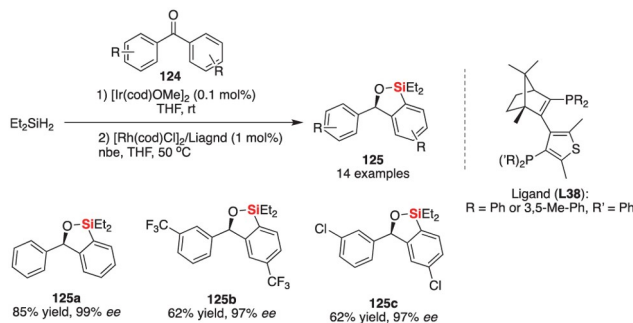
**Scheme 56** Enantioselective rhodium-catalyzed intramolecular C(sp<sup>2</sup>)–H silylation of metallocenes (color online).



**Scheme 57** Enantioselective rhodium-catalyzed intramolecular C(sp<sup>2</sup>)–H silylation of metallocenes (color online).



**Scheme 58** Enantioselective rhodium-catalyzed intramolecular C(sp<sup>3</sup>)–H silylation (color online).



**Scheme 59** Enantioselective rhodium-catalyzed intramolecular C(sp<sup>2</sup>)–H silylation (color online).

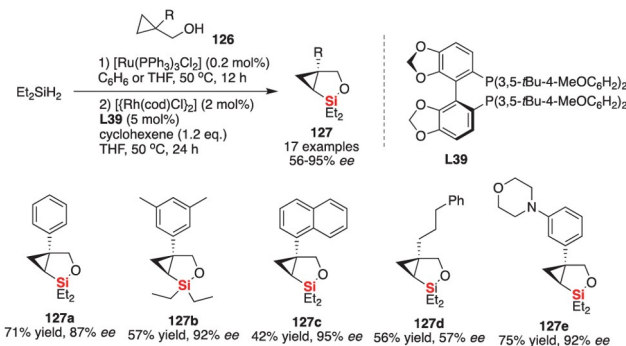
group and catalyzed by the combination of [Rh(cod)Cl]<sub>2</sub> and chiral bisphosphine ligands, which was recognized as a site-selective silylation of enantioenriched chiral diarylmethanols in high yield with excellent enantioselectivity [135].

Subsequently in 2016, Hartwig and Lee [136] developed an enantioselective intramolecular silylation of cyclopropanes **126** based on *in-situ* formed silyl ether-linked hydrosilanes, which constitutes a highly enantioselective Si–C bond-forming silylation of an alkyl C–H bond and functionalization of the C(sp<sup>3</sup>)–H bond in a cyclopropane to form chiral silacycles **127** (Scheme 60). The enantioselective silylation process tolerates a wide range of functional groups with the aid of chiral bisphosphine **L39** and Rh complex. In addition, the observed KIE data (about 2.1) suggests that the C–H bond activation is turnover-limiting and enantioselectivity-determining process for this silylation reaction.

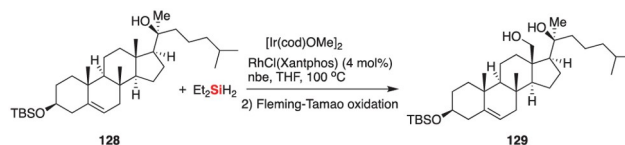
To modify the structure of drug-like molecule, Hartwig and co-workers [137] developed a rhodium-catalyzed intramolecular silylation of alkyl C–H bonds that occurs with unusual selectivity for the C(sp<sup>3</sup>)–H bonds locating  $\delta$ -position to the silicon-tethered oxygen atom of an *in-situ* formed alcohol-derived silyl ether from dehydrogenative coupling of tertiary alcohols **128** with diethylsilane (Scheme 61). Although this silylation is not an enantioselective fashion, this regioselective process provides a facile method to synthesize drug-like 1,4-diols **129** by a hydroxyl-directed C(sp<sup>3</sup>)–H bond functionalization and is distinct from the iridium-catalyzed silylation for the synthesis of 1,3-diols from alcohols. Thus the highly regioselective [(Xantphos)Rh(Cl)]-catalyzed silylation occurred at a primary C–H bond of  $\delta$ -position to the silicon-tethered hydroxyl group over typically more reactive C(sp<sup>3</sup>)–H bonds more proximal to the same functional group. Similar to previous reports, recent and exciting progress on the intramolecular silylation of chiral substrates further revealed the importance of silicon-tethered strategy in the enantioselective construction of a new additional central chirality [138].

Similarly, Zhao and co-workers [139] have successfully developed a rhodium-catalyzed dehydrogenative Si–C coupling-type silylation with Et<sub>2</sub>SiH<sub>2</sub>, which provided a highly efficient method to access structurally diverse silacycles, including dibenzooxasilines and ferrocene oxasilolanes with a broad substituent scope. Notably, the asymmetric dehydrogenative silylation of 2-ferrocenyl-substituted phenolic silyl ethers resulted into enantioenriched planar-chiral ferrocenes bearing a six-membered oxasilines **131** with good yields (51%–82%) and enantioselectivities (90%–95% *ee*) (Scheme 62).

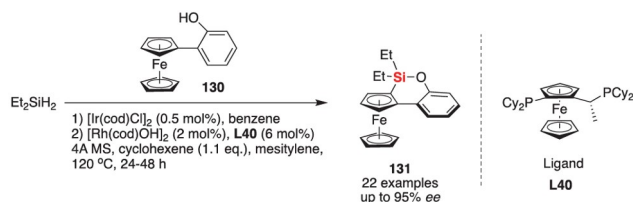
Although asymmetric intramolecular dehydrogenative silylation between Si–H and C–H bonds has been determined before 2017 [127–136], the combined intermolecular dehydrogenative C–H silylation with tandem desymmetrization of silacyclobutanes was a really novel reaction process at that time. In this context, He and co-workers [140] reported an interesting method to construct silicon-stereogenic dibenzosiloles **133** through rhodium-catalyzed tandem desymmetrization of silacyclobutanes and intermolecular



**Scheme 60** Enantioselective rhodium-catalyzed intramolecular C(sp<sup>3</sup>)–H silylation (color online).

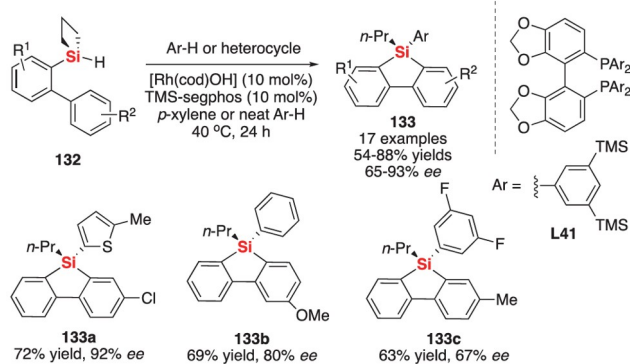


**Scheme 61** Enantioselective rhodium-catalyzed intramolecular C(sp<sup>3</sup>)–H silylation (color online).



**Scheme 62** Enantioselective rhodium-catalyzed C(sp<sup>2</sup>)–H silylation (color online).

dehydrogenative silylation hinged on the C–H silylation (Scheme 63). In this reaction, mechanistic studies showed that silacyclobutanes **132** initially underwent desymmetric C–H silylation with the aid of a reactive Si–H bond, producing a chiral hydrosilane intermediate that ultimately furnished the intermolecular Si–C coupling reaction to access silicon-stereogenic dibenzosilole product. Subsequently in 2021, He and Yu *et al.* [141] reported that a combined computational and experimental study to clarify the Rh-catalyzed C–H silylation with silacyclobutanes. The key findings in this reaction mechanism include: (1) the active catalytic species is a [Rh]–H but not the previously proposed [Rh]–Cl species; (2) the [Rh]–H is generated *via* a reductive elimination and b-hydride (b-H) elimination sequence; (3) the oxidative addition of SCBs is identified as the regio- and enantio-determining steps; (4) based on the reaction mechanism, the discretely *in-situ* formed [Rh]–H is shown to be a more efficient catalyst in C–H silylation with SCBs. Through this combined computational and experimental study, He and co-workers [142] further improved this reaction in this work in comparison to that of the previous method.

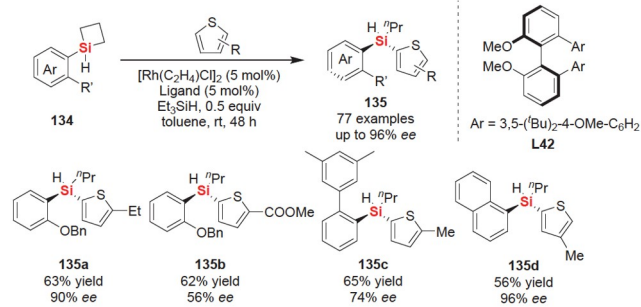


**Scheme 63** Enantioselective rhodium-catalyzed C(sp<sup>2</sup>)-H silylation of silacyclobutanes (color online).

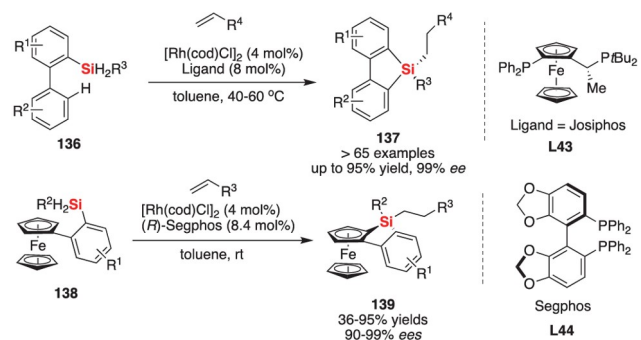
On the basis of their previous findings [140–142], He and co-workers [143] developed a modified protocol that enabled enantioselective intermolecular C–H silylation reactions, which made a wide scope of acyclic silicon-stereogenic hydrosilanes **135** in high yields and excellent enantioselectivities (Scheme 64). In this work, the employment of [Rh]–H catalyst that *in-situ* formed from the reaction system was proposed to be a more reactive catalyst as opposed to the commonly used [Rh]–Cl catalyst. In addition, the placement of a steric blocking group next to the Si center might be another important factor to guarantee the high level of enantioselective control in this reaction.

To construct silicon-stereogenic silacycles by C–H silylation, He and co-workers [144] developed a highly enantioselective tandem C–H silylation/alkene hydrosilylation reaction with readily available dihydrosilanes and alkenes to construct structurally diverse silicon-stereogenic silanes in a single step with good to excellent yields and enantioselectivities (Scheme 65). The desired products **137** or **139** featured with architecturally complex and functionally tetrasubstituted structures. This work further revealed the powerful potentials of Joisphos **L43** in the asymmetric Rh-controlled desymmetrization of dihydrosilanes.

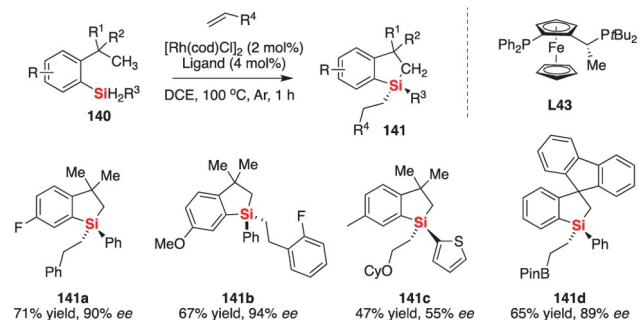
In 2020, He and co-workers [145] developed an efficient intramolecular C(sp<sup>3</sup>)-H silylation and tandem alkene hydrosilylation for the enantioselective synthesis of silicon-stereogenic dihydrobenzosiloles **141** (Scheme 66). This process involves double Si–C bond-forming reaction, as claimed asymmetric C(sp<sup>3</sup>)-H silylation of dihydrosilanes and followed by a stereospecific hydrosilylation with another molecule of alkene. In this work, a wide range of dihydrosilanes and alkenes displaying good functional group-tolerance with good to excellent yields and enantioselectivities. Very recently, the same group described an enantioselective synthesis of chiral 6-member-bridged dihydrodibenzosilines featuring axial and central chirality in excellent enantioselectivities (Scheme 67) [146]. A wide range of silicon-stereogenic dihydrodibenzosilines **143**



**Scheme 64** Enantioselective rhodium-catalyzed C(sp<sup>2</sup>)-H silylation of silacyclobutanes (color online).

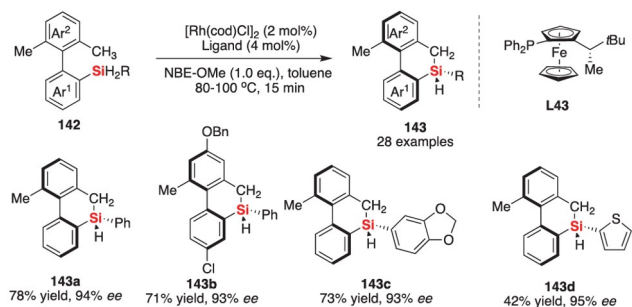


**Scheme 65** Enantioselective rhodium-catalyzed tandem C–H silylation/alkene hydrosilylation (color online).

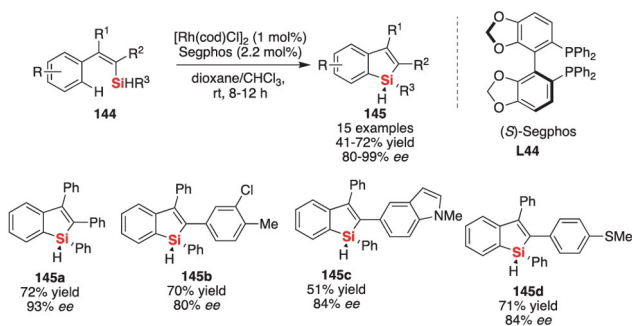


**Scheme 66** Enantioselective rhodium-catalyzed intramolecular C(sp<sup>3</sup>)-H silylation and tandem alkene hydrosilylation (color online).

containing both silicon-central and axial chiralities are conveniently constructed through intramolecular dehydrogenative C–H silylation with the aid of chiral Rh/Joisphos (**L43**) catalyst system and with a modified NBE-OMe (5-(methoxymethyl)bicyclo-[2.2.1]hept-2-ene) as the hydrogen acceptor. It should be noted that reaction time is very important because the yield of the desired product increased while the *ee* value decreased over time, in which the loss of *ee* might suffer from the side reaction between Rh catalysts with the newly formed monohydrosilane. Later, He and co-workers [147] further demonstrated an enantioselective rhodium-catalyzed intramolecular dehydrogenative C–H silylation process of aryl dihydrosilanes **144** (Scheme 68), which enables the facile synthesis of a variety of silicon-



**Scheme 67** Enantioselective rhodium-catalyzed intramolecular C(sp<sup>3</sup>)-H silylation (color online).

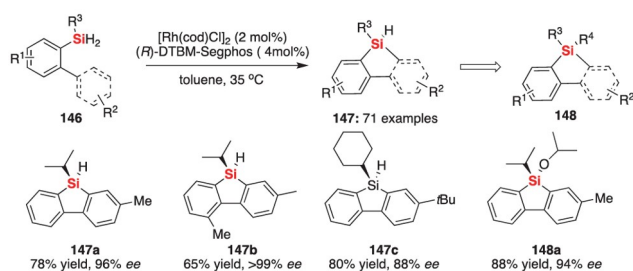


**Scheme 68** Enantioselective rhodium-catalyzed intramolecular C(sp<sup>3</sup>)-H silylation (color online).

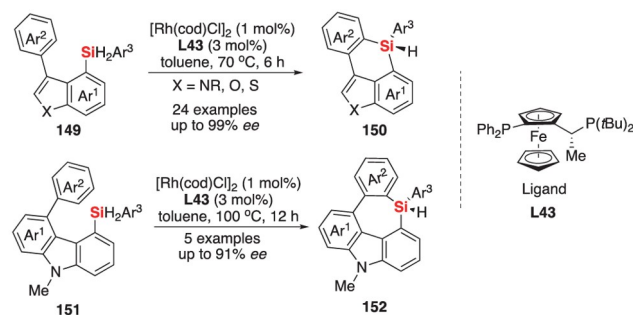
stereogenic 1H-benzosiloles **145** (15 examples) and structurally similar 1H-benzosilolometallocenes (10 examples) in good yields with good to excellent chemo-, regio-, and stereocontrol (up to 99% ee).

Very recently, He and co-workers [148] developed a general method for the construction of silicon-stereogenic monohydrosilanes **147** through enantioselective Rh-catalyzed intramolecular dehydrogenative coupling between Si-H bond of dihydrosilane and aryl C(sp<sup>2</sup>)-H bonds (Scheme 69). This Si-H functionalization provided a wide scope of silicon-stereogenic monohydrosilanes with different substituents on the aryl rings and Si centers. In addition, the remaining Si-H bond on the chiral monohydrosilanes could be further transformed to access chiral tetraorganosilanes **148** by hydrosilylation with alkene or alkyne, silylation of alcohol, hydrosilylation of ketone, and Si-H/C-H dehydrogenative coupling reaction. It also found that the silicon stereochemistry had a >99% retention under the above reaction conditions.

In 2021, He and co-workers [149] expanded the general aryl substrates to indole-derived heterocycles **149** or **151** in the intramolecular C-H silylation, in which they reported an enantioselective rhodium-catalyzed intramolecular silylation to the construction of six- and seven-membered silicon-stereogenic silacycles **150** or **152** with excellent enantioselectivities (Scheme 70). These silacycle products, silicon-bridged heterocycles, exhibited bright blue fluorescence and



**Scheme 69** Enantioselective rhodium-catalyzed intramolecular C(sp<sup>2</sup>)-H silylation (color online).

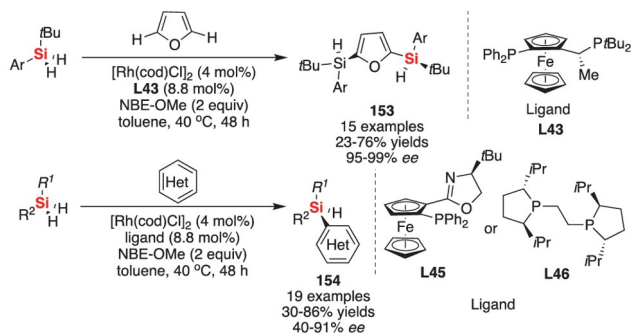


**Scheme 70** Enantioselective rhodium-catalyzed intramolecular C(sp<sup>2</sup>)-H silylation (color online).

potential functions for their application in the field of organic optoelectronic materials. In terms of the enantioselective Si-H bond activation, this process underwent a direct dehydrogenative C-H silylation through intramolecular Si-C cross-coupling cyclization that occurred with both C-H activation and Si-H bond functionalization. In addition, the elaboration of the chiral monohydrosilane product delivered structurally diverse tetraorgano-substituted silicon-stereogenic silacycles without the loss of enantiopurity.

## 5.2 Rh-catalyzed intermolecular C-H silylation

Intermolecular C-H silylation is a challenging research topic, and no C-H silylation with high stereoselectivity has been reported for a long time. Very recently, He and co-workers [150] reported an interesting intermolecular rhodium-catalyzed C-H silylation of heteroarenes for the enantioselective synthesis of acyclic silicon-stereogenic heteroarylsilanes (Scheme 71). This process featuring dehydrogenative Si-H/C-H cross-coupling provided a new strategy for the preparation of a variety of bis-Si-stereogenic silanes **153** or acyclic heteroarylated silicon-stereogenic monohydrosilanes **154** in good chemo-, regio-, and stereocontrol fashion. Similarly, Huang and Chen *et al.* [151] also reported a desymmetrization of dihydrosilanes with S-heterocycles, such as thianaphthene and thiophene derivatives, *via* intermolecular C-H silylation. The protocol provided a series of silicon-stereogenic monohydrosilanes with high



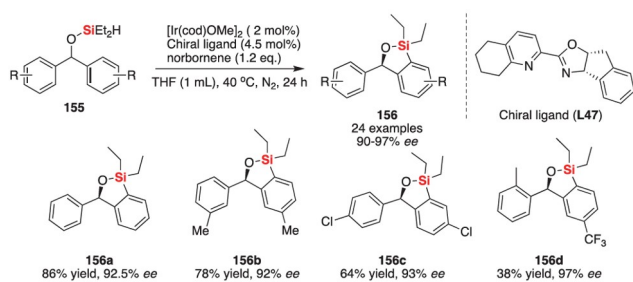
**Scheme 71** Enantioselective rhodium-catalyzed intermolecular C(sp<sup>3</sup>)-H silylation (color online).

yields (up to 90%), moderate to excellent enantioselectivity (63%–99% *ee*) and good regioselectivity.

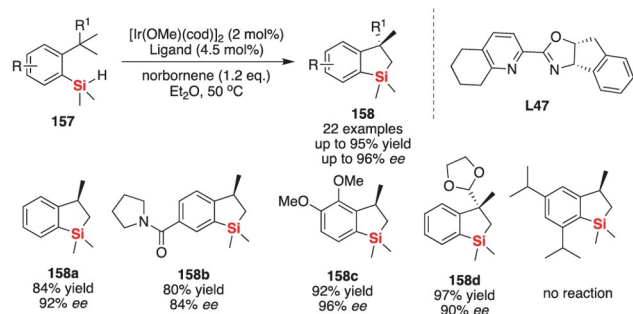
### 5.3 Rh-catalyzed intermolecular C–H silylation

Similar to the rhodium catalysis, iridium complexes were also found to be effective catalysts and have been widely used in the intermolecular C–H silylation of arene and heteroarenes [152]. However, there are a few examples related to the enantioselective control of iridium-catalyzed C–H silylation. In 2017, Hartwig and Shi *et al.* [153] reported an Ir-catalyzed intramolecular silylation of various symmetrical diarylmethanol derivatives to form Si-containing silacycles, chiral cyclic silyl ethers **156**, in good excellent yields with high enantioselectivity (up to 97% *ee*). The pyridinyl-oxazoline ligand **L47** was proved to be a crucial factor that enabled the enantioselective silylations of C–H bonds occurred in the presence of chiral Ir complex. In addition, this excellent stereoselectivity also translated to the kinetic resolution of unsymmetrical and racemic diarylmethoxysilanes to give the enantioenriched cyclic silyl ether **156** with good enantioselectivity (Scheme 72).

The same group also reported a highly enantioselective intramolecular C(sp<sup>3</sup>)-H silylations of primary C(sp<sup>3</sup>)-H bonds promoted by the iridium complex generated from [Ir(COD)OMe]<sub>2</sub> and chiral oxazoline-containing dinitrogen ligands [154]. The reactions provided a facile process to the synthesis of chiral dihydrobenzosiloles **158** in high yields with excellent enantioselectivities (up to 96% *ee*) by desymmetric functionalization of methyl groups under mild conditions (Scheme 73). The synthetic potential of this reaction was also illustrated by sequential C(sp<sup>3</sup>)-H and C(sp<sup>2</sup>)-H silylations as well as diastereoselective C–H silylations/functionalizations of a natural-product derivative containing point chirality and multiple types of C–H bonds. In 2019, the density functional theory calculations were performed by Huang and co-workers [155] to reveal the iridium-catalyzed intramolecular silylation of methyl C(sp<sup>3</sup>)-H bonds. The experimental results showed that the *in-situ* generated iridium(III) silyl dihydride species was the true



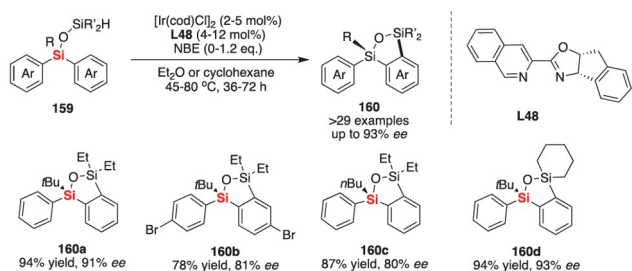
**Scheme 72** Enantioselective iridium-catalyzed intermolecular C(sp<sup>2</sup>)-H silylation (color online).



**Scheme 73** Iridium-catalyzed intramolecular silylation of methyl C–H bonds (color online).

active catalyst, in which the iridium(III) disilyl hydride species would generate from the migratory insertion and the transmetalation. In addition, the C–H silylation reaction was found to take place through an Ir(III)/Ir(V) catalytic cycle, and the C(sp<sup>3</sup>)-H bond oxidative addition was proved to be the rate- and enantioselectivity-determining step. Notably, the steric repulsion and C–H···π interaction between chiral ligand and substrate were found to account for the high enantioselectivity.

Despite a hot and growing attention on the catalytic asymmetric synthesis of silacycle compounds by C–H silylation, the enantioselective construction of silicon-stereogenic centers through desymmetrization strategy remains a challenging topic in organosilicon chemistry [156]. Inspired by previous iridium-catalyzed intramolecular C–H silylation of siloxane-tethered arene and hydrosilane that reported by Xu's group [157], Zhao and co-workers [158] recently realized an enantioselective strategy for the construction of silicon-stereogenic diarylsilanol-derived silacycles **160** that could be converted to chiral diol catalyst cores (PSiOLs) and its derivatives as a P-ligand possessing both Si and P-stereocenters (Scheme 74). Notably, in this reaction, it was observed that the *tert*-butyl group linked with silicon atom on the silanol moiety largely affected the yield and enantioselective control. When the *tert*-butyl group was changed to methyl, *n*-butyl, isopropyl, cyclohexyl, or benzyl groups, the enantioselectivities of the products were decreased to some extent under slightly modified reaction conditions.

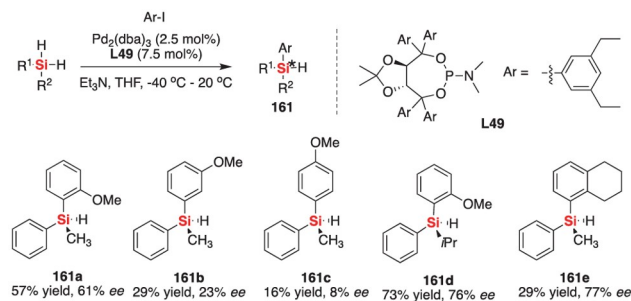


**Scheme 74** Iridium-catalyzed intramolecular C–H silylation (color online).

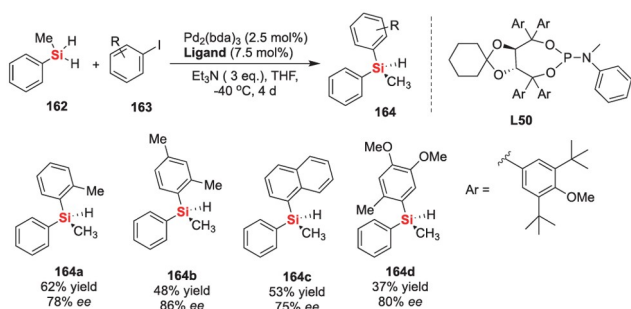
## 6 Cross-coupling of hydrosilanes with aryl halides

Although the potential of transition-metal-catalyzed silicon-carbon bond-forming cross-coupling reaction has attracted much attention in the past decades [159], limited progress has been reported in catalytic asymmetric Si–C bond-forming silylation of aryl halides with hydrosilanes. In addition, the synthesis of silicon-stereogenic organosilicon compounds through catalytic asymmetric silicon-carbon bond-forming silylation with aryl halides and hydrosilanes is really a challenging task. In 2012, Yamanoi and Nishihara [160] have described the first enantioselective arylation of dihydrosilanes with aryl iodides with the aid of chiral palladium catalyst systems with TADDOL-based phosphoramidite **L49** as chiral ligand (Scheme 75), and it was found to be effective for selective arylation of secondary silanes with promising enantioselectivity (up to 77% *ee*). The experimental results indicated that the substitution pattern of the substituent on hydrosilanes or the phenyl ring of both aryl iodides has a nonignored effect on the enantioselectivity. For example, quite low yields and enantioselectivities were achieved with *meta*- and *para*-substituted aryl iodides. Notably, the authors further investigated this asymmetric arylation of dihydrosilanes for the synthesis of low-molecular-weight circularly polarized luminescence (CPL) materials [161].

At present, the improvement of enantioselective control of transition-metal-catalyzed arylation of dihydrosilanes is still a challenging topic. In 2016, Xu and co-workers [162] also reported an enantioselective Pd-catalyzed silicon-carbon bond-forming arylation of hydrosilanes with aryl iodides for the direct synthesis of silicon-stereogenic silanes on the basis of a systematic optimization of a TADDOL-derived monodentate phosphoramidite ligand (Scheme 76). The identification of a new TADDOL-derived phosphoramidite ligand **L50** provided a new catalyst system to access chiral silanes **164** with moderate to good yield and enantioselectivity (up to 86% *ee*) under mild conditions. Furthermore, Xu and co-workers [163] have also performed a DFT study to gain mechanistic insights into the asymmetric palladium-catalyzed arylation of dihydrosilanes with aryl iodides. Ac-



**Scheme 75** Enantioselective palladium-catalyzed Si–C bond-forming silylation of aryl iodides (color online).



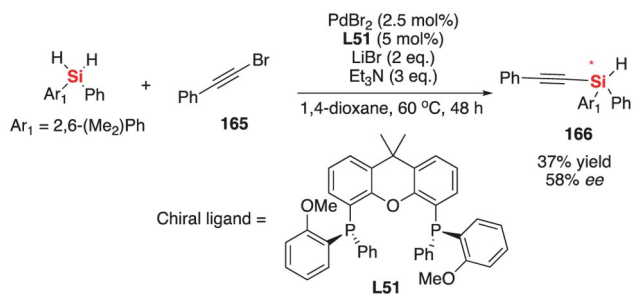
**Scheme 76** Enantioselective palladium-catalyzed Si–C bond-forming silylation of aryl iodides (color online).

ording to the calculation, the transmetalation step between  $\text{LPd}^{\text{II}}(\text{Ar})(\text{I})$  Pd–Ar bond and dihydrosilane Si–H bond was found to be the rate-determining or the enantioselective determining step. And the chiral P-ligand played with a long-distance chirality transfer manner for the discriminating Si–H bond activation of dihydrosilane, in which the aryl-aryl interactions between the steric bulky aryl group in P-ligand ( $\text{Ar}^1$ ) and aryl group in substrate **2** was responsible for the conformational adjustment during the rate-determining transmetalation step.

Very recently, Xu and co-workers [164] developed the first example of palladium-catalyzed C(sp)–Si cross coupling reaction of alkynyl bromides and hydrosilanes for the catalytic synthesis of alkynylsilanes with moderate to good yields and excellent chemoselectivity. Furthermore, this method aided by Xantphos-like chiral phosphine ligand (**L51**) allowed to make silicon-stereogenic alkynylsilane **166** with moderate enantioselectivity (58% *ee*) based on this catalytic asymmetric hydrosilylation (Scheme 77).

## 7 Conclusion and outlook

In the past decades, the enantioselective functionalization process of silicon-hydrogen bonds of hydrosilane compounds has been continuously developed with the aid of chiral catalyst systems, providing a series of new synthetic methods or strategies for the synthesis of chiral silicon-



**Scheme 77** Enantioselective palladium-catalyzed Si-C bond-forming silylation of aryl iodides (color online).

containing compounds with high efficiency and stereoselectivity. Especially, catalytic hydrosilylation reactions, Si-H insertion reactions, C-H silylation reactions and silicon-carbon bond-forming cross-coupling reactions, have been determined as major processes for the enantioselective version of Si-H bond functionalization. During the studies on stereoselective control of silicon-hydrogen bond functionalizations in the above transformations, a large number of chiral ligands were used to optimize the reaction conditions, and various transition metal catalytic systems with excellent performance were successfully constructed. Notably, platinum, rhodium, copper, nickel, iron, cobalt and other metal-based chiral catalyst systems exhibited personalized ability in catalytic asymmetric hydrosilylation reaction of alkenes or alkynes under the promotion of corresponding chiral phosphine ligands or nitrogen ligands, thereby completing the highly stereoselective silicon-hydrogen bond functionalization reaction process. As described in this review, transition metal catalyst systems such as rhodium, iridium, copper or palladium can exhibit excellent catalytic performance in silicon-hydrogen insertion reactions, C-H silylation reactions, or other functionalization reactions of silicon-hydrogen bonds. These experiment results further enrich the chiral organosilicon chemistry of hydrosilanes. Although the great achievements of the Si-H bond functionalization reaction process are comprehensively demonstrated in this review, the successful Si-H bond conversion reaction process is still very limited compared with the carbon-hydrogen bond functionalization reaction. It is well-known that the functionalization reaction process of silicon-hydrogen bonds is still a challenging topic in comparison to C-H bond functionalization. We believe that the asymmetric silicon-hydrogen bond functionalization reaction will not only be limited to these types of reactions presented in this review, but also new reactions that will be developed with continuous efforts in the future. To solve the problem of enantioselective control of Si-H bond functionalization, the development of new chiral ligands and their corresponding metal catalysis systems will not only further enhance the enantioselectivity of challenging reaction, such as the palladium-catalyzed silicon-carbon bond-forming

cross-coupling reaction, but also are expected to realize new types of enantioselective silicon-hydrogen bond functionalization reactions such as multicomponent reaction systems involving the activation of silicon-hydrogen bonds. Given the readily available sources and abundant structures of hydrosilane compounds, further investigation on the functionalization of silicon-hydrogen bonds will be beneficial to the development of organosilicon chemistry. We expect more chemists to be engaged in related fields of Si-H bond functionalization and jointly promote the rapid development of chiral silicon chemistry. Finally, we would like to conclude with a passage from Prof. Robert Corriu who is one of the founders of organosilicon chemistry in France: "In this area the only limitation for the chemist is mainly his own creativity" from the topic of "Where organosilicon chemistry is going?" [165]. We believe that the creation of more and more new strategies for the catalytic asymmetric silicon-hydrogen bond-forming transformations will appear in the near future [166].

**Acknowledgements** This work was supported by the National Natural Science Foundation of China (22072035), the Special Support Program for High-level Talents of Zhejiang Province (2021R51005), the "Ten-Thousand Talents Plan" of Hangzhou city, Hangzhou Innovation Team (TD2020015), and Zhejiang Provincial Natural Science Foundation of China (LY21B030007, LY22B020006). The authors thank X.F. Chen and X.J. Fang for their assistance in this work.

**Conflict of interest** The authors declare no conflict of interest.

- For recent reviews, see: (a) Zuo Y, Liang X, Yin J, Gou Z, Lin W. *Coord Chem Rev*, 2021, 447: 214166; (b) Zheng L, Nie XX, Wu Y, Wang P. *Eur J Org Chem*, 2021, 2021: 6006-6014; (c) Zuo Y, Gou Z, Quan W, Lin W. *Coord Chem Rev*, 2021, 438: 213887; (d) Zhang X, Fang J, Cai C, Lu G. *Chin Chem Lett*, 2021, 32: 1280-1292; (e) Wang H, Chen S, Li Y, Liu Y, Jing Q, Liu X, Liu Z, Zhang X. *Adv Energy Mater*, 2021, 11: 2101057
- Patai S, Rappoport Z. *The Chemistry of Organic Silicon Compounds*. New York: John Wiley & Sons, 1989
- Pawlenko S. *Organosilicon Chemistry*. Berlin: Walter de Gruyter, 1986
- (a) Mata S, López LA, Vicente R. *Angew Chem Int Ed*, 2018, 57: 11422-11426; (b) Onoe M, Baba K, Kim Y, Kita Y, Tobisu M, Chatani N. *J Am Chem Soc*, 2012, 134: 19477-19488; (c) Liu ZL, Yang C, Xue QY, Zhao M, Shan CC, Xu YH, Loh TP. *Angew Chem Int Ed*, 2019, 58: 16538-16542; (d) Nishino S, Hirano K, Miura M. *Chem Eur J*, 2020, 26: 8725-8728
- Kuciński K, Stachowiak-Dłużyńska H, Hreczycho G. *Coord Chem Rev*, 2022, 459: 214456
- For recent reviews, see: (a) Corey JY. *Chem Rev*, 2016, 116: 11291-11435; (b) Chaulagain MR, Sormunen GJ, Montgomery J. *J Am Chem Soc*, 2007, 129: 9568-9569; (c) Murphy SK, Zeng M, Herzon SB. *Science*, 2017, 356: 956-959
- (a) Price FP. *J Am Chem Soc*, 1947, 69: 2600-2604; (b) Eaboran CE. *Organosilicon Compounds*. Edinburgh: Butterworths Publications, 1960
- (a) Iglesias M, Fernández-Alvarez FJ, Oro LA. *Coord Chem Rev*, 2019, 386: 240-266; (b) Li Z, Yu Z, Luo X, Li C, Wu H, Zhao W, Li H, Yang S. *RSC Adv*, 2020, 10: 33972-34005
- Wang H, Lu G, Sormunen GJ, Malik HA, Liu P, Montgomery J. *J*

- Am Chem Soc*, 2017, 139: 9317–9324
- 10 Gui YY, Hu N, Chen XW, Liao LL, Ju T, Ye JH, Zhang Z, Li J, Yu DG. *J Am Chem Soc*, 2017, 139: 17011–17014
- 11 Peng D, Zhang Y, Du X, Zhang L, Leng X, Walter MD, Huang Z. *J Am Chem Soc*, 2013, 135: 19154–19166
- 12 Wang C, Teo WJ, Ge S. *ACS Catal*, 2017, 7: 855–863
- 13 Łowicki D, Bezlada A, Mlynarski J. *Adv Synth Catal*, 2014, 356: 591–595
- 14 Zuo Z, Zhang L, Leng X, Huang Z. *Chem Commun*, 2015, 51: 5073–5076
- 15 Weber S, Glavic M, Stöger B, Pittenauer E, Podewitz M, Veiros LF, Kirchner K. *J Am Chem Soc*, 2021, 143: 17825–17832
- 16 Lu W, Zhu X, Yang L, Wu X, Xie X, Zhang Z. *ACS Catal*, 2021, 11: 10190–10197
- 17 Chakraborty S, Blacque O, Fox T, Berke H. *ACS Catal*, 2013, 3: 2208–2217
- 18 Seliger J, Dong X, Oestreich M. *Angew Chem Int Ed*, 2019, 58: 1970–1974
- 19 (a) Wang X, Huang SS, Zhang FJ, Xie JL, Li Z, Xu Z, Ye F, Xu LW. *Org Chem Front*, 2021, 8: 6577–6584; (b) Yin G, Xu L. *Chin J Org Chem*, 2021, 41: 4839–4840; (c) Zhu J, Chen S, He C. *J Am Chem Soc*, 2021, 143: 5301–5307
- 20 (a) Troegel D, Stohrer J. *Coord Chem Rev*, 2011, 255: 1440–1459; (b) Almeida LD, Wang H, Junge K, Cui X, Beller M. *Angew Chem Int Ed*, 2021, 60: 550–565
- 21 (a) Miller ZD, Dorel R, Montgomery J. *Angew Chem Int Ed*, 2015, 54: 9088–9091; (b) Hu MY, Lian J, Sun W, Qiao TZ, Zhu SF. *J Am Chem Soc*, 2019, 141: 4579–4583
- 22 Sommer LH, Pietrusza EW, Whitmore FC. *J Am Chem Soc*, 1947, 69: 188
- 23 (a) Speier JL, Webster JA, Barnes GH. *J Am Chem Soc*, 1957, 79: 974–979; (b) Hofmann R, Vlatković M, Wiesbrock F. *Polymers*, 2017, 9: 534; (c) Li N, Dong XY, Zhang JL, Yang KF, Zheng ZJ, Zhang WQ, Gao ZW, Xu LW. *RSC Adv*, 2017, 7: 50729–50738
- 24 (a) Lukin RY, Kuchkaev AM, Sukhov AV, Bekmukhamedov GE, Yakhvarov DG. *Polymers*, 2020, 12: 2174; (b) Osakada K, Tsuchido Y, Tanabe M. *Coord Chem Rev*, 2020, 412: 213195
- 25 Szymaniak AA, Zhang C, Coombs JR, Morken JP. *ACS Catal*, 2018, 8: 2897–2901
- 26 (a) Riener K, Högerl MP, Gigler P, Kühn FE. *ACS Catal*, 2012, 2: 613–621; (b) Liu W, Lu W, Yang L, Wu X, Zhang Z. *Tetrahedron*, 2022, 109: 132632
- 27 Naito T, Yoneda T, Ito J, Nishiyama H. *Synlett*, 2012, 23: 2957–2960
- 28 Bergens SH, Noheda P, Whelan J, Bosnich B. *J Am Chem Soc*, 1992, 114: 2121–2128
- 29 (a) Hua Y, Nguyen HH, Scaggs WR, Jeon J. *Org Lett*, 2013, 15: 3412–3415; (b) Hua Y, Nguyen HH, Trog G, Berlin AS, Jeon J. *Eur J Org Chem*, 2014, 2014: 5890–5895
- 30 Chung JYL, Shevlin M, Klapars A, Journet M. *Org Lett*, 2016, 18: 1812–1815
- 31 Li HL, Huang WS, Ling FY, Li L, Yan JH, Xu H, Xu LW. *Chem Asian J*, 2021, 16: 1730–1734
- 32 Tamao K, Nakamura K, Ishii H, Yamaguchi S, Shiro M. *J Am Chem Soc*, 1996, 118: 12469–12470
- 33 Naganawa Y, Namba T, Kawagishi M, Nishiyama H. *Chem Eur J*, 2015, 21: 9319–9322
- 34 Chang X, Ma PL, Chen HC, Li CY, Wang P. *Angew Chem Int Ed*, 2020, 59: 8937–8940
- 35 (a) Huang YH, Wu Y, Zhu Z, Zheng S, Ye Z, Peng Q, Wang P. *Angew Chem Int Ed*, 2022, 61: e202113052; (b) Wu Y, Wang P. *Angew Chem Int Ed*, 2022, 61: e202205382
- 36 Zhao ZY, Nie YX, Tang RH, Yin GW, Cao J, Xu Z, Cui YM, Zheng ZJ, Xu LW. *ACS Catal*, 2019, 9: 9110–9116
- 37 He T, Liu LC, Ma WP, Li B, Zhang QW, He W. *Chem Eur J*, 2020, 26: 17011–17015
- 38 (a) Xu LW, Li L, Lai GQ, Jiang JX. *Chem Soc Rev*, 2011, 40: 1777–1790; (b) Xu LW. *Angew Chem Int Ed*, 2012, 51: 12932–12934
- 39 Kiso Y, Yamamoto K, Tamao K, Kumada M. *J Am Chem Soc*, 1972, 94: 4373–4374
- 40 (a) Uozumi Y, Hayashi T. *J Am Chem Soc*, 1991, 113: 9887–9888; (b) Uozumi Y, Sang-Yong L, Hayashi T. *Tetrahedron Lett*, 1992, 33: 7185–7188; (c) Uozumi Y, Kitayama K, Hayashi T. *Tetrahedron-Asymmetry*, 1993, 4: 2419–2422; (d) Hayashi T. *Catal Today*, 2000, 62: 3–15; (e) Heller B, Gutnov A, Fischer C, Drexler HJ, Spannenberg A, Redkin D, Sundermann C, Sundermann B. *Chem Eur J*, 2007, 13: 1117–1128
- 41 (a) Kitayama K, Uozumi Y, Hayashi T. *J Chem Soc Chem Commun*, 1995, 1533; (b) Pioda G, Togni A. *Tetrahedron-Asymmetry*, 1998, 9: 3903–3910; (c) Pedersen HL, Johannsen M. *Chem Commun*, 1999, 24: 2517–2518; (d) Weber I, Jones GB. *Tetrahedron Lett*, 2001, 42: 6983–6986; (e) Hayashi T, Hirate S, Kitayama K, Tsuji H, Torii A, Uozumi Y. *J Org Chem*, 2001, 66: 1441–1449; (f) Jensen JF, Svendsen BY, la Cour TV, Pedersen HL, Johannsen M. *J Am Chem Soc*, 2002, 124: 4558–4559; (g) Guo XX, Xie JH, Hou GH, Shi WJ, Wang LX, Zhou QL. *Tetrahedron-Asymmetry*, 2004, 15: 2231–2234; (h) Li X, Song J, Xu D, Kong L. *Synthesis*, 2008, 2008: 925–931; (i) Zhang F, Fan QH. *Org Biomol Chem*, 2009, 7: 4470–4474; (j) Junge K, Wendt B, Enthaler S, Beller M. *ChemCatChem*, 2010, 2: 453–458; (k) Han JW, Hayashi T. *Tetrahedron-Asymmetry*, 2010, 21: 2193–2197; (l) Park HS, Han JW, Shintani R, Hayashi T. *Tetrahedron-Asymmetry*, 2013, 24: 418–420; (m) Han JW, Hayashi T. *Tetrahedron-Asymmetry*, 2014, 25: 479–484; (n) Park HS, Kim MY, Ahn HJ, Han JW. *Bull Korean Chem Soc*, 2016, 37: 795–796
- 42 Gibson S, Rudd M. *Adv Synth Catal*, 2007, 349: 781–795
- 43 Wang YF, He YH, Su Y, Ji Y, Li R. *J Org Chem*, 2022, 87: 2831–2844
- 44 (a) Widenhoefer RA, DeCarli MA. *J Am Chem Soc*, 1998, 120: 3805–3806; (b) Perch NS, Widenhoefer RA. *J Am Chem Soc*, 1999, 121: 6960–6961; (c) Perch NS, Pei T, Widenhoefer RA. *J Org Chem*, 2000, 65: 3836–3845
- 45 Kochi T, Ichinose K, Shigekane M, Hamasaki T, Kakiuchi F. *Angew Chem Int Ed*, 2019, 58: 5261–5265
- 46 Long PW, Xu JX, Bai XF, Xu Z, Zheng ZJ, Yang KF, Li L, Xu LW. *RSC Adv*, 2018, 8: 22944–22951
- 47 (a) Sumida Y, Yorimitsu H, Oshima K. *J Org Chem*, 2009, 74: 7986–7989; (b) Benohoud M, Tuokko S, Pihko PM. *Chem Eur J*, 2011, 17: 8404–8413; (c) Gandhamsetty N, Park J, Jeong J, Park SW, Park S, Chang S. *Angew Chem Int Ed*, 2015, 54: 6832–6836
- 48 Gu XW, Sun YL, Xie JL, Wang XB, Xu Z, Yin GW, Li L, Yang KF, Xu LW. *Nat Commun*, 2020, 11: 2904
- 49 (a) Oestreich M, Rendler S. *Angew Chem Int Ed*, 2005, 44: 1661–1664; (b) Rendler S, Oestreich M, Butts CP, Lloyd-Jones GC. *J Am Chem Soc*, 2007, 129: 502–503
- 50 (a) Zhang M, Zhang A. *Appl Organometal Chem*, 2010, 24: 751–757; (b) Raya-Barón Á, Oña-Burgos P, Fernández I. *ACS Catal*, 2019, 9: 5400–5417
- 51 (a) Yamamoto K, Hayashi T, Zembayashi M, Kumada M. *J Organomet Chem*, 1976, 118: 161–181; (b) Yamamoto K, Hayashi T, Uramoto Y, Ito R, Kumada M. *J Organomet Chem*, 1976, 118: 331–348; (c) Tamao K, Tohma T, Inui N, Nakayama O, Ito Y. *Tetrahedron Lett*, 1990, 31: 7333–7336; (d) Fu PF, Brard L, Li Y, Marks TJ. *J Am Chem Soc*, 1995, 117: 7157–7168
- 52 (a) Chen J, Cheng B, Cao M, Lu Z. *Angew Chem Int Ed*, 2015, 54: 4661–4664; (b) Nikonov GI. *ChemCatChem*, 2015, 7: 1918–1919; (c) Chen J, Cao M, Cheng B, Lu Z. *Synlett*, 2015, 26: 2332–2335
- 53 Cheng B, Liu W, Lu Z. *J Am Chem Soc*, 2018, 140: 5014–5017
- 54 Chen C, Wang H, Sun Y, Cui J, Xie J, Shi Y, Yu S, Hong X, Lu Z. *iScience*, 2020, 23: 100985
- 55 (a) Greenwood NN, Earnshaw A. *Chemistry of the Elements*. 2nd Ed. London: Butterworth, 1997. 1114; (b) Obligacion JV, Chirik PJ. *Nat Rev Chem*, 2018, 2: 15–34; (c) Wen H, Liu G, Huang Z. *Coord Chem Rev*, 2019, 386: 138–153
- 56 Harrod JF, Chalk AJ. *J Am Chem Soc*, 1965, 87: 1133
- 57 Sun J, Deng L. *ACS Catal*, 2016, 6: 290–300



- 58 Cheng B, Lu P, Zhang H, Cheng X, Lu Z. *J Am Chem Soc*, 2017, 139: 9439–9442
- 59 Wen H, Wang K, Zhang Y, Liu G, Huang Z. *ACS Catal*, 2019, 9: 1612–1618
- 60 Wang XB, Zheng ZJ, Xie JL, Gu XW, Mu QC, Yin GW, Ye F, Xu Z, Xu LW. *Angew Chem Int Ed*, 2020, 59: 790–797
- 61 Dian L, Marek I. *Org Lett*, 2020, 22: 4914–4918
- 62 Wang L, Lu W, Zhang J, Chong Q, Meng F. *Angew Chem Int Ed*, 2022, 61: e202205624
- 63 Levine DS, Tilley TD, Andersen RA. *Chem Commun*, 2017, 53: 11881–11884
- 64 Zhan G, Teng HL, Luo Y, Lou SJ, Nishiura M, Hou Z. *Angew Chem Int Ed*, 2018, 57: 12342–12346
- 65 (a) Rendler S, Oestreich M. *Angew Chem Int Ed*, 2007, 46: 498–504; (b) Díez-González S, Nolan SP. *Acc Chem Res*, 2008, 41: 349–358
- 66 Gribble Jr. MW, Pirmot MT, Bandar JS, Liu RY, Buchwald SL. *J Am Chem Soc*, 2017, 139: 2192–2195
- 67 Xu QF, Yang P, Zhang X, You SL. *Synlett*, 2020, 32: 505–510
- 68 (a) Xu JL, Xu ZY, Wang ZL, Ma WW, Sun XY, Fu Y, Xu YH. *J Am Chem Soc*, 2022, 144: 5535–5542; (b) Li S, Xu JL, Xu YH. *Org Lett*, 2022, 24: 6054–6059
- 69 Zhang M, Ji Y, Zhang Z, Zhang C. *Org Lett*, 2022, 24: 2756–2761
- 70 Du X, Huang Z. *ACS Catal*, 2017, 7: 1227–1243
- 71 Shi R, Zhang Z, Hu X. *Acc Chem Res*, 2019, 52: 1471–1483
- 72 Bai D, Wu F, Chang L, Wang M, Wu H, Chang J. *Angew Chem Int Ed*, 2022, 61: e202114918
- 73 (a) Sánchez-Page B, Munarriz J, Jiménez MV, Pérez-Torrente JJ, Blasco J, Subias G, Passarelli V, Álvarez P. *ACS Catal*, 2020, 10: 13334–13351; (b) Hu MY, He P, Qiao TZ, Sun W, Li WT, Lian J, Li JH, Zhu SF. *J Am Chem Soc*, 2020, 142: 16894–16902
- 74 He P, Hu MY, Zhang XY, Zhu SF. *Synthesis*, 2022, 54: 49–66
- 75 (a) Pan G, Hu C, Hong S, Li H, Yu D, Cui C, Li Q, Liang N, Jiang Y, Zheng L, Jiang L, Liu Y. *Nat Commun*, 2021, 12, 64: 1–9; (b) Kaur B, Raza R, Stashick MJ, Branda NR. *Org Chem Front*, 2019, 6: 1253–1256
- 76 (a) Dong C, Yuan Y, Cui YM, Zheng ZJ, Cao J, Xu Z, Xu LW. *Appl Organometal Chem*, 2018, 32: e4037; (b) Xu JX, Chen MY, Zheng ZJ, Cao J, Xu Z, Cui YM, Xu LW. *ChemCatChem*, 2017, 9: 3111–3116
- 77 Igawa K, Yoshihiro D, Ichikawa N, Kokan N, Tomooka K. *Angew Chem Int Ed*, 2012, 51: 12745–12748
- 78 Ye F, Xu Z, Xu LW. *Acc Chem Res*, 2021, 54: 452–470
- 79 Long PW, Bai XF, Ye F, Li L, Xu Z, Yang KF, Cui YM, Zheng ZJ, Xu LW. *Adv Synth Catal*, 2018, 360: 2825–2830
- 80 Puerta-Oteo R, Munarriz J, Polo V, Jiménez MV, Pérez-Torrente JJ. *ACS Catal*, 2020, 10: 7367–7380
- 81 Chakrapani H, Liu C, Widenhofer RA. *Org Lett*, 2003, 5: 157–159
- 82 Fan BM, Xie JH, Li S, Wang LX, Zhou QL. *Angew Chem Int Ed*, 2007, 46: 1275–1277
- 83 Tang RH, Xu Z, Nie YX, Xiao XQ, Yang KF, Xie JL, Guo B, Yin GW, Yang XM, Xu LW. *iScience*, 2020, 23: 101268
- 84 Li K, Nie M, Tang W. *Green Synthesis Catal*, 2020, 1: 171–174
- 85 Xie JL, Xu Z, Zhou HQ, Nie YX, Cao J, Yin GW, Bouillon JP, Xu LW. *Sci China Chem*, 2021, 64: 761–769
- 86 Park JW. *Chem Commun*, 2022, 58: 491–504
- 87 Guo J, Shen X, Lu Z. *Angew Chem Int Ed*, 2017, 56: 615–618
- 88 Monfette S, Turner ZR, Semproni SP, Chirik PJ. *J Am Chem Soc*, 2012, 134: 4561–4564
- 89 Wen H, Wan X, Huang Z. *Angew Chem Int Ed*, 2018, 57: 6319–6323
- 90 Guo J, Wang H, Xing S, Hong X, Lu Z. *Chem*, 2019, 5: 881–895
- 91 Jin S, Liu K, Wang S, Song Q. *J Am Chem Soc*, 2021, 143: 13124–13134
- 92 You Y, Ge S. *Angew Chem Int Ed*, 2021, 60: 20684–20688
- 93 You Y, Ge S. *Angew Chem Int Ed*, 2021, 60: 12046–12052
- 94 Sun Y, Guo J, Shen X, Lu Z. *Nat Commun*, 2022, 13: 650
- 95 Huang X, Nguyen MH, Pu M, Zhang L, Chi YR, Wu YS, Zhou JS. *Angew Chem Int Ed*, 2020, 59: 10814–10818
- 96 Guo Z, Wen H, Liu G, Huang Z. *Org Lett*, 2021, 23: 2375–2379
- 97 Lu W, Zhao Y, Meng F. *J Am Chem Soc*, 2022, 144: 5233–5240
- 98 Keipour H, Carreras V, Ollevier T. *Org Biomol Chem*, 2017, 15: 5441–5456
- 99 Zhang H, Li L, Shen F, Cai T, Shen R. *Chin J Org Chem*, 2020, 40: 873–885
- 100 Zhu SF, Zhou QL. *Acc Chem Res*, 2012, 45: 1365–1377
- 101 Zhang YZ, Zhu SF, Wang LX, Zhou QL. *Angew Chem Int Ed*, 2008, 47: 8496–8498
- 102 Dakin LA, Ong PC, Panek JS, Staples RJ, Stavropoulos P. *Organometallics*, 2000, 19: 2896–2908
- 103 Wu J, Chen Y, Panek JS. *Org Lett*, 2010, 12: 2112–2115
- 104 Carreras V, Besnard C, Gandon V, Ollevier T. *Org Lett*, 2019, 21: 9094–9098
- 105 Wu J, Panek JS. *J Org Chem*, 2011, 76: 9900–9918
- 106 Huang EH, Zhang YQ, Cui DQ, Zhu XQ, Li X, Ye LW. *Org Lett*, 2022, 24: 196–201
- 107 Zhai XY, Wang XQ, Wu B, Zhou YG. *Chin J Chem*, 2022, 40: 21–27
- 108 Yasutomi Y, Suematsu H, Katsuki T. *J Am Chem Soc*, 2010, 132: 4510–4511
- 109 Wang JC, Xu ZJ, Guo Z, Deng QH, Zhou CY, Wan XL, Che CM. *Chem Commun*, 2012, 48: 4299–4301
- 110 Ball ZT. *Acc Chem Res*, 2013, 46: 560–570
- 111 Sambasivan R, Ball ZT. *J Am Chem Soc*, 2010, 132: 9289–9291
- 112 Chen D, Zhu DX, Xu MH. *J Am Chem Soc*, 2016, 138: 1498–1501
- 113 Jagannathan JR, Fettinger JC, Shaw JT, Franz AK. *J Am Chem Soc*, 2020, 142: 11674–11679
- 114 (a) Yang LL, Evans D, Xu B, Li WT, Li ML, Zhu SF, Houk KN, Zhou QL. *J Am Chem Soc*, 2020, 142: 12394–12399; (b) Yang LL, Cao J, Zhao TY, Zhu SF, Zhou QL. *J Org Chem*, 2021, 86: 9692–9698
- 115 Yang LL, Ouyang J, Zou HN, Zhu SF, Zhou QL. *J Am Chem Soc*, 2021, 143: 6401–6406
- 116 Tseberlidis G, Caselli A, Vicente R. *J Organomet Chem*, 2017, 835: 1–5
- 117 Huang MY, Yang JM, Zhao YT, Zhu SF. *ACS Catal*, 2019, 9: 5353–5357
- 118 Nakagawa Y, Chanthamath S, Fujisawa I, Shibatomi K, Iwasa S. *Chem Commun*, 2017, 53: 3753–3756
- 119 Lee CL, Chen D, Chang XY, Tang Z, Che CM. *Organometallics*, 2020, 39: 2642–2652
- 120 Keipour H, Ollevier T. *Org Lett*, 2017, 19: 5736–5739
- 121 Gu H, Han Z, Xie H, Lin X. *Org Lett*, 2018, 20: 6544–6549
- 122 Kan SBJ, Lewis RD, Chen K, Arnold FH. *Science*, 2016, 354: 1048–1051
- 123 (a) Li B, Dixneuf PH. *Chem Soc Rev*, 2021, 50: 5062–5085; (b) Cheng C, Hartwig JF. *Chem Rev*, 2015, 115: 8946–8975; (c) Xu Z, Xu LW. *ChemSusChem*, 2015, 8: 2176–2179; (d) Xu Z, Huang WS, Zhang J, Xu LW. *Synthesis*, 2015, 47: 3645–3668; (e) Ge Y, Huang X, Ke J, He C. *Chem Catal*, 2022, 2: 2898–2928
- 124 Cui YM, Lin Y, Xu LW. *Coord Chem Rev*, 2017, 330: 37–52
- 125 (a) Cheng C, Hartwig JF. *Science*, 2014, 343: 853–857; (b) Cheng C, Hartwig JF. *J Am Chem Soc*, 2014, 136: 12064–12072
- 126 Toutov AA, Liu WB, Betz KN, Fedorov A, Stoltz BM, Grubbs RH. *Nature*, 2015, 518: 80–84
- 127 Shibata T, Shizuno T, Sasaki T. *Chem Commun*, 2015, 51: 7802–7804
- 128 (a) Fischer C, Defieber C, Suzuki T, Carreira EM. *J Am Chem Soc*, 2004, 126: 1628–1629; (b) Defieber C, Grützmacher H, Carreira E. *Angew Chem Int Ed*, 2008, 47: 4482–4502
- 129 Kuninobu Y, Yamauchi K, Tamura N, Seiki T, Takai K. *Angew Chem Int Ed*, 2013, 52: 1520–1522
- 130 Murai M, Takeuchi Y, Yamauchi K, Kuninobu Y, Takai K. *Chem Eur J*, 2016, 22: 6048–6058
- 131 Zhang QW, An K, Liu LC, Yue Y, He W. *Angew Chem Int Ed*, 2015, 54: 6918–6921
- 132 Murai M, Matsumoto K, Takeuchi Y, Takai K. *Org Lett*, 2015, 17:

- 3102–3105
- 133 Murai M, Takeshima H, Morita H, Kuninobu Y, Takai K. *J Org Chem*, 2015, 80: 5407–5414
- 134 Li B, Driess M, Hartwig JF. *J Am Chem Soc*, 2014, 136: 6586–6589
- 135 Lee T, Wilson TW, Berg R, Ryberg P, Hartwig JF. *J Am Chem Soc*, 2015, 137: 6742–6745
- 136 Lee T, Hartwig JF. *Angew Chem Int Ed*, 2016, 55: 8723–8727
- 137 Karmel C, Li B, Hartwig JF. *J Am Chem Soc*, 2018, 140: 1460–1470
- 138 (a) Zuo Z, Xu S, Zhang L, Gan L, Fang H, Liu G, Huang Z. *Organometallics*, 2019, 38: 3906–3911; (b) Chen J, Shi Z, Lu P. *Org Lett*, 2021, 23: 7359–7363; (c) Chen J, Shi Z, Li C, Lu P. *Chem Sci*, 2021, 12: 10598–10604
- 139 Zhao WT, Lu ZQ, Zheng H, Xue XS, Zhao D. *ACS Catal*, 2018, 8: 7997–8005
- 140 Zhang QW, An K, Liu LC, Zhang Q, Guo H, He W. *Angew Chem Int Ed*, 2017, 56: 1125–1129
- 141 Zhang L, An K, Wang Y, Wu YD, Zhang X, Yu ZX, He W. *J Am Chem Soc*, 2021, 143: 3571–3582
- 142 Zhang QW, An K, Liu LC, Guo S, Jiang C, Guo H, He W. *Angew Chem Int Ed*, 2016, 55: 6319–6323
- 143 An K, Ma W, Liu LC, He T, Guan G, Zhang QW, He W. *Nat Commun*, 2022, 13: 847
- 144 Mu D, Yuan W, Chen S, Wang N, Yang B, You L, Zu B, Yu P, He C. *J Am Chem Soc*, 2020, 142: 13459–13468
- 145 Yang B, Yang W, Guo Y, You L, He C. *Angew Chem Int Ed*, 2020, 59: 22217–22222
- 146 Guo Y, Liu MM, Zhu X, Zhu L, He C. *Angew Chem Int Ed*, 2021, 60: 13887–13891
- 147 Yuan W, You L, Lin W, Ke J, Li Y, He C. *Org Lett*, 2021, 23: 1367–1372
- 148 Ma W, Liu LC, An K, He T, He W. *Angew Chem Int Ed*, 2021, 60: 4245–4251
- 149 Chen S, Mu D, Mai PL, Ke J, Li Y, He C. *Nat Commun*, 2021, 12: 1249
- 150 Chen S, Zhu J, Ke J, Li Y, He C. *Angew Chem Int Ed*, 2022, 61: e202117820
- 151 Mu D, Pan S, Wang X, Liao X, Huang Y, Chen J. *Chem Commun*, 2022, 58: 7388–7391
- 152 (a) Zhang M, Gao S, Tang J, Chen L, Liu A, Sheng S, Zhang AQ. *Chem Commun*, 2021, 57: 8250–8263; (b) Yan ZB, Peng M, Chen QL, Lu K, Tu YQ, Dai KL, Zhang FM, Zhang XM. *Chem Sci*, 2021, 12: 9748–9753; (c) Esteruelas MA, Martínez A, Oliván M, Oñate E. *J Am Chem Soc*, 2020, 142: 19119–19131; (d) Karmel C, Hartwig JF. *J Am Chem Soc*, 2020, 142: 10494–10505; (e) Karmel C, Rubel CZ, Kharitonova EV, Hartwig JF. *Angew Chem Int Ed*, 2020, 59: 6074–6081
- 153 Su B, Zhou TG, Li XW, Shao XR, Xu PL, Wu WL, Hartwig JF, Shi ZJ. *Angew Chem Int Ed*, 2017, 56: 1092–1096
- 154 Su B, Hartwig JF. *J Am Chem Soc*, 2017, 139: 12137–12140
- 155 Zhang M, Liang J, Huang G. *J Org Chem*, 2019, 84: 2372–2376
- 156 (a) Ye F, Xu LW. *Synlett*, 2021, 32: 1281–1288; (b) Yuan W, He C. *Synthesis*, 2022, 54: 1939–1950
- 157 Lin Y, Jiang KZ, Cao J, Zheng ZJ, Xu Z, Cui YM, Xu LW. *Adv Synth Catal*, 2017, 359: 2247–2252
- 158 Zhang H, Zhao D. *ACS Catal*, 2021, 11: 10748–10753
- 159 (a) Yamagishi H, Saito H, Shimokawa J, Yorimitsu H. *ACS Catal*, 2021, 11: 10095–10103; (b) Duan J, Wang K, Xu GL, Kang S, Qi L, Liu XY, Shu XZ. *Angew Chem Int Ed*, 2020, 59: 23083–23088; (c) Miura H, Masaki Y, Fukuta Y, Shishido T. *Adv Synth Catal*, 2020, 362: 2642–2650; (d) Lim S, Cho H, Jeong J, Jang M, Kim H, Cho SH, Lee E. *Org Lett*, 2020, 22: 7387–7392; (e) Wang S, Sun M, Zhang H, Zhang J, He Y, Feng Z. *CCS Chem*, 2021, 3: 2164–2173; (f) Wang M, Yu M, Wang W, Lin W, Luo F. *Chin J Org Chem*, 2019, 39: 3145–3153
- 160 Kurihara Y, Nishikawa M, Yamanoi Y, Nishihara H. *Chem Commun*, 2012, 48: 11564–11566
- 161 Koga S, Ueki S, Shimada M, Ishii R, Kurihara Y, Yamanoi Y, Yuasa J, Kawai T, Uchida T, Iwamura M, Nozaki K, Nishihara H. *J Org Chem*, 2017, 82: 6108–6117
- 162 Chen L, Huang JB, Xu Z, Zheng ZJ, Yang KF, Cui YM, Cao J, Xu LW. *RSC Adv*, 2016, 6: 67113–67117
- 163 (a) Xu Z, Xu JZ, Zhang J, Zheng ZJ, Cao J, Cui YM, Xu LW. *Chem Asian J*, 2017, 12: 1749–1757; (b) Yang JJ, Xu Z, Nie YX, Lu SQ, Zhang J, Xu LW. *J Org Chem*, 2020, 85: 14360–14368
- 164 Zhou XH, Fang XJ, Ling FY, Xu Z, Hong LQ, Ye F, Xu LW. *Org Chem Front*, 2022, 9: 5891–5898
- 165 Corriu R. *J Organomet Chem*, 2003, 686: 1
- 166 During the revision of this manuscript, Xu and co-workers recently reported an unprecedented strategy to access silicon-stereogenic organosilicons from racemic substrates. In this report, the novel designed chiral ligand SiMOS-Phos was crucial in the dynamic kinetic asymmetric hydrosilylation of “silicon-centered” racemic hydrosilanes, providing a wide range of the silicon-stereogenic benzosiloles with good enantioselectivities (up to 96:4 *er*). See: Zeng Y, Fang XJ, Tang RH, Xie JY, Zhang FJ, Xu Z, Nie YX, Xu LW. *Angew Chem Int Ed*, 2022, 61: e202214147